Molecular and neuronal mechanisms underlying context-dependent processing of odor valence in *Caenorhabditis elegans*

A Dissertation

Presented to

The Faculty of the Graduate School of Arts and Sciences

Brandeis University

Interdepartmental Program in Neuroscience

Dr. Piali Sengupta, Advisor

In Partial Fulfillment

of the Requirements for the Degree

Doctor of Philosophy

by

Munzareen Khan

February 2022

The signed version of this form is on file in the Graduate School of Arts and Sciences.

This dissertation, directed and approved by Munzareen Khan's Committee, has been accepted and approved by the Faculty of Brandeis University in partial fulfillment of the requirements for the degree of:

DOCTOR OF PHILOSOPHY

Wendy Cadge, Dean
Graduate School of Arts and Sciences

Dissertation Committee:

Dr. Piali Sengupta, Department of Biology
Dr. Donald B. Katz, Department of Psychology
Dr. Stephen Van Hooser, Department of Biology
Dr. Yun Zhang, Department of Organismic and Evolutionary Biology, Harvard University

ACKNOWLEDGEMENTS

As I reflect on my education journey, I realize that there is very little that I have achieved on my own. None of it would have been possible without the support, encouragement, and understanding I received from my family, mentors, friends, and colleagues. First, I would like to thank my mentor Piali for patiently guiding me over the last couple years and always encouraging me to push my boundaries. I am a better scientist as a result of Piali's high expectations and infectious enthusiasm for science. Beyond science, her work ethic, and dedication to mentoring and creating an inclusive lab environment has truly made a difference in my graduate school experience. Piali, I will always strive to be as good a mentor to my future mentees, as you were to me.

To all Sengupta lab members, past and present- thank you for all the help over the years. I don't think there has been a single day without me asking for help with experimental design, analysis and just life in general. You all made lab feel like home. Special shout out goes to Michael O'Donnell, without whom I would not be able to complete my Ph.D. Mike, you have been an incredible support. Thank you for being so amazingly generous with your time when it came to mentoring graduate students in the Sengupta lab. You have encouraged me to always connect the dots and think critically about my project, which contributed to the scientist I am today.

I would also like to acknowledge my committee and the graduate program at Brandeis, including the administrative staff. The inclusive environment of Brandeis and the commitment to scientific rigor has made my graduate school experience truly worthwhile. To Steve and Don – thank you for your guidance and support with this project. Thank you also to my external examiner, Yun, for agreeing to be a part of my

committee. I would also like to acknowledge all my professors, past mentors, and teachers in school. My development into the scientist I am today began years back when you encouraged me to push my boundaries.

Finally, without a network of support from family, this would not have been possible. To my parents, ammu (mom) Zobeda Mahmood and abbu (dad) Imranul Hoque Khan, thank you for being more than incredible. You have always allowed me to pursue my dreams, and always stood out like a beacon of hope, supporting me through it all. Your endless sacrifices led me here, so I dedicate my Ph.D. to you. To my siblings Ishraque and Iram – thank you for always being there and allowing me to lean on you for support. I also want to thank my grandparents and both of my khalamonis (aunts), my khalu (uncle), my in-laws, and all my cousins for being the best support system that I could ever ask for. To my husband Shimul, thank you for all you do to help me reach my goals and dreams. You are amazingly generous with your time and I simply could not have done this without your support. Thank you for everything that you have helped me accomplish. And finally to my daughter Zayda- you are just three years old as I write this, but you have given me the most profound reason and meaning to my life. You have taught me to persevere when things get difficult. Thank you for being my source of joy, love, and fun. I love you.

I am fully aware that my education is a privilege. Many children across the world do not have access to education, especially girls. To those women who have paved the path for me and for my right to education, thank you for this amazing gift. And to those who will come after me, I promise to take every opportunity to support education equity, especially for girls and women.

ABSTRACT

Molecular and neuronal mechanisms underlying context-dependent processing of odor valence in *Caenorhabditis elegans*

A dissertation presented to the Faculty of the
Graduate School of Arts and Sciences of Brandeis University
Waltham, Massachusetts

By Munzareen Khan

The survival of all animals is critically dependent on their ability to detect and respond appropriately to environmental cues. It is particularly important for animals to integrate information such as internal state and contextual cues in order to generate flexible and adaptive behaviors. One of the most important sensory modalities is olfaction; animals rely on olfaction to locate food sources, avoid pathogens and predators, and communicate with each other. However, a given odorant can elicit attractive or repulsive responses depending on context, intensity, and experience. How odor valence is robustly but flexibly encoded in neural circuits remains to be fully explored. Using the small nematode *Caenorhabditis elegans,* I have characterized a context- and concentration-dependent olfactory plasticity paradigm to a subset of bacterial food-produced medium-chain alcohols such as 1-hexanol. Specifically, I show that the behavioral response of *C. elegans* to 1-hexanol is inverted from attraction to avoidance in the presence of saturating levels of a second attractive bacteria-produced chemical. I have found that, by engaging distinct intracellular signal transduction pathways, the single AWC sensory neuron pair can invert its odorant response sign and drive context-dependent changes in behavioral preference to an odorant. In addition, I

have also described a push-pull opposing component circuit that drives concentration-dependent behavioral preference to hexanol. The results described in this dissertation suggest that sensory neurons can dynamically encode the hedonic valences of stimuli and that odor discrimination can take place at the level of sensory neurons.

TABLE OF CONTENTS

LIST OF TABLES

LIST OF FIGURES

CHAPTER 1

CHAPTER 2

CHAPTER 1

General Introduction

1.1 Plasticity in sensory systems

Animals must sense and respond to environmental stimuli in an experience- and context-dependent manner for optimal survival. Since environmental stimuli fluctuate constantly, sensory behaviors must be flexible and adaptive. The nervous system has the remarkable ability to change its structure and/or function to drive appropriate behavioral responses that allows organisms to adapt and thrive in their dynamic environment. This phenomenon is broadly termed as plasticity. The concept of plasticity of the brain and nervous system can be traced back to William James's seminal work, *The Principles of Psychology* (1980), in which he describes behavior, habits, and instincts to be under the influence of our external world. He states,

> Plasticity, … in the wide sense of the word, means the possession of a structure weak enough to yield to an influence, but strong enough not to yield all at once.… Organic matter, especially nervous tissue, seems endowed with a very extraordinary degree of plasticity of this sort; so that we may without hesitation lay down as our first proposition the following, that the phenomena of habit in living beings are due to the plasticity of the organic materials of which their bodies are composed. (p. 106)

Context- and experience-dependent modulation of sensory behaviors can be driven by various mechanisms, which include changes in intrinsic neuronal functions, alteration in synaptic signaling, and/or changes in the composition of neural circuits (Abott & Regehr, 2004; Pascual-Leone et al., 2005; Gulyaeva, 2017; Baroncelli & Lunghi, 2021; Bernhardi et al., 2017; Marder, 2012; Schaefer et al., 2017). Thus, plasticity in sensory systems can be driven entirely by changes at the sensory neuron level, as well as changes in downstream circuit dynamics, including plasticity at the level of central synapses.

The visual system provides an excellent example of a sensory system that adapts rapidly to environmental changes and responds to cues over a broad dynamic

range. One of the primary tasks of the visual system is to remain sensitive as the ambient light intensity varies over many orders of magnitude, and to adapt to different intensities of light. For example, upon entering a dark room from a well-lit environment, the retina goes through rapid changes which helps us adapt to a darker environment (Koch et al., 1982; Koutalos & Yau, 1996; Pugh & Lamb, 1990). There is over a million-fold change in light intensity between a bright sunny day and a starlit night. How does the visual system adjust to such broad ranges of light? This feat is accomplished by a few different mechanisms including changes in pupil size, compartmentalized functions of rods and cones, compensatory changes in photopigments, and feedback mechanisms to control the responsiveness of photoreceptors (Koch et al., 1982; Koutalos & Yau, 1996; Pugh & Lamb, 1990) (Dunn et al., 2007; Fain et al., 2001) (Ke et al., 2014; Radonjic et al., 2011). Molecular mechanisms guiding light/dark adaptation have also been extensively characterized. For example, intracellular calcium concentrations serve as an internal regulator of a series of feedback loops that modulate various steps of the phototransduction process to adjust gain control and sensitivity and evade saturation (Fain & Matthews; Koch et al., 1982; Koutalos & Yau, 1996; Matthews et al., 1988; Nakatani & Yau, 1988; Torre et al., 1986) (Pugh & Lamb, 1990). As a consequence, photoreceptors retain the ability to respond to a single photon over at least seven magnitudes of light intensity.

Sensory systems are not only influenced by contextual experience but can also be modulated by internal state. A key modulator of internal state is satiety, and satiety state-dependent behavioral modulation has been extensively studied in multiple systems, including in *Drosophila.* In general, starved flies are more tolerant of innately

aversive odors (Bracker et al., 2013). On the contrary, food-related odors are less appealing by a satiated fly (Root et al., 2011, Ko et al., 2015). For example, the satiety state in flies has been shown to influence their preference for apple cider vinegar (Huetteroth & Waddell, 2011; Root et al., 2011). Prior work has shown that fruit flies are attracted to low concentrations of apple cider vinegar, and that the Or42b expressing olfactory sensory neurons that project to the DM1 glomerulus are particularly important for this behavioral response (Semmelhack & Wang, 2009). Starved, but not fed adult flies, exhibit strong seeking behavior when they smell the odor of apple cider vinegar. Global insulin signaling and a local neuropeptide pathway work cooperatively in peripheral sensory neurons and downstream circuits to tune the behavioral response of flies to food odor (Semmelhack & Wang, 2009). More recent studies have built on this finding, and have shown that starvation upregulates appetitive and downregulates aversive olfactory channels, via parallel neuromodulatory pathways,
to fine tune and regulate overall hedonic valence of food odors (Root et al., 2011; Ko et al., 2015; Inagaki et al, 2012). Specifically, satiety-dependent neuromodulators facilitate synaptic outputs from Or42b olfactory receptor neurons and suppression of those from Or85a —neuronal populations that mediate odor-guided attraction and aversion behaviors, respectively (Root et al., 2011; Ko et al., 2015; Inagaki et al., 2012).

Sensory plasticity is also modulated by learned association. In 1956, Galambos et al. published the first electrophysiological study of the auditory cortex and reported associative-learning related plasticity in A1 neurons (Galambos, 1956). In the auditory system, individual neurons have receptive fields tuned to a certain frequency, and each neuron is maximally sensitive and responsive to that frequency. Galambos et al. (1956)

found that click-shock pairing, a type of classical conditioning, was accompanied by significant increases in the amplitude of A1-evoked potentials to the conditioned stimulus in cats (Galambos, 1956). Additional auditory conditioning studies have also shown that neurons in rodent area A1 often revealed dramatic shifts in their frequency tuning functions such that their best frequencies shifted in an experience-dependent manner to the direction of the shock-predictive tone (Bakin & Weinberger, 1990; Diamond & Weinberger, 1984).

Our nervous system essentially acts as a sensor and any sensor risks saturation and loss of functionality without employing mechanisms of gain control and fine tuning. Plasticity allows organisms to adjust the sensitivity of the sensory system which helps them thrive and adapt to their changing environments. Examples of plasticity can be found in every sensory modality. As discussed above, mechanisms driving sensory plasticity can vary widely and can take place at different levels of the nervous system. Since my thesis research focuses on chemosensation and olfactory plasticity, I discuss and highlight relevant background information and findings in this modality in greater depth throughout the rest of this chapter.

1.1 Chemosensation

Chemosensation is a fundamental sensory process shared by all living organisms and it is critical for survival. For most species, the ability to detect and respond appropriately to chemosensory stimuli serves as the primary window to the sensory world. Almost all organisms use chemosensation to avoid predators, find reproductive partners, and assess the availability and quality of food. Responses to

chemosensory stimuli are present even in the simplest organisms, including bacteria, mold, and protozoans. Furthermore, the biochemical process of chemosensation involves recognition of chemical molecules in the environment by specialized chemosensory structures and signal transduction pathways, such that the information can be translated into signals that the nervous system can then interpret.

Valence of chemical signals are largely driven by innate preferences and learned association with past experiences (Knaden & Hansson, 2014; Li & Liberles, 2015; Mori & Sakano, 2021; Sachse & Beshel, 2016; Stowers & Kuo, 2015; Takahashi, 2014). Behavioral responses to chemical signals can also be extensively modulated by internal and external context (Grunwald Kadow, 2019; Stowers & Liberles, 2016). Thus, chemosensation has been a particularly useful modality in which to study mechanisms of sensory behavioral plasticity. The senses of smell and taste (gustatory system) are often referred to together as the chemosensory system, since they both give the nervous system information about the chemical environment. As my dissertation focuses on olfactory plasticity in *C. elegans,* I will focus primarily on the topic of olfaction (here defined as the ability to detect and respond to volatile odorants). First, I will describe the structure of the olfactory system and olfactory signaling mechanisms in mammals and insects, followed by a review of comparative features of olfaction in *C. elegans.*

1.2.1 Comparative olfaction – olfactory system organization and signaling mechanisms in *M. musculus* and *D. melanogaster*

The fact that all living organisms rely on olfaction for survival may be the reason behind the striking organizational and mechanistic similarities that are found between olfactory systems of diverse species. The olfactory systems of insects and mammals have analogous anatomical features and use similar molecular logic for olfactory coding (Hildebrand & Shepherd, 1997). Comparison of olfaction across diverse species reveals unexpected similarities and surprising differences among chemosensory systems. Here, I will describe the structure and function of the olfactory systems of mice and *Drosophila,* two very well studied organisms in the olfaction field.

Olfactory system organization

M. musculus

In most mammals, including mice, the olfactory system can be divided into two main parts: (1) the main olfactory epithelium (MOE)(Graziadei & Metcalf, 1971), comprising of a layer of dense olfactory sensory neurons (OSNs) in the nasal cavity (Buck & Axel, 1991), where transduction of volatile odorants take place, and (2) the vomeronasal organ (VNO), also referred to as the accessory olfactory system, which is dedicated to the detection of pheromones (Clancy et al., 1984; Zancanaro & Carla, 2014). The olfactory epithelium is connected to the main olfactory bulb (MOB), whereas olfactory information from VNO is transmitted to the accessory olfactory bulb, which occupies a distinct area. Odorant receptors (ORs), a type of G protein-coupled receptor, are expressed on the surface of the cilia which protrude from the OSN's dendrite into the mucus covering the surface of the epithelium (Buck & Axel, 1991). Each OSN

expresses only one type of OR, but an odorant can bind multiple ORs expressed on different OSNs (Buck & Axel, 1991; Mombaerts et al., 1996; Vassar et al., 1994). Instead of expressing the classical olfactory receptors, a minority of neurons in the mammalian olfactory system expresses the much smaller trace amine-associated receptors (TAARs), another class of G protein- coupled receptors (Borrowsky et al., 2001; Johnson et al., 2012). It has been shown that TAAR2–TAAR9 function as olfactory receptors for volatile amine odorants in vertebrates (Liberles, 2015). Several TAARs detect natural odors derived from urine, microbial metabolism, and other ecological sources, thus serving as an important contributor in translating ethological chemosensory information into relevant behaviors. Finally, it has also been shown that a distinct set of neurons in the main olfactory epithelium, expresses both receptor guanylate cyclase and a non-GPCR olfactory receptor, encoded by the membrane spanning 4-pass A (MS4A) genes (Greer et al., 2016). These cells are thought to mediate the social acquisition of food preference and confer responses to ethologically relevant ligands, including fatty acids and pheromones (Greer et al., 2016, Munger et al., 2010; Hu et al., 2007).

In addition to peripheral olfactory structures, the mammalian olfactory system also consists of central brain regions which are responsible for further odor processing. Structures on the surface of the main olfactory bulb, known as glomeruli, serve as a connector for terminals of the olfactory nerve and the dendrites of projection neurons, which connect to the olfactory cortex and higher centers of the brain, for further processing of odors (Shepherd, 1994)(Figure 1.1). The main olfactory bulb reaches, among other structures, the olfactory (piriform) cortex, and the entorhinal cortex. The

main target of the accessory olfactory bulb is the medial anterior and posterior cortical amygdala (Dulac et al., 2003; Bear et al., 2016). These structures are involved in odor perception and translation of odor information into emotions, memory, and learning. The axons of OSNs expressing the same odorant receptors converge onto the same glomerulus, allowing for the organization and segregation of different types of olfactory information (Figure 1.1) (Mombaerts et al., 1996; Vassar et al., 1994).

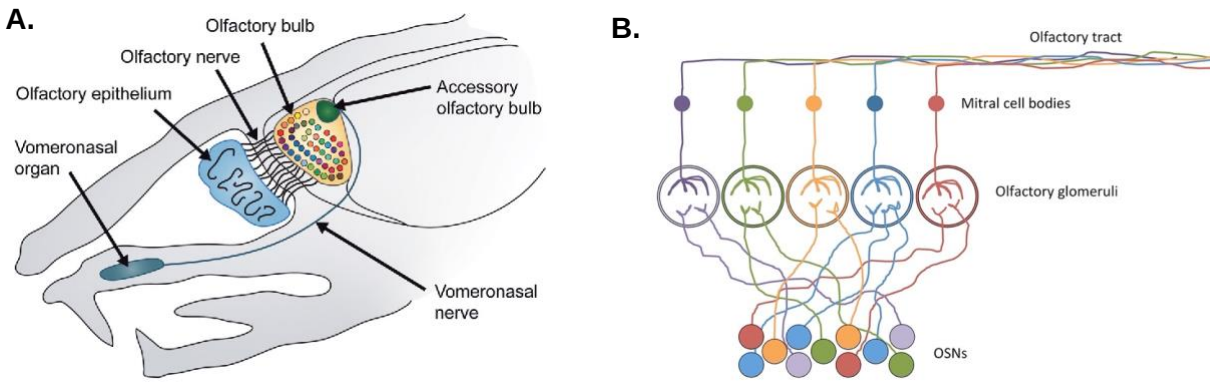

Figure 1.1. (A) Schematic representation of olfactory organs in mice (DeMaria & Ngai, 2010). **(B)** Olfactory system organization of mammals. (Wikibooks)

D. melanogaster

The chemosensory system of the *Drosophila* has analogous anatomical features as mice. *Drosophila* chemosensory structures can also be functionally segregated into olfactory and pheromone sensing systems. Primarily, the olfactory organs consist of the antenna and maxillary palp (Figure 1.2). Both organs contain sensory hairs, known as sensilla, which contains the dendrites of olfactory receptor neurons ORNs (Ayer & Carlson, 1992; de Bruyne et al., 1999; Dweck et al., 2016). The sensilla are categorized

into three distinct morphological types- basiconic, coelonoic, and trichoid (Shanbhag et al., 2000). The basiconic sensilla responds to odorants whereas primary detection of pheromones occurs at the trichoid sensilla (Clyne et al., 1999; van der Goes van Naters & Carlson, 2007). Olfactory receptors in fruit flies comprise of three families: the odorant receptors (ORs), gustatory receptors (GRs) (Vosshall & Stocker, 2007) (Vosshal & Stocker, 2007), and ionotropic receptors (IRs) (Benton et al., 2009). ORs and IRs both serve as chemosensors in the insect olfactory system and they function as ligand-gated ion channels (Sato et al., 2008; Wicher et al., 2008). Both types of receptors are expressed on the olfactory sensory neurons (OSNs) of the main olfactory organ, the antenna, but they are housed in different types of sensilla: IRs in coeloconic sensilla and ORs in basiconic and trichoid sensilla. OR channels consist of two subunits: a conserved co-receptor (Orco) subunit and a highly divergent odorant receptor (OR) subunit that contains the odorant-binding site (Larsson et al., 2004; Butterwick et al., 2018). Unlike the mammalian system, ORNs in the antenna have now been reported to co-express chemosensory receptors, which may contribute to enhanced odor discrimination abilities (McLaughlin et al., 2021; Task et al., 2020). In the glomeruli, ORNs synapse onto antennal lobe projection neurons (PNs), which are second-order neurons connected to higher processing areas, such as the mushroom body and lateral horn (Figure 1.2). The mushroom body structures are important for olfactory learning and memory, while the lateral horn functions both in learned and innate olfactory response (de Belle & Heisenberg, 1994; Perisse et al., 2013; Heisenberg, 2003; Fisek & Wislon, 2014). Both of these structures are implicated in decoding the biological value or valence of odors (Strutz et al., 2014).

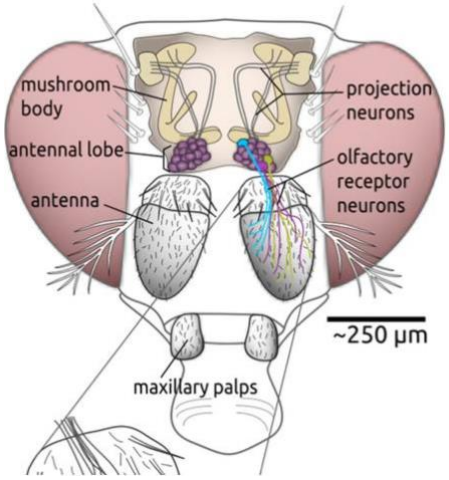

Figure 1.2. Schematic representation of olfactory organs in *Drosophila.* Adapted from (Strauch et al., 2014)

Signal transduction

M. musculus

In mice, odorant transduction begins when ligands (odorants) bind to specific olfactory receptors on the external surface of the cilia located on the dendrites of OSNs (Buck & Axel, 1991; Touhara, 2002, 2007). On sensing a ligand, the G protein-coupled seven transmembrane domain receptor (GPCR) is activated, which sets off a signaling cascade (Bakalyar & Reed, 1990; Dhallan et al., 1990; Steven J. Kleene, 2008; S. J. Kleene & Gesteland, 1991; Lowe & Gold, 1993; Nakamura & Gold, 1987; Reisert et al., 2003). In mammals, the principal pathway involves GPCR mediated activation of the G-protein, G_{olf}. The activated G protein stimulates adenylate cyclase which synthesize the second messenger cyclic adenosine monophosphate (cAMP). Increase in cAMP opens cyclic nucleotide-gated ion channels that permit cation influx, which in turn leads to depolarization of olfactory neurons. This change in neural activity is conducted passively to the axon of the receptor neuron, where action potentials are generated onto

the olfactory bulb then relayed to higher processing areas (Frings & Lindemann, 1988; Lynch & Barry, 1989; Maue & Dionne, 1987; Trotier & MacLeod, 1986) (Figure 1.3A). Conversely, neurons in the VNO show differential expression of two G-protein subunits, Gαi2 and Gαo (Jia & Halpern, 1996; Berghard & Buck, 1996). Activation of these G-proteins are the first steps of a phospholipase C-mediated signaling cascade in the VNO (Chamero et al., 2012). Furthermore, neurons in the VNO send axons to mitral cells in the glomerular region of the accessory olfactory bulb (Baum & Kelliher, 2009; Clapham & Neer, 1997). Olfactory signal transduction in the peripheral olfactory structures is then relayed to central brain regions which are responsible for further odor processing. Specifically, activity of the main olfactory bulb is relayed to the olfactory (piriform) cortex, and the entorhinal cortex, whereas activity of neurons in the accessory olfactory bulb are relayed to different central brain regions, including the amygdala and hypothalamus (Dulac et al., 2003; Bear et al., 2016). The further processing that occurs in these various regions initiates appropriate emotional, visceral, and behavioral responses to olfactory stimuli. For example, the piriform cortex serves a critical role in odor discrimination and perception, synthetic processing of complex odorant mixtures, experience- and state-dependent olfactory sensory gating, short-term odor habituation, and odor memory (Neville & Haberly, 2004; Wilson & Sullivan, 2011). Conversely, the amygdala participates primarily in innate aversive and appetitive behaviors (Root et al., 2014).

D. melanogaster

As discussed above, in fruit flies, olfactory sensory neurons rely primarily on odorant receptors (ORs) and ionotropic receptors (IRs) to convert odor stimuli into neural activity and subsequently behavior. Unlike mammalian ORs, these channels can be directly activated by chemical stimuli (Sato et. al., 2008; Wicher et al., 2008) Chemosensory signal transduction in fruit flies starts at the antenna and maxillary palp, which is covered with sensilla. The odorant enters through tiny pores in the sensillum and diffuses in and binds to an odorant binding protein (Carraher et al., 2015). Odorant binding proteins transport the odorant molecule to receptor(s) and co-receptor(s) (Orco) on the surface of olfactory receptor neurons (Larsson et al., 2004; Butterwick et al., 2018). This results in the neuron firing an action potential down the axon into the antennal lobe or the subesophogeal ganglion. The antennal lobes contain projection neurons, which are mostly excitatory, and local neurons, which are mostly inhibitory. The projection neurons send their axon to higher centers of the insect brain, such as the mushroom body and lateral horn. As discussed above, the mushroom body have been shown to regulate olfactory learning and memory, and the lateral horn regulates both innate and learned olfactory responses (de Belle & Heisenberg, 1994; Perisse et al., 2013; Heisenberg, 2003; Fisek & Wislon, 2014). In *Drosophila,* the hedonic valence of olfactory stimuli is primarily determined by the lateral horn (Strutz et al., 2014). Activity of the inhibitory projection neurons (iPNs), which exclusively target the lateral horn, encodes positive hedonic valence or intensity information and conveying these features into separate domains in the lateral horn (Strutz et al., 2014). Recent work has also found that the activity of mushroom body neurons encodes innate valence information

of an odor as well as the physiological state of the animal to drive appropriate behavioral responses to olfactory stimuli (Siju et al., 2020).

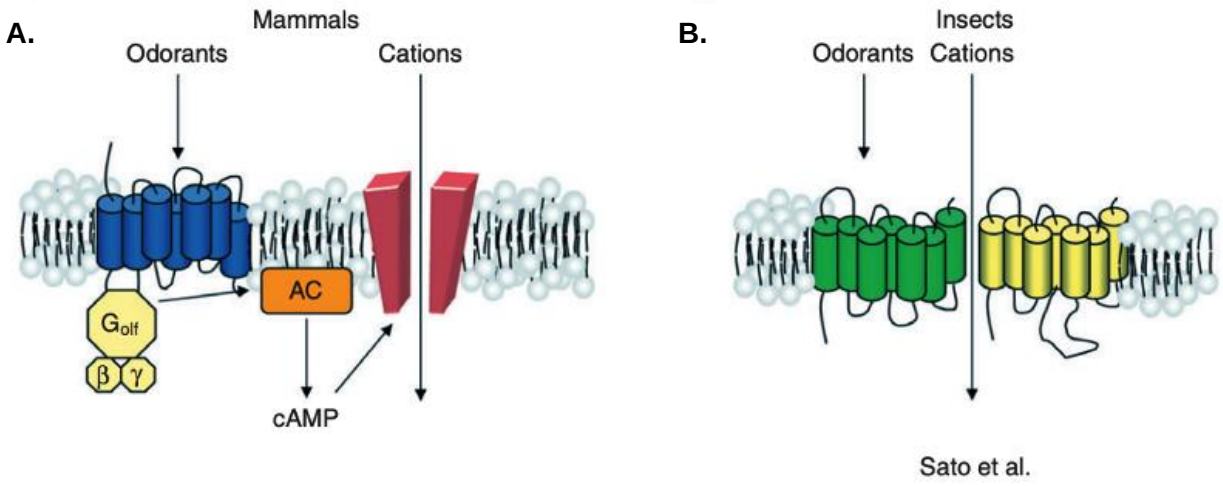

Figure 1.3. Models of signal transduction mechanisms in olfactory systems in **(A)** mammals, and **(B)** insect ORs. Adapted from (Pellegrino & Nakagawa, 2009)

1.2.2 Chemosensory plasticity

Chemosensation is critical for the survival of almost all organisms. However, since environmental stimuli can fluctuate and is highly variable, organisms have developed neuronal plasticity mechanisms which allow context- and state-dependent processing of chemosensory stimuli. To ensure survival, organisms have evolved mechanisms to modulate their olfactory responses in changing physiological conditions such as feeding state, circadian rhythm, and mating status. State-dependent chemosensory plasticity such as those in reproductive behaviors and feeding conditions occurs throughout the animal kingdom. For example, after mating, antennal neurons in insects become less sensitive to pheromones (Kromann et al., 2015). Moreover, studies

have also shown that antennal sensitivity of many inspect species can vary by the time of the day, and the sensitivity is largely determined by differential regulation of olfactory receptors (Gadenne et al., 2016; Krishnan et al., 1999; Page & Koelling, 2003).

Satiety and reproductive states can directly act on sensory neurons to modulate their activity. However, downstream olfactory circuits have also been shown to faithfully relay stimuli information to allow contextual integration of information. For example, neuromodulatory transmission in the main olfactory bulb in the mammalian olfactory system, sharpens the tuning curves of mitral cells, thereby enhancing odor discriminability (Chaudhury et al., 2010; Ma & Luo, 2012). However, there are missing gaps in our understanding of how contextual information is encoded in olfactory circuits. The nematode *C. elegans*, with its compact yet well-studied nervous system, provides a powerful model for mechanistic dissection of odor aversion and attraction behavior.

1.3 Chemosensation in *C. elegans*

For the small nematode *Caenorhabditis elegans,* most information about the environment comes through detection of chemicals, or chemosensation. In the wild, *C. elegans* live in soil, rotten fruit and plant matter and this complex environment contains both food bacteria as well as dangerous pathogens (Brenner, 1974). In order to thrive in a rich and complex chemosensory environment, these nematodes have to detect and discriminate between hundreds of olfactory cues, over a broad concentration range. In *C. elegans,* chemosensory signals also regulate different aspects of development and physiology including life span (Apfeld & Kenyon, 1999; Schafer, 2006), body size and lipid homeostasis (Fujiwara et al., 2002; Lanjuin & Sengupta, 2002) (Mak et al., 2006;

Mukhopadhyay et al., 2005) (Ashrafi et al., 2003), mating (Liu & Sternberg, 1995), and locomotory behaviors such as egg-laying, pharyngeal pumping, and food-related behavioral states (Avery & Horvitz, 1990; Nurrish et al., 1999; Waggoner et al., 1998). Chemotaxis assays in laboratories have been used to identify multiple aqueous and volatile chemicals detected by *C. elegans*, although the repertoire of their responses is likely to be much larger. Water soluble (gustatory) attractants include ions such as salts, cyclic nucleotides, amino acids, biotin, and basic pH (Dusenbery, 1974) (Ward). Volatile odorants can be detected in the nanomolar range and include structurally diverse chemicals including alcohols, ketones, esters, aldehydes, amines, organic acids, and aromatic compounds (Bargmann et al.1993). *C. elegans* also exhibit avoidance behaviors to a wide range of chemical stimuli including long-chain alcohols, detergents, heavy metals, bitter alkaloids, etc. (Bargmann et al., 1993; Hilliard et al., 2002). Finally, a family of small molecules called ascarosides act as pheromones and have been shown to mediate a number of behaviors including sex-specific attraction or repulsion, aggregation, and development into the dauer stage, which are resistant to harsh environmental conditions (Butcher et al.; Golden & Riddle, 1982 2005; 1984; Izrayelit et al., 2012; Jang et al., 2012; Macosko et al., 2009 ; Simon & Sternberg, 2002; Srinivasan et al., 2012 ; Srinivasan et al., 2008).

1.3.1 Organization of the chemosensory system of *C. elegans*

As mentioned in the earlier section, individual chemicals can be attractants or repellents, or they can regulate physiology and development of the animal. How are such diverse chemical cues discriminated from one another? Adaptability of

chemosensory signal transduction mechanisms and the neuronal circuitry drives robust yet flexible responses to such diverse cues. An adult hermaphrodite *C. elegans* has 302 neurons and ~32 of them are predicted to mediate responses to chemical stimuli (Ward et al. 1975; Ware et al.1975; White et al., 1986). Chemosensory neurons are localized at both the head and the tail, however, most research has focused on the neurons within the anterior sensilla pair, the amphids (Hilliard et al., 2002) (Figure 1.4). The amphids are a pair of organs that each contain sensory dendrites of 12 sensory neurons in the head (Ward, 1973; Ware et al., 1975; White et al., 1986). The dendrites of these neurons terminate in specialized sensory cilia, a subset of which protrudes through a pore and is exposed to the environment to allow detection of chemicals (Perkins et al.; Ward et al.; Ware et al.) (Figure 1.4).

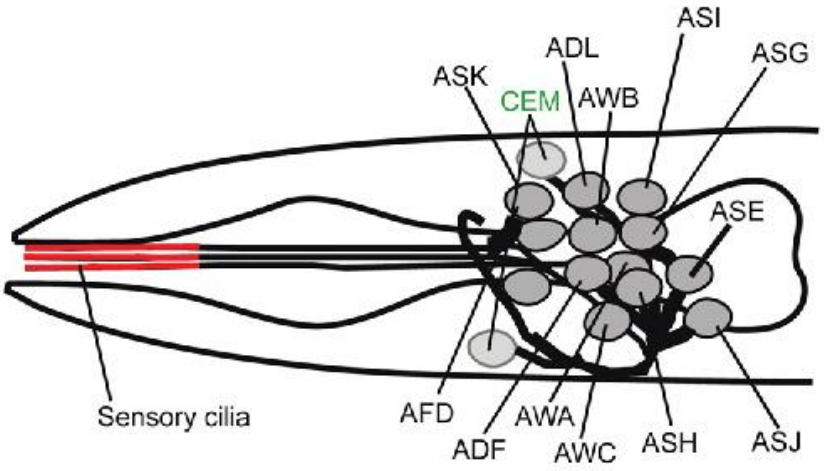

Figure 1.4. Schematic of head chemosensory neurons, including the male-specific CEM neurons, in *C. elegans.* Adapted from (Chute & Srinivasan, 2014)

Each neuron is designated with a unique name, typically consisting of three or four letters which specify the location of the neuron (amphid or phasmid) along with a description of the cilia (winged, single, etc.). Distinct subsets of these neurons generally drive attraction or avoidance. In general, the ASE neurons detect soluble attractants, whereas the AWC and AWA neurons detect volatile attractants (Bargmann et al., 1993). The ASH, ADL, and AWB neurons have been shown to detect volatile repellants (Chao et al., 2004; Troemel et al., 1997). Unlike the others in this group, the ASH and ADL neurons can sense both soluble and volatile repellents; the neurons detect high osmolarity, heavy metals such as $Cd^{2+}$and Cu^{2+} (Sambongi et al., 1999), 1-octanol (Troemel et al., 1995), SDS, etc. ASH neurons can also respond to mechanosensory stimuli, thus serving as a polymodal nociceptive neuron (Kaplan & Horvitz, 1993). ADL, along with ASK and ASI, has also been shown to play a role in the detection of pheromones (de Bono & Maricq, 2005; Jang et al., 2012; Kim et al., 2009; McGrath et al., 2011; Park et al.; Sambongi et al.). Other amphid neurons play minor roles in promoting attraction and avoidance of chemicals. (Bargmann and Horvitz 1991; Sambongi et al. 1999; Hilliard et al. 2002). Table 1.1 summarizes chemical responses driven by individual chemical neurons.

Table 1.1: Chemical responses mediated by individual chemosensory neurons in *C. elegans*
Adapted from (Ferkey et al., 2021) Table 1

Chemical stimulus	Neuron(s)	Soluble (S) or Volatile (V)
Attractants		
Cyclic nucleotides cAMP cGMP	ASE (ADF, ASG, ASI)	S

Chemical stimulus	Neuron(s)	Soluble (S) or Volatile (V)
Cations Na^+ K^+	ASEL (ADF, ASG, ASI) ASER (ASEL)	S
Anions Cl^-	ASER (ADF, ASG, ASI)	S
Basic pH	ASEL	S
Amino acids Lysine Histidine Cysteine Methionine	ASE (ASG, ASI, ASK)	S
Biotin	ASE (ADF, ASG, ASI)	S
Pyrazine	AWA	V
Diacetyl (low)	AWA	V
Diacetyl (intermediate)	AWA, AWC	V
2,4,5-Trimethylthiazole (low)	AWA, AWC	V
Butyric acid	AWA (AWC ?)	V
Isobutyric acid	AWA (AWC ?)	V
Benzyl proprionate	AWA, AWC	V
Benzaldehyde (low)	AWC (AWA)	V
Isoamyl alcohol (low)	AWC (AWA)	V
2-Butanone	AWC^{ON}	V
Acetone	AWC^{ON}	V
Dimethylthiazole	AWC	V
1-Methylpyrrole	AWC	V

Chemical stimulus	Neuron(s)	Soluble (S) or Volatile (V)
1-Pentanol	AWC	V
2-Cyclohexylethanol	AWC	V
2-Ethoxythiazole	AWC	V
2-Isobutylthiazole	AWC (AWA ?)	V
2-Methylpyrazine	AWC (AWA ?)	V
4-Chlorobenzyl mercaptan	AWC (AWA ?)	V
Benzyl mercaptan	AWC (AWA ?)	V
2-Heptanone	AWC^{ON}	V
2,3-Pentanedione (low)	AWC^{OFF}	V
2,3-Pentanedione (intermediate)	AWA, AWC	V
Acidic pH	ASH, ADF, ASK, ASE	S
Basic pH (>10.5)	ASH	S
Copper	ASH, ADL, ASE	S
Cadmium	ASH, ADL, ASE	S
SDS	ASH (ASK, ASI, ASJ) PHA, PHB (antagonistic)	S
Bitters quinine	ASH (ASK)	S
Diacetyl (high)	ASH	V
2,4,5-Trimethylthiazole (high)		V
Benzaldehyde (high)	ASH (AWB)	V

Chemical stimulus	Neuron(s)	Soluble (S) or Volatile (V)
Isoamyl alcohol (high)	ASH (ADL, AWB)	V
Alcohols 1-Octanol (100%) 1-Octanol (30%)	ASH (ADL, AWB—off food) ASH	V
Ketones 2-Nonanone	AWB (ASH)	V
Serrawettin W2	AWB	S
Phenazine-1-carboxamide	ASJ	S
Pyochelin	ASJ	S
Dodecanoic acid	ASH (ADL?, ADF ?) PHA PHB	S

The chemosensory neurons converge onto a small subset of interneurons, which play a major role in signal processing and integration, and ultimately drive behavioral outputs. The majority of the amphid olfactory neurons synapse onto at least one member of the first-layer interneurons- AIA, AIB, AIY, and AIZ (Ward et al.; Ware et al., 1975; White et al.) (Figure 1.5).Chemosensory neurons which mediate responses to toxic chemicals display distinct connectivity patterns to downstream interneurons from those sensing attractive chemicals. For example, the neurons which mediate responses to attractive chemicals primarily synapse onto first layer interneurons, whereas ASH, ADL and AWB nociceptive neurons, have also been shown to synapse directly into command interneurons and motor neurons which generate backward movements (White et al.). Differential recruitment of downstream neurons allows for more fine tuning

of behavioral responses and ultimately dictates if the animal moves forward or backward in response to chemical stimuli (Gray et al.; Tsalik & Hobert).

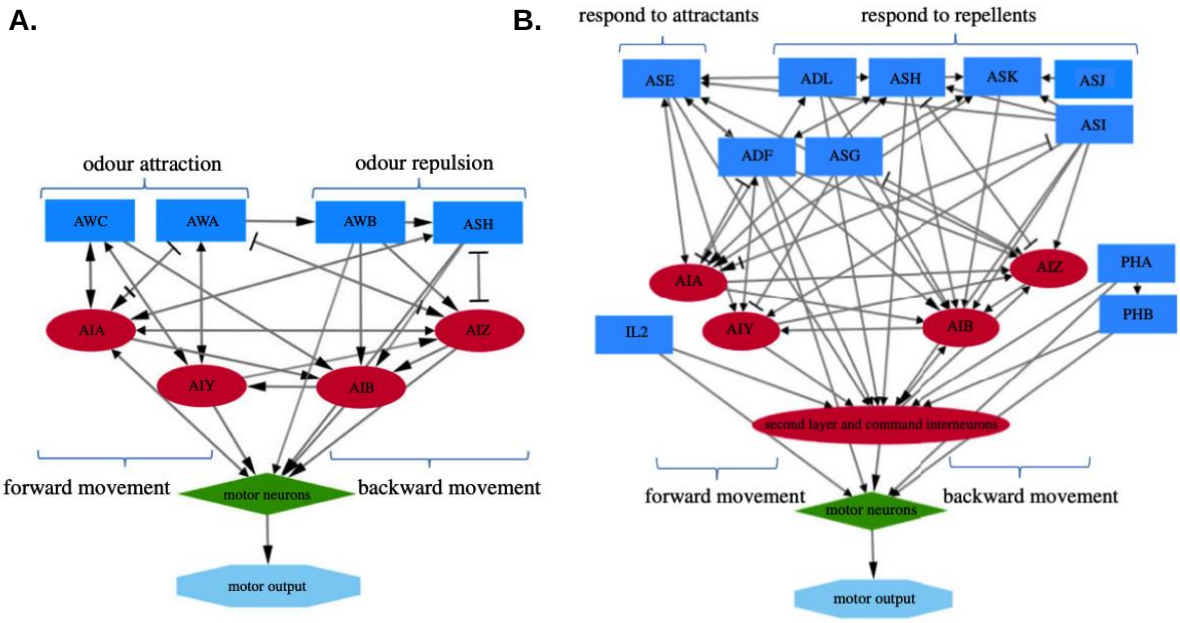

Figure 1.5. *C. elegans* neural circuits driving behavior towards (A) volatile odorants and (B) soluble chemicals (Metaxakis et al., 2018)

1.3.2 Signal transduction in chemosensory neurons in *C. elegans*

GPCRs

As described above, *C. elegans* uses distinct subsets of sensory neurons driving attraction and repulsion to chemical stimuli. Segregated detection of chemosensory stimuli can contribute to odorant specificity. However, this factor alone cannot contribute to all the odorant specificity since *C. elegans* has a limited repertoire of chemosensory neurons but can respond to a large number of chemosensory stimuli. This suggests that additional intracellular mechanisms exist to establish odorant specificity. As in other organisms, many chemicals are sensed by the seven transmembrane G protein-

coupled receptors in *C. elegans.* Thousands of chemosensory candidate receptors have been identified through genomic analysis and expression analysis using promoter GFP fusion reporters (Fredriksson & Schioth, 2005; Thomas & Robertson, 2008)(Troemel et al., 1995). Unlike mammalian and insect olfactory neurons which typically express a single type of odorant receptor (Buck and Axel, 1991), *C. elegans* expresses multiple types of odorant receptors in a single chemosensory neuron (N. Chen et al., 2005; Colosimo et al., 2004; McCarroll et al., 2005; Troemel et al., 1995). To date, only six chemosensory receptors have been paired with a ligand, partly due to the large number size of the *C. elegans* chemoreceptor gene family.

G-proteins

Perhaps the most remarkable aspect of the relatively small chemosensory system of *C. elegans* is their ability to discriminate among attractive chemicals. Single chemosensory neurons are not only able to respond to multiple odorants, but in the presence of a background chemical, they continue responding to other chemicals sensed by the neuron and can chemotax up a gradient of the second attractive chemical (Bargmann et al., 1993.; Ward, 1973). The ability of worms to discriminate between cues detected by the same neuron suggests that downstream signaling cascades can diverge. When ligands bind to GPCRs, it causes a conformational change and engages downstream heterotrimeric G proteins, which then transduce the signals from olfactory receptors to different intracellular pathways (McCudden et al., 2005; Weis, 2018). The *C. elegans* genome encodes 21 Gα, 2 Gβ, and 2 Gγ subunits (Janset et al., 1999; (Cuppen et al., 2003; Roayaie et al., 1998; Zwaal et al.,1997). Four Gα

subunits encoded by the worm genome share high homology to mammalian G_s, $G_{i/o}$, G_q, $G_{12/13}$ α subunits, respectively. Additional alpha subunits include fourteen G_i-like *gpa* genes that are expressed in subsets of chemosensory neurons (Jansen et al., 1999). A single sensory neuron can express multiple *gpa* genes. Several of the *C. elegans* Gα subunits have been shown to either positively or negatively regulate chemosensation (Lans et al., 2004). For example, *odr-3* encodes a Gα subunit important for odorant detection in several chemosensory neurons (L'Etoile et al., 2002; Lans et al., 2004). The weak olfactory responses that persist in *odr-3* mutants are eliminated in *odr-3 gpa-3* double mutants, suggesting that *gpa-3* has a positive chemosensory function. *gpa-5* mutants have no defect on their own, but they suppress defects of *odr-3* mutants to chemotax to the attractive odorant diacetyl, suggesting that *gpa-5* is a negative regulator of chemosensation (Jansen et al., 1999; Lans et al., 2004).

C. elegans has two Gβ (GPB-1 and GPB-2) and two Gγ (GPC-1 and GPC-2) subunits (Jansen et al.). GPC-1 is expressed in some sensory neurons whereas GPB-2 and GPC-2 are widely expressed (Zwaal et al., 1997). Knockdown of GPB-1 in ASH results in defects in quinine and high osmolarity avoidance (Esposito et al., 2007). While GPB-2 and GPC-1 are not directly required for chemosensation, they play an important role in chemosensory adaptation. For example, GPB-2 contributes to olfactory adaptation of the attractant benzalydehyde (Matsuki et al., 2006; O'Halloran et al., 2009), and GPC-1 is required for adaptation to salts (Jansen et al., 2002).

Receptor guanylyl cyclases (rGCs)

rGCs produce cGMP, the second messenger that regulates signal transduction in a subset of chemosensory neurons. CNG channels (discussed below) are gated by intracellular cGMP levels, thus synthesis and breakdown of cGMP is a key regulator of chemosensory neuron activity. rGCs can act downstream of GPCRs via activation of G-proteins and/or ligands can directly bind to the extracellular domains of rGCS and activate them. An example of G-protein activated rGCs are the ODR-1 and DAF-11 rGCs. Both ODR-1 and DAF-11 are required for AWC-mediated chemotaxis to benzaldehyde, isoamyl alcohol, and butanone and for AWB-mediated repulsion from 2-nonanone (Birnby et al. 2000; L'Etoile and Bargmann 2000; Ferkey et al., 2021). GCY-14 and GCY-22 are important rGCs that regulate responses to salt and salt ions. GCY-22 act in ASER, the sensory neuron that promotes chemotaxis to the salt concentration last associated with food (Smith et al. 2013; Kunitomo et al. 2013; Luo et al. 2014). GCY-14 is localized to the ASEL cilia and is required both for chemotaxis to Na^+ and Li^+ ions and for the response of ASEL to high pH (Ortiz et al. 2006). It has been shown that GCY-14 can be directly activated by increases in pH (Murayama et al., 2013; Ferkey et al, 2021). rGCs have also been implicated in olfactory adaptation. GCY-28 is expressed in the axons of AWC neurons where it drives butanone exposure-induced behavioral preference switch after prolonged starvation (Tsunozaki et al., 2008).

Ion channels

CNG channels

Signal transduction in a subset of chemosensory neurons is dependent on cyclic nucleotide-gated (CNG) channels, encoded by the *tax-2* and *tax-4* genes (Chao et al., 2004; Coburn & Bargmann, 1996). TAX-2 and TAX-4 proteins are localized to the cilia of a subset of neurons including AWC and AWB neurons, and mutants for these genes are unable to chemotax to odorants sensed by those neurons (Birnby et al., 2000; Coburn & Bargmann, 1996; Komatsu et al., 1996; L'Etoile & Bargmann, 2000; Vowels & Thomas, 1994) (Figure 1.5A). TAX-2/4 channels are gated by the cyclic guanosine monophosphate (cGMP) second messenger. In general, activation of receptor guanylyl cyclases (rGCs) by G proteins can set off a cGMP cascade (Figure 1.6A). rGCs synthesize cGMP, thus odorant binding and downstream signaling increases intracellular cGMP levels and opens the CNG channels resulting in neural activity due to ion influx (Figure 1.6A). One exception to this mechanism is the AWC neurons in which odorant binding to the receptor has shown to hyperpolarize the neuron, likely due to a decrease in the intracellular cGMP levels (Chalasani et al., 2007; "Correction for Zaslaver et al., Hierarchical sparse coding in the sensory system of Caenorhabditis elegans," 2015). Phosphodiesterases (PDEs) hydrolyze cGMP and thus can be crucial regulators of activity in chemosensory neurons. However, no *C. elegans* PDE has been shown to play a direct role in regulating chemosensory signaling, although some are involved in driving adaptation to odorants (O'Halloran et al., 2009).

TRPV channels

Sensory signal transduction in another set of chemosensory neurons is dependent on transient receptor potential vanilloid (TRPV) channels, encoded by the *osm-9* and *ocr-2* genes (Colbert & Bargmann, 1997; Tobin et al., 2002). Results from gene expression and translational reporter analyses have shown that these proteins are localized to the cilia of a subset of chemosensory neurons, including, ASH, ADL, and AWA neurons (Colbert & Bargmann, 1997; Tobin et al., 2002). OSM-9/OCR-2 signaling depends on polyunsaturated fatty acids (PUFAs), although the specific enzymes that act downstream of G-proteins are yet to be identified (Kahn-Kirby et al., 2004) (Figure 1.6B).

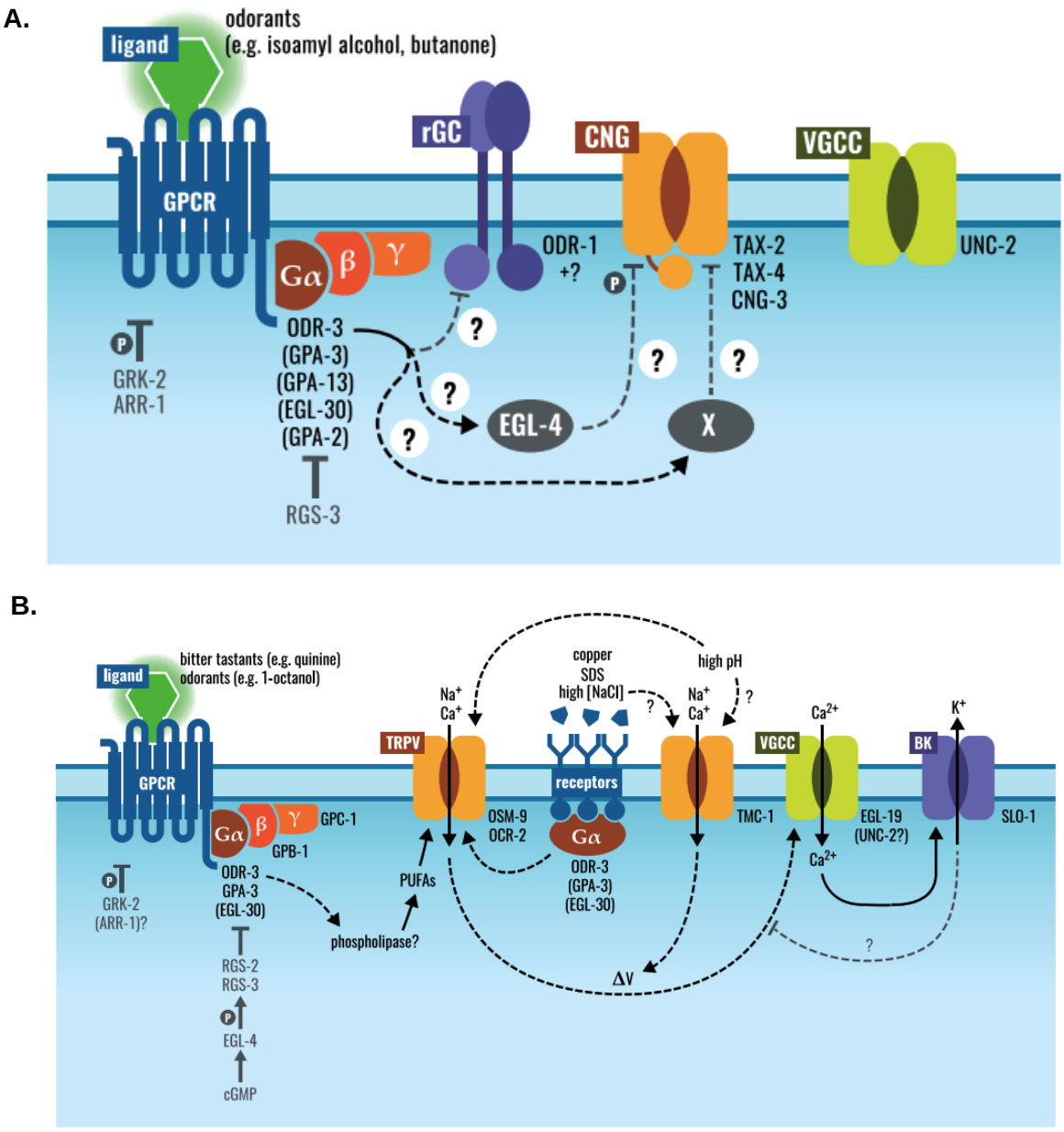

Figure 1.6. Chemosensory signal transduction pathways in *C. elegans.* **(A)** CNG channel mediated signaling in AWC and **(B)** TRPV channel mediated signaling in ASH (Ferkey et al., 2021) (Figure 4)

In chemosensory signaling cascades in *C. elegans,* activation of ion channels is a key last step to convert sensory stimuli into electrical activity in chemosensory neurons (Zagotta & Siegelbaum, 1996). The majority of chemosensory neurons exhibit

one of the following neuronal responses to chemosensory stimuli: (1) increase in cytoplasmic calcium in response to chemosensory stimuli, presumably due to depolarization, (2) decrease in cytoplasmic calcium in response to chemicals, presumably due to hyperpolarization, along with increases in calcium upon decrease in chemical cue concentrations, and increase in cytoplasmic calcium in response to both presentation and removal of chemical (biphasic) (Ferkey et al., 2021). Differential activity patterns in chemosensory neurons can contribute to flexibility and fine tuning of behavioral responses.

1.3.3 Chemotaxis navigation strategies in *C. elegans*

In a complex chemosensory environment, most chemical cues are perceived as gradients, where concentration and strength of the stimuli is directly correlated to proximity to the stimuli. How does *C. elegans* navigate up/down odor gradients? Detailed behavioral analysis and motion-tracking studies have shown that *C. elegans primarily* navigates gradients using a biased random walk strategy, or klinokinesis although additional mechanisms are also employed (Gray et al., 2005; Pierce-Shimomura et al., 1999; Ryu & Samuel; Yoshida et al.; Zariwala et al., 2003)(Figure 1.7A). This strategy of chemotaxis involves regulating frequency of sharp turns, also known as pirouettes, in response to changes in stimulus concentration. When moving towards an attractive chemical, worms decrease their turning frequency and increase forward runs, whereas the oppositive strategy is employed when navigating away from a repulsive stimulus (Pierce-Shimomura et al., 1999).

Previous work has also shown that worms can bias their turning direction and steer to the preferred direction, a strategy known as weathervaning or klinotaxis (Iino & Yoshida, 2009; Ward, 1973)(Figure 1.7B). Klinotaxis involves gradual turns up a gradient and toward the line of steepest ascent (Iino & Yoshida, 2009). In this behavior, worms regulate the curving rate bias by detecting the odor gradient, gradually curving towards the higher concentration (Iino & Yoshida, 2009; Yoshida et al., 2012). (Figure 1.7B) It has been shown that *C. elegans* can use both strategies towards the same chemical stimuli, at different time points. For example, worms exhibit a concentration-dependent response to the volatile odorant isoamyl alcohol (IAA). Lower concentrations of IAA are attractive while high concentrations of the chemical are repulsive (Yoshida et al., 2012). It has been shown that in response to dilute IAA, worms used klinokinesis to drive attraction, and they changed their behavioral strategy to positive klinotaxis at later time points of the assay (Yoshida et al., 2012). However, avoidance of high concentration IAA was driven by both klinotaxis and klinokinesis at early time points, followed by a complete switch to klinokinetic-driven behavior at later time points of the assay (Yoshida et al., 2012).

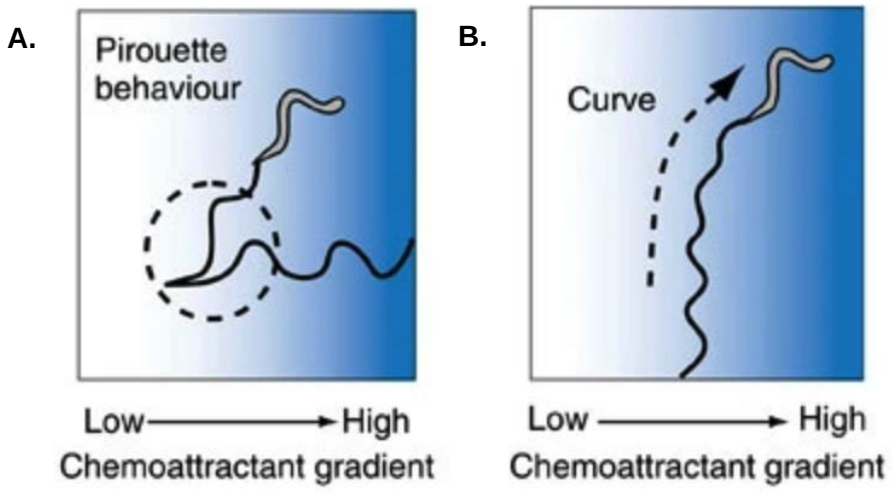

Figure 1.7. Schematic representation of different chemotactic navigation strategies in *C. elegans.* **(A)** klinokinesis, **(B)** klinotaxis (Yoshida et al., 2012) (Figure 3)

Changes in locomotory patterns are controlled by sensory input via chemosensory neurons (Gray et al., 2005; Wakabayashi et al., 2004). However, it has been shown that manipulating the activity of first order interneurons can drive specific chemotactic behavior, suggesting that navigational strategy may be determined at the interneuron level (Kocabas et al., 2012). For example, AWC chemosensory neurons are known to drive attraction to volatile odorants, and ASH chemosensory neurons drive repulsion to nociceptive chemosensory stimuli. ASH and AWC have inhibitory connections onto the AIA interneurons, while both neurons activate the AIB interneuron (Figure 1.5). The two interneurons play opposing roles in regulating motor movements, with AIA suppressing and AIB promoting turns, respectively (Gray et al., 2005; Iino & Yoshida, 2009; Luo et al., 2014; Piggott et al., 2011). These interneurons have been studied in the context of several olfactory circuits, and their activities have been shown to drive distinct navigation strategies and behavioral outputs (Gray et al., 2005; Iino & Yoshida, 2009; Larsch et al., 2015; Tsalik & Hobert, 2003).

1.3.4 Examples of chemosensory plasticity in *C. elegans*

Chemosensory responses in *C. elegans* are modulated by internal and external context, past experience, memory, sex, and life stage (Leinwand et al., 2015) (Gruner et al., 2014; Hart & Chao, 2010; Ryan et al., 2014). Behavioral plasticity can result from changes in sensory neurons and intracellular pathways, but it can also be driven by plasticity at the circuit level. Examples of plasticity in both levels have been shown in *C. elegans.* Here, I will summarize a few examples of sensory and circuit level plasticity described in *C. elegans*.

Examples of plasticity in sensory neurons

Modulation of chemoreceptor expression levels in a single chemosensory neuron have been shown to contribute to behavioral flexibility (Ryan et al., 2014) (Gruner et al., 2014). For example, feeding status, developmental stage, and sex can alter the expression of ODR-10, a receptor in the AWA sensory neurons that responds to the attractant diacetyl, a food associated odor (Ryan et al., 2014). In males, expression of ODR-10 is low, allowing them to prioritize finding mates (Ryan et al., 2014). Overexpression of *odr-10* has been shown to increase food attraction in males and decrease off-food exploration. By contrast, *odr-10* loss diminished food exploration behaviors in both sexes (Ryan et al. 2014). *C. elegans* larvae from both sexes have equal *odr-10* expression, and thereby both sexes prioritize feeding over exploration and exhibit equal food attraction (Ryan et al., 2014). Furthermore, expression of srh-234 receptors in the ADL neuron is also regulated by integration of sensory and internal feeding state signals from both sensory signaling and circuit mediated feedback (Gruner

et al., 2014). Regulation of multiple factors including, insulin signaling, neuropeptides, and channels allow for differential expression of the chemoreceptor gene, allowing animals to precisely respond to changes in internal and external conditions (Gruner et al., 2014). These examples illustrate how modulation of chemoreceptor gene expression in a single neuron can drive context-dependent behavioral plasticity.

Internal nutritional state of starvation and satiety can also modulate chemosensory responses at the sensory neuron level. For example, in salt chemotaxis learning, exposure to NaCl in the absence of food causes worms to avoid normally attractive concentrations of NaCl (Saeki et al., 2001; Tomioka et al., 2006). The pair of ASE neurons are the major NaCl-sensing neurons in *C. elegans* (Bargmann & Horvitz, 1991; Hukema et al., 2008). ASE left (ASEL) and ASE right (ASER) are the left and right neurons in the ASE neuron pair, respectively and they have been shown to be functionally distinct in driving context-dependent response to salt. Specifically, it has been shown that following prolonged exposure to NaCl, the changes in calcium responses of ASER and ASEL were asymmetric: the response of ASER increased whereas that of ASEL decreased after NaCl conditioning (Oda et al., 2011). A more recent study has shown that the ASG neuron plays a pivotal role in driving salt chemotaxis upon starvation (Jang et al., 2019). Although the neuron does not directly respond to changes in salt concentrations, it showed increased starvation-induced activity which resulted in bias of turning behaviors to efficiently navigate worms toward food sources (Jang et al., 2019).

Examples of circuit level plasticity

Circuit level plasticity driving changes in behavior have been studied in the context of pathogen avoidance. Microbes are abundant in the natural environment of *C. elegans.* Depending on the bacterial strain, bacteria can either serve as a food source for these nematodes or pathogenic bacteria may cause infection in the nematode host. Innate recognition of bacterial metabolites can produce immediate behavioral responses. However, ingestion of nutritive or pathogenic bacteria can modulate internal states that underlie long-lasting behavioral changes. For example, *C. elegans* displays associative olfactory conditioning upon exposure to the pathogenic bacterium *Pseudomonas aeruginosa* strain PA14. Infection following the ingestion of *P. aeruginosa* PA14, which is not only a nutritive food source for *C. elegans* causes an aversive learned response that is distinct from the effect of feeding on nutritive non-pathogenic bacteria. Worms that have never ingested the pathogenic bacterium, show either mild attraction or does not avoid odors associated with the pathogenic bacteria (Ha et al., 2010; Harris et al.; Zhang et al., 2005). The initial innate preference of *C. elegans* for PA14 over *E. coli* OP50 was found to be reversed after feeding on PA14, with a subsequent preference for *E. coli* OP50 and aversion to PA14 (Ha et al., 2010; Harris et al.; Zhang et al., 2005). Several studies have localized the site of learning within sensorimotor circuits that underlies the learned change in bacterial preference. For example, it has been shown that exposure to PA14 increases serotonin in the ADF chemosensory neurons which acts via serotonin receptors in downstream interneurons to promote aversive learning (Zhang et al., 2005). Specifically, a subset of interneurons, such as AIY, AIZ, and AIB neurons, are required for navigation towards food sources in

naive animals, but not required for learned behavior. In contrast, SMD and RIM neurons are not required for naive food choice but are required for the learned change in food preference after PA14 exposure (Jin et al., 2016; Zhang et al., 2005). This modulation requires serotonergic signaling from ADF and learning dependent expression change in insulin-like peptides (Chen et al., 2013; Ha et al., 2010; Zhang et al., 2005).

Sensory responses can also be acutely regulated by the presence of absence of food. For example, in the presence of food, *C. elegans* are repelled by the long-chain volatile alcohol octanol, however in the absence of food, they display diminished repulsion to octanol (Chao et al., 2004). This acute modulation of chemosensory responses is also driven by serotonin (5-HT) signaling, which acts on sensory neurons as well as interneurons. Genetic evidence suggests that the presence of food increases overall levels of the modulatory neurotransmitter serotonin (Avery & Horvitz; Colbert & Bargmann) (Sze et al.). MOD-1 and SER-1 receptors function in the AIB or AIY and the RIA interneurons, respectively, to modulate ASH-mediated aversive responses to dilute octanol and thereby gate the sensitivity of the circuit (Chao et al., 2004; Harris et al., 2014)(Harris et al., 2009)(Zahratka et al., 2015). The above examples highlight that plasticity mechanisms can operate at multiple levels in the neuronal circuitry, generating flexible context- and experience-dependent behaviors. Both intracellular and intercellular plasticity mechanisms can contribute to fine-tuning of behavioral responses and allow the relatively compact nervous system of *C. elegans* to meet the computational demands as more complex nervous systems.

1.4 Rationale for dissertation research

It is clear from the examples shared in this chapter that chemosensation is a major regulator of many biological processes across taxa. Furthermore, it is also evident that chemosensory plasticity can take place at different levels of the circuit and can also be driven by innate preferences, learned associations, as well as context. At any given moment, organisms across all types of niches have a very complex chemical environment around them. Many prey organisms are able to detect the presence of predators even against a background of high chemical diversity. How do chemosensory systems discriminate and assign value to a stimulus to drive appropriate behavioral responses in fluctuating environments? What is the role of plasticity in chemosensory neuron responses themselves to olfactory behavioral plasticity? In the following chapters, I explore the mechanisms driving context- and concentration dependent plasticity to medium-chain alcohols in *C. elegans*. In Chapter 2, I examined the neuronal and molecular pathways necessary for the behavioral preference to the alcohol 1-hexanol, and how neuronal signaling is altered in a context-dependent manner to drive attraction and avoidance. In Chapter 3, I explored how functional reorganization of a neural circuit can drive concentration-dependent behavioral preference to 1-hexanol.

Deficits in processing sensory inputs, and in the ability to correctly alter behavior based on experience underlie many neurological syndromes such as schizophrenia and autism spectrum disorders. Likewise, deficits in olfactory function and plasticity are also perturbed in wide variety of diseases including Alzheimer's, Huntington's, and Parkinson's disease (Lazic et al., 2007; Mesholam et al., 1998; Wesson et al., 2010). A

complete description of the etiology of these and other disorders requires an understanding of how healthy neurons can sense and integrate sensory information.

The experimental amenability, as a result of availability of powerful genetic and molecular tools and robust behavioral assays, make *C. elegans* an ideal experimental system in which to characterize mechanisms of behavioral plasticity. Furthermore, *C. elegans* homologs have been identified for 60–80% of human genes (Kaletta & Hengartner, 2006), and 12 out of 17 known signal transduction pathways are conserved in *C. elegans* and human (NRC, 2000). Although the structure of the olfactory system and peripheral chemosensory mechanisms are divergent between mammals and *C. elegans*, regulatory mechanisms have been reported to be more conserved (Consortium, 1998; Kuwabara & O'Neil, 2001; Lai et al., 2000; Luedtke et al., 2010). Since molecular and neuronal mechanisms in *C. elegans* are highly conserved, studying chemosensory plasticity mechanisms in *C. elegans* will result in a more comprehensive understanding of the pathways by which neurons respond to signals and adjust their responses based on the animal's experience and context. Furthermore, findings in this dissertation may also provide insights into how similar computations can encode context-dependent processing of stimulus in diverse nervous systems and across sensory modalities.

References

Apfeld, J., et al. (1999). Regulation of lifespan by sensory perception in Caenorhabditis elegans. *Nature, 402*(6763), 804-809. doi:10.1038/45544

Ashrafi, K., et al. (2003). Genome-wide RNAi analysis of Caenorhabditis elegans fat regulatory genes. *Nature, 421*(6920), 268-272. doi:10.1038/nature01279

Avery, L., et al. (1990). Effects of starvation and neuroactive drugs on feeding in Caenorhabditis elegans. *J Exp Zool, 253*(3), 263-270. doi:10.1002/jez.1402530305

Ayer, R. K., Jr., et al. (1992). Olfactory physiology in the Drosophila antenna and maxillary palp: acj6 distinguishes two classes of odorant pathways. *J Neurobiol, 23*(8), 965-982. doi:10.1002/neu.480230804

Bakalyar, H. A., et al. (1990). Identification of a specialized adenylyl cyclase that may mediate odorant detection. *Science, 250*(4986), 1403-1406. doi:10.1126/science.2255909

Bakin, J. S., et al. (1990). Classical conditioning induces CS-specific receptive field plasticity in the auditory cortex of the guinea pig. *Brain Res, 536*(1-2), 271-286. doi:10.1016/0006-8993(90)90035-a

Bargmann, C. I., et al. (1993). Odorant-selective genes and neurons mediate olfaction in C. elegans. *Cell, 74*(3), 515-527. doi:10.1016/0092-8674(93)80053-h

Bargmann, C. I., et al. (1991). Chemosensory neurons with overlapping functions direct chemotaxis to multiple chemicals in C. elegans. *Neuron, 7*(5), 729-742. doi:10.1016/0896-6273(91)90276-6

Birnby, D. A., et al. (2000). A transmembrane guanylyl cyclase (DAF-11) and Hsp90 (DAF-21) regulate a common set of chemosensory behaviors in caenorhabditis elegans. *Genetics, 155*(1), 85-104. doi:10.1093/genetics/155.1.85

Blundell, J., et al. (2010). Appetite control: methodological aspects of the evaluation of foods. *Obes Rev, 11*(3), 251-270. doi:10.1111/j.1467-789X.2010.00714.x

Brenner, S. (1974). The genetics of Caenorhabditis elegans. *Genetics, 77*(1), 71-94. doi:10.1093/genetics/77.1.71

Buck, L., et al. (1991). A novel multigene family may encode odorant receptors: a molecular basis for odor recognition. *Cell, 65*(1), 175-187. doi:10.1016/0092-8674(91)90418-x

Butcher, R. A., et al. (2007). Small-molecule pheromones that control dauer development in Caenorhabditis elegans. *Nat Chem Biol, 3*(7), 420-422. doi:10.1038/nchembio.2007.3

Chalasani, S. H., et al. (2007). Dissecting a circuit for olfactory behaviour in Caenorhabditis elegans. *Nature, 450*(7166), 63-70. doi:10.1038/nature06292

Chao, M. Y., et al. (2004). Feeding status and serotonin rapidly and reversibly modulate a Caenorhabditis elegans chemosensory circuit. *Proc Natl Acad Sci U S A, 101*(43), 15512-15517. doi:10.1073/pnas.0403369101

Chaudhury, D., et al. (2010). Olfactory bulb habituation to odor stimuli. *Behav Neurosci, 124*(4), 490-499. doi:10.1037/a0020293

Chen, N., et al. (2005). Identification of a nematode chemosensory gene family. *Proc Natl Acad Sci U S A, 102*(1), 146-151. doi:10.1073/pnas.0408307102

Chen, Z., et al. (2013). Two insulin-like peptides antagonistically regulate aversive olfactory learning in C. elegans. *Neuron, 77*(3), 572-585. doi:10.1016/j.neuron.2012.11.025
Clancy, A. N., et al. (1984). Sexual behavior and aggression in male mice: involvement of the vomeronasal system. *J Neurosci, 4*(9), 2222-2229. Retrieved from https://www.ncbi.nlm.nih.gov/pubmed/6541245
Clyne, P. J., et al. (1999). A novel family of divergent seven-transmembrane proteins: candidate odorant receptors in Drosophila. *Neuron, 22*(2), 327-338. doi:10.1016/s0896-6273(00)81093-4
Coburn, C. M., et al. (1996). A putative cyclic nucleotide-gated channel is required for sensory development and function in C. elegans. *Neuron, 17*(4), 695-706. doi:10.1016/s0896-6273(00)80201-9
Colbert, H. A., et al. (1997). Environmental signals modulate olfactory acuity, discrimination, and memory in Caenorhabditis elegans. *Learn Mem, 4*(2), 179-191. doi:10.1101/lm.4.2.179
Colosimo, M. E., et al. (2004). Identification of thermosensory and olfactory neuron-specific genes via expression profiling of single neuron types. *Curr Biol, 14*(24), 2245-2251. doi:10.1016/j.cub.2004.12.030
Consortium, C. e. S. (1998). Genome sequence of the nematode C. elegans: a platform for investigating biology. *Science, 282*(5396), 2012-2018. doi:10.1126/science.282.5396.2012
Correction for Zaslaver et al., Hierarchical sparse coding in the sensory system of Caenorhabditis elegans. (2015). *Proc Natl Acad Sci U S A, 112*(13), E1688-1689. doi:10.1073/pnas.1504344112
de Bono, M., et al. (2005). Neuronal substrates of complex behaviors in C. elegans. *Annu Rev Neurosci, 28*, 451-501. doi:10.1146/annurev.neuro.27.070203.144259
de Bruyne, M., et al. (1999). Odor coding in a model olfactory organ: the Drosophila maxillary palp. *J Neurosci, 19*(11), 4520-4532. Retrieved from https://www.ncbi.nlm.nih.gov/pubmed/10341252
DeMaria, S., et al. (2010). The cell biology of smell. *J Cell Biol, 191*(3), 443-452. doi:10.1083/jcb.201008163
Dhallan, R. S., et al. (1990). Primary structure and functional expression of a cyclic nucleotide-activated channel from olfactory neurons. *Nature, 347*(6289), 184-187. doi:10.1038/347184a0
Diamond, D. M., et al. (1984). Physiological plasticity of single neurons in auditory cortex of the cat during acquisition of the pupillary conditioned response: II. Secondary field (AII). *Behav Neurosci, 98*(2), 189-210. Retrieved from https://www.ncbi.nlm.nih.gov/pubmed/6721922
Dunn, F. A., et al. (2007). Light adaptation in cone vision involves switching between receptor and post-receptor sites. *Nature, 449*(7162), 603-606. doi:10.1038/nature06150
Dusenbery, D. B. (1974). Analysis of chemotaxis in the nematode Caenorhabditis elegans by countercurrent separation. *J Exp Zool, 188*(1), 41-47. doi:10.1002/jez.1401880105
Dweck, H. K., et al. (2016). Olfactory channels associated with the Drosophila maxillary palp mediate short- and long-range attraction. *Elife, 5*. doi:10.7554/eLife.14925

Esposito, G., et al. (2007). Efficient and cell specific knock-down of gene function in targeted C. elegans neurons. *Gene, 395*(1-2), 170-176. doi:10.1016/j.gene.2007.03.002
Fain, G. L., et al. (1990). Calcium and the mechanism of light adaptation in vertebrate photoreceptors. *Trends Neurosci, 13*(9), 378-384. doi:10.1016/0166-2236(90)90023-4
Fain, G. L., et al. (2001). Adaptation in vertebrate photoreceptors. *Physiol Rev, 81*(1), 117-151. doi:10.1152/physrev.2001.81.1.117
Ferkey, D. M., et al. (2021). Chemosensory signal transduction in Caenorhabditis elegans. *Genetics, 217*(3). doi:10.1093/genetics/iyab004
Fishilevich, E., et al. (2005). Genetic and functional subdivision of the Drosophila antennal lobe. *Curr Biol, 15*(17), 1548-1553. doi:10.1016/j.cub.2005.07.066
Fredriksson, R., et al. (2005). The repertoire of G-protein-coupled receptors in fully sequenced genomes. *Mol Pharmacol, 67*(5), 1414-1425. doi:10.1124/mol.104.009001
Frings, S., et al. (1988). Odorant response of isolated olfactory receptor cells is blocked by amiloride. *J Membr Biol, 105*(3), 233-243. doi:10.1007/BF01871000
Fujiwara, M., et al. (2002). Regulation of body size and behavioral state of C. elegans by sensory perception and the EGL-4 cGMP-dependent protein kinase. *Neuron, 36*(6), 1091-1102. doi:10.1016/s0896-6273(02)01093-0
Gadenne, C., et al. (2016). Plasticity in Insect Olfaction: To Smell or Not to Smell? *Annu Rev Entomol, 61*, 317-333. doi:10.1146/annurev-ento-010715-023523
Galambos, R. (1956). Suppression of auditory nerve activity by stimulation of efferent fibers to cochlea. *J Neurophysiol, 19*(5), 424-437. doi:10.1152/jn.1956.19.5.424
Golden, J. W., et al. (1982). A pheromone influences larval development in the nematode Caenorhabditis elegans. *Science, 218*(4572), 578-580. doi:10.1126/science.6896933
Golden, J. W., et al. (1984). The Caenorhabditis elegans dauer larva: developmental effects of pheromone, food, and temperature. *Dev Biol, 102*(2), 368-378. doi:10.1016/0012-1606(84)90201-x
Goldman, A. L., et al. (2005). Coexpression of two functional odor receptors in one neuron. *Neuron, 45*(5), 661-666. doi:10.1016/j.neuron.2005.01.025
Gray, J. M., et al. (2005). A circuit for navigation in Caenorhabditis elegans. *Proc Natl Acad Sci U S A, 102*(9), 3184-3191. doi:10.1073/pnas.0409009101
Gruner, M., et al. (2014). Feeding state, insulin and NPR-1 modulate chemoreceptor gene expression via integration of sensory and circuit inputs. *PLoS Genet, 10*(10), e1004707. doi:10.1371/journal.pgen.1004707
Grunwald Kadow, I. C. (2019). State-dependent plasticity of innate behavior in fruit flies. *Curr Opin Neurobiol, 54*, 60-65. doi:10.1016/j.conb.2018.08.014
Ha, H. I., et al. (2010). Functional organization of a neural network for aversive olfactory learning in Caenorhabditis elegans. *Neuron, 68*(6), 1173-1186. doi:10.1016/j.neuron.2010.11.025
Harris, G., et al. (2014). Dissecting the signaling mechanisms underlying recognition and preference of food odors. *J Neurosci, 34*(28), 9389-9403. doi:10.1523/JNEUROSCI.0012-14.2014

Hart, A. C., et al. (2010). From Odors to Behaviors in Caenorhabditis elegans. In A. Menini (Ed.), *The Neurobiology of Olfaction*. Boca Raton (FL).
Hildebrand, J. G., et al. (1997). Mechanisms of olfactory discrimination: converging evidence for common principles across phyla. *Annu Rev Neurosci, 20*, 595-631. doi:10.1146/annurev.neuro.20.1.595
Hilliard, M. A., et al. (2002). C. elegans responds to chemical repellents by integrating sensory inputs from the head and the tail. *Curr Biol, 12*(9), 730-734. doi:10.1016/s0960-9822(02)00813-8
Huetteroth, W., et al. (2011). Hungry flies tune to vinegar. *Cell, 145*(1), 17-18. doi:10.1016/j.cell.2011.03.018
Hukema, R. K., et al. (2008). Gustatory plasticity in C. elegans involves integration of negative cues and NaCl taste mediated by serotonin, dopamine, and glutamate. *Learn Mem, 15*(11), 829-836. doi:10.1101/lm.994408
Iino, Y., et al. (2009). Parallel use of two behavioral mechanisms for chemotaxis in Caenorhabditis elegans. *J Neurosci, 29*(17), 5370-5380. doi:10.1523/JNEUROSCI.3633-08.2009
Izrayelit, Y., et al. (2012). Targeted metabolomics reveals a male pheromone and sex-specific ascaroside biosynthesis in Caenorhabditis elegans. *ACS Chem Biol, 7*(8), 1321-1325. doi:10.1021/cb300169c
Jang, H., et al. (2012). Neuromodulatory state and sex specify alternative behaviors through antagonistic synaptic pathways in C. elegans. *Neuron, 75*(4), 585-592. doi:10.1016/j.neuron.2012.06.034
Jansen, G., et al. (1999). The complete family of genes encoding G proteins of Caenorhabditis elegans. *Nat Genet, 21*(4), 414-419. doi:10.1038/7753
Jansen, G., et al. (2002). The G-protein gamma subunit gpc-1 of the nematode C.elegans is involved in taste adaptation. *EMBO J, 21*(5), 986-994. doi:10.1093/emboj/21.5.986
Kahn-Kirby, A. H., et al. (2004). Specific polyunsaturated fatty acids drive TRPV-dependent sensory signaling in vivo. *Cell, 119*(6), 889-900. doi:10.1016/j.cell.2004.11.005
Kaletta, T., et al. (2006). Finding function in novel targets: C. elegans as a model organism. *Nat Rev Drug Discov, 5*(5), 387-398. doi:10.1038/nrd2031
Kaplan, J. M., et al. (1993). A dual mechanosensory and chemosensory neuron in Caenorhabditis elegans. *Proc Natl Acad Sci U S A, 90*(6), 2227-2231. doi:10.1073/pnas.90.6.2227
Ke, J. B., et al. (2014). Adaptation to background light enables contrast coding at rod bipolar cell synapses. *Neuron, 81*(2), 388-401. doi:10.1016/j.neuron.2013.10.054
Kim, K., et al. (2009). Two chemoreceptors mediate developmental effects of dauer pheromone in C. elegans. *Science, 326*(5955), 994-998. doi:10.1126/science.1176331
Kleene, S. J. (2008). The Electrochemical Basis of Odor Transduction in Vertebrate Olfactory Cilia. *Chemical Senses, 33*(9), 839-859. doi:10.1093/chemse/bjn048
Kleene, S. J., et al. (1991). Calcium-activated chloride conductance in frog olfactory cilia. *J Neurosci, 11*(11), 3624-3629. Retrieved from https://www.ncbi.nlm.nih.gov/pubmed/1941099

Knaden, M., et al. (2014). Mapping odor valence in the brain of flies and mice. *Curr Opin Neurobiol, 24*(1), 34-38. doi:10.1016/j.conb.2013.08.010
Kocabas, A., et al. (2012). Controlling interneuron activity in Caenorhabditis elegans to evoke chemotactic behaviour. *Nature, 490*(7419), 273-277. doi:10.1038/nature11431
Koch, C., et al. (1982). Retinal ganglion cells: a functional interpretation of dendritic morphology. *Philos Trans R Soc Lond B Biol Sci, 298*(1090), 227-263. doi:10.1098/rstb.1982.0084
Komatsu, H., et al. (1996). Mutations in a cyclic nucleotide-gated channel lead to abnormal thermosensation and chemosensation in C. elegans. *Neuron, 17*(4), 707-718. doi:10.1016/s0896-6273(00)80202-0
Koutalos, Y., et al. (1996). Regulation of sensitivity in vertebrate rod photoreceptors by calcium. *Trends Neurosci, 19*(2), 73-81. doi:10.1016/0166-2236(96)89624-x
Krishnan, B., et al. (1999). Circadian rhythms in olfactory responses of Drosophila melanogaster. *Nature, 400*(6742), 375-378. doi:10.1038/22566
Kromann, S. H., et al. (2015). Concurrent modulation of neuronal and behavioural olfactory responses to sex and host plant cues in a male moth. *Proc Biol Sci, 282*(1799), 20141884. doi:10.1098/rspb.2014.1884
Kuwabara, P. E., et al. (2001). The use of functional genomics in C. elegans for studying human development and disease. *J Inherit Metab Dis, 24*(2), 127-138. doi:10.1023/a:1010306731764
L'Etoile, N. D., et al. (2000). Olfaction and odor discrimination are mediated by the C. elegans guanylyl cyclase ODR-1. *Neuron, 25*(3), 575-586. doi:10.1016/s0896-6273(00)81061-2
Lai, C. H., et al. (2000). Identification of novel human genes evolutionarily conserved in Caenorhabditis elegans by comparative proteomics. *Genome Res, 10*(5), 703-713. doi:10.1101/gr.10.5.703
Lanjuin, A., et al. (2002). Regulation of chemosensory receptor expression and sensory signaling by the KIN-29 Ser/Thr kinase. *Neuron, 33*(3), 369-381. doi:10.1016/s0896-6273(02)00572-x
Lans, H., et al. (2004). A network of stimulatory and inhibitory Galpha-subunits regulates olfaction in Caenorhabditis elegans. *Genetics, 167*(4), 1677-1687. doi:10.1534/genetics.103.024786
Larsch, J., et al. (2015). A Circuit for Gradient Climbing in C. elegans Chemotaxis. *Cell Rep, 12*(11), 1748-1760. doi:10.1016/j.celrep.2015.08.032
Lazic, S. E., et al. (2007). Olfactory abnormalities in Huntington's disease: decreased plasticity in the primary olfactory cortex of R6/1 transgenic mice and reduced olfactory discrimination in patients. *Brain Res, 1151*, 219-226. doi:10.1016/j.brainres.2007.03.018
Leinwand, S. G., et al. (2015). Circuit mechanisms encoding odors and driving aging-associated behavioral declines in Caenorhabditis elegans. *Elife, 4*, e10181. doi:10.7554/eLife.10181
Li, Q., et al. (2015). Aversion and attraction through olfaction. *Curr Biol, 25*(3), R120-R129. doi:10.1016/j.cub.2014.11.044
Liu, K. S., et al. (1995). Sensory regulation of male mating behavior in Caenorhabditis elegans. *Neuron, 14*(1), 79-89. doi:10.1016/0896-6273(95)90242-2

Lowe, G., et al. (1993). Contribution of the ciliary cyclic nucleotide-gated conductance to olfactory transduction in the salamander. *J Physiol, 462*, 175-196. doi:10.1113/jphysiol.1993.sp019550
Luedtke, S., et al. (2010). The regulation of feeding and metabolism in response to food deprivation in Caenorhabditis elegans. *Invert Neurosci, 10*(2), 63-76. doi:10.1007/s10158-010-0112-z
Luo, L., et al. (2014). Dynamic encoding of perception, memory, and movement in a C. elegans chemotaxis circuit. *Neuron, 82*(5), 1115-1128. doi:10.1016/j.neuron.2014.05.010
Lynch, J. W., et al. (1989). Action potentials initiated by single channels opening in a small neuron (rat olfactory receptor). *Biophys J, 55*(4), 755-768. doi:10.1016/S0006-3495(89)82874-7
Ma, M., et al. (2012). Optogenetic activation of basal forebrain cholinergic neurons modulates neuronal excitability and sensory responses in the main olfactory bulb. *J Neurosci, 32*(30), 10105-10116. doi:10.1523/JNEUROSCI.0058-12.2012
Macosko, E. Z., et al. (2009). A hub-and-spoke circuit drives pheromone attraction and social behaviour in C. elegans. *Nature, 458*(7242), 1171-1175. doi:10.1038/nature07886
Mak, H. Y., et al. (2006). Polygenic control of Caenorhabditis elegans fat storage. *Nat Genet, 38*(3), 363-368. doi:10.1038/ng1739
Matsuki, M., et al. (2006). Goalpha regulates olfactory adaptation by antagonizing Gqalpha-DAG signaling in Caenorhabditis elegans. *Proc Natl Acad Sci U S A, 103*(4), 1112-1117. doi:10.1073/pnas.0506954103
Matthews, H. R., et al. (1988). Photoreceptor light adaptation is mediated by cytoplasmic calcium concentration. *Nature, 334*(6177), 67-69. doi:10.1038/334067a0
Maue, R. A., et al. (1987). Patch-clamp studies of isolated mouse olfactory receptor neurons. *J Gen Physiol, 90*(1), 95-125. doi:10.1085/jgp.90.1.95
McCarroll, S. A., et al. (2005). Identification of transcriptional regulatory elements in chemosensory receptor genes by probabilistic segmentation. *Curr Biol, 15*(4), 347-352. doi:10.1016/j.cub.2005.02.023
McCudden, C. R., et al. (2005). G-protein signaling: back to the future. *Cell Mol Life Sci, 62*(5), 551-577. doi:10.1007/s00018-004-4462-3
McGrath, P. T., et al. (2011). Parallel evolution of domesticated Caenorhabditis species targets pheromone receptor genes. *Nature, 477*(7364), 321-325. doi:10.1038/nature10378
Mesholam, R. I., et al. (1998). Olfaction in neurodegenerative disease: a meta-analysis of olfactory functioning in Alzheimer's and Parkinson's diseases. *Arch Neurol, 55*(1), 84-90. doi:10.1001/archneur.55.1.84
Metaxakis, A., et al. (2018). Multimodal sensory processing in Caenorhabditis elegans. *Open Biol, 8*(6). doi:10.1098/rsob.180049
Mombaerts, P., et al. (1996). Visualizing an olfactory sensory map. *Cell, 87*(4), 675-686. doi:10.1016/s0092-8674(00)81387-2
Mori, K., et al. (2021). Olfactory Circuitry and Behavioral Decisions. *Annu Rev Physiol, 83*, 231-256. doi:10.1146/annurev-physiol-031820-092824

Mukhopadhyay, S., et al. (2005). A structural perspective of the flavivirus life cycle. *Nat Rev Microbiol, 3*(1), 13-22. doi:10.1038/nrmicro1067
Nakamura, T., et al. (1987). A cyclic nucleotide-gated conductance in olfactory receptor cilia. *Nature, 325*(6103), 442-444. doi:10.1038/325442a0
Nakatani, K., et al. (1988). Calcium and light adaptation in retinal rods and cones. *Nature, 334*(6177), 69-71. doi:10.1038/334069a0
Nurrish, S., et al. (1999). Serotonin inhibition of synaptic transmission: Galpha(0) decreases the abundance of UNC-13 at release sites. *Neuron, 24*(1), 231-242. doi:10.1016/s0896-6273(00)80835-1
O'Halloran, D. M., et al. (2009). Regulators of AWC-mediated olfactory plasticity in Caenorhabditis elegans. *PLoS Genet, 5*(12), e1000761. doi:10.1371/journal.pgen.1000761
Page, T. L., et al. (2003). Circadian rhythm in olfactory response in the antennae controlled by the optic lobe in the cockroach. *J Insect Physiol, 49*(7), 697-707. doi:10.1016/s0022-1910(03)00071-4
Park, D., et al. (2012). Interaction of structure-specific and promiscuous G-protein-coupled receptors mediates small-molecule signaling in Caenorhabditis elegans. *Proc Natl Acad Sci U S A, 109*(25), 9917-9922. doi:10.1073/pnas.1202216109
Pellegrino, M., et al. (2009). Smelling the difference: controversial ideas in insect olfaction. *J Exp Biol, 212*(Pt 13), 1973-1979. doi:10.1242/jeb.023036
Perkins, L. A., et al. (1986). Mutant sensory cilia in the nematode Caenorhabditis elegans. *Dev Biol, 117*(2), 456-487. doi:10.1016/0012-1606(86)90314-3
Pierce-Shimomura, J. T., et al. (1999). The fundamental role of pirouettes in Caenorhabditis elegans chemotaxis. *J Neurosci, 19*(21), 9557-9569. Retrieved from https://www.ncbi.nlm.nih.gov/pubmed/10531458
Piggott, B. J., et al. (2011). The neural circuits and synaptic mechanisms underlying motor initiation in C. elegans. *Cell, 147*(4), 922-933. doi:10.1016/j.cell.2011.08.053
Pugh, E. N., Jr., et al. (1990). Cyclic GMP and calcium: the internal messengers of excitation and adaptation in vertebrate photoreceptors. *Vision Res, 30*(12), 1923-1948. doi:10.1016/0042-6989(90)90013-b
Radonjic, A., et al. (2011). The dynamic range of human lightness perception. *Curr Biol, 21*(22), 1931-1936. doi:10.1016/j.cub.2011.10.013
Reisert, J., et al. (2003). The Ca-activated Cl channel and its control in rat olfactory receptor neurons. *J Gen Physiol, 122*(3), 349-363. doi:10.1085/jgp.200308888
Ressler, K. J., et al. (1994). Information coding in the olfactory system: evidence for a stereotyped and highly organized epitope map in the olfactory bulb. *Cell, 79*(7), 1245-1255. doi:10.1016/0092-8674(94)90015-9
Root, C. M., et al. (2011). Presynaptic facilitation by neuropeptide signaling mediates odor-driven food search. *Cell, 145*(1), 133-144. doi:10.1016/j.cell.2011.02.008
Ryan, D. A., et al. (2014). Sex, age, and hunger regulate behavioral prioritization through dynamic modulation of chemoreceptor expression. *Curr Biol, 24*(21), 2509-2517. doi:10.1016/j.cub.2014.09.032
Ryu, W. S., et al. (2002). Thermotaxis in Caenorhabditis elegans analyzed by measuring responses to defined Thermal stimuli. *J Neurosci, 22*(13), 5727-5733. doi:20026542

Sachse, S., et al. (2016). The good, the bad, and the hungry: how the central brain codes odor valence to facilitate food approach in Drosophila. *Curr Opin Neurobiol, 40*, 53-58. doi:10.1016/j.conb.2016.06.012
Saeki, S., et al. (2001). Plasticity of chemotaxis revealed by paired presentation of a chemoattractant and starvation in the nematode Caenorhabditis elegans. *J Exp Biol, 204*(Pt 10), 1757-1764. Retrieved from https://www.ncbi.nlm.nih.gov/pubmed/11316496
Sambongi, Y., et al. (1999). Sensing of cadmium and copper ions by externally exposed ADL, ASE, and ASH neurons elicits avoidance response in Caenorhabditis elegans. *Neuroreport, 10*(4), 753-757. doi:10.1097/00001756-199903170-00017
Sato, K., et al. (2008). Insect olfactory receptors are heteromeric ligand-gated ion channels. *Nature, 452*(7190), 1002-1006. doi:10.1038/nature06850
Schafer, W. R. (2006). Neurophysiological methods in C. elegans: an introduction. *WormBook*, 1-4. doi:10.1895/wormbook.1.111.1
Semmelhack, J. L., et al. (2009). Select Drosophila glomeruli mediate innate olfactory attraction and aversion. *Nature, 459*(7244), 218-223. doi:10.1038/nature07983
Sengupta, P. (2007). Generation and modulation of chemosensory behaviors in C. elegans. *Pflugers Arch, 454*(5), 721-734. doi:10.1007/s00424-006-0196-9
Shanbhag, S. R., et al. (2000). Atlas of olfactory organs of Drosophila melanogaster 2. Internal organization and cellular architecture of olfactory sensilla. *Arthropod Struct Dev, 29*(3), 211-229. doi:10.1016/s1467-8039(00)00028-1
Simon, J. M., et al. (2002). Evidence of a mate-finding cue in the hermaphrodite nematode Caenorhabditis elegans. *Proc Natl Acad Sci U S A, 99*(3), 1598-1603. doi:10.1073/pnas.032225799
Srinivasan, J., et al. (2008). A blend of small molecules regulates both mating and development in Caenorhabditis elegans. *Nature, 454*(7208), 1115-1118. doi:10.1038/nature07168
Srinivasan, J., et al. (2012). A modular library of small molecule signals regulates social behaviors in Caenorhabditis elegans. *PLoS Biol, 10*(1), e1001237. doi:10.1371/journal.pbio.1001237
Stowers, L., et al. (2015). Mammalian pheromones: emerging properties and mechanisms of detection. *Curr Opin Neurobiol, 34*, 103-109. doi:10.1016/j.conb.2015.02.005
Stowers, L., et al. (2016). State-dependent responses to sex pheromones in mouse. *Curr Opin Neurobiol, 38*, 74-79. doi:10.1016/j.conb.2016.04.001
Strauch, M., et al. (2014). More than apples and oranges--detecting cancer with a fruit fly's antenna. *Sci Rep, 4*, 3576. doi:10.1038/srep03576
Sze, J. Y., et al. (2000). Food and metabolic signalling defects in a Caenorhabditis elegans serotonin-synthesis mutant. *Nature, 403*(6769), 560-564. doi:10.1038/35000609
Takahashi, L. K. (2014). Olfactory systems and neural circuits that modulate predator odor fear. *Front Behav Neurosci, 8*, 72. doi:10.3389/fnbeh.2014.00072
Thomas, J. H., et al. (2008). The Caenorhabditis chemoreceptor gene families. *BMC Biol, 6*, 42. doi:10.1186/1741-7007-6-42

Tobin, D. M., et al. (2002). Combinatorial expression of TRPV channel proteins defines their sensory functions and subcellular localization in C. elegans neurons. *Neuron, 35*(2), 307-318. doi:10.1016/s0896-6273(02)00757-2
Tomioka, M., et al. (2006). The insulin/PI 3-kinase pathway regulates salt chemotaxis learning in Caenorhabditis elegans. *Neuron, 51*(5), 613-625. doi:10.1016/j.neuron.2006.07.024
Torre, V., et al. (1986). Role of calcium in regulating the cyclic GMP cascade of phototransduction in retinal rods. *Proc Natl Acad Sci U S A, 83*(18), 7109-7113. doi:10.1073/pnas.83.18.7109
Touhara, K. (2002). Odor discrimination by G protein-coupled olfactory receptors. *Microsc Res Tech, 58*(3), 135-141. doi:10.1002/jemt.10131
Touhara, K. (2007). Deorphanizing vertebrate olfactory receptors: recent advances in odorant-response assays. *Neurochem Int, 51*(2-4), 132-139. doi:10.1016/j.neuint.2007.05.020
Troemel, E. R., et al. (1995). Divergent seven transmembrane receptors are candidate chemosensory receptors in C. elegans. *Cell, 83*(2), 207-218. doi:10.1016/0092-8674(95)90162-0
Troemel, E. R., et al. (1997). Reprogramming chemotaxis responses: sensory neurons define olfactory preferences in C. elegans. *Cell, 91*(2), 161-169. doi:10.1016/s0092-8674(00)80399-2
Trotier, D., et al. (1986). Intracellular recordings from salamander olfactory supporting cells. *Brain Res, 374*(2), 205-211. doi:10.1016/0006-8993(86)90413-0
Tsalik, E. L., et al. (2003). Functional mapping of neurons that control locomotory behavior in Caenorhabditis elegans. *J Neurobiol, 56*(2), 178-197. doi:10.1002/neu.10245
van der Goes van Naters, W., et al. (2007). Receptors and neurons for fly odors in Drosophila. *Curr Biol, 17*(7), 606-612. doi:10.1016/j.cub.2007.02.043
Vassar, R., et al. (1994). Topographic organization of sensory projections to the olfactory bulb. *Cell, 79*(6), 981-991. doi:10.1016/0092-8674(94)90029-9
Vassar, R., et al. (1993). Spatial segregation of odorant receptor expression in the mammalian olfactory epithelium. *Cell, 74*(2), 309-318. doi:10.1016/0092-8674(93)90422-m
Vosshall, L. B., et al. (2007). Molecular architecture of smell and taste in Drosophila. *Annu Rev Neurosci, 30*, 505-533. doi:10.1146/annurev.neuro.30.051606.094306
Vosshall, L. B., et al. (2000). An olfactory sensory map in the fly brain. *Cell, 102*(2), 147-159. doi:10.1016/s0092-8674(00)00021-0
Vowels, J. J., et al. (1994). Multiple chemosensory defects in daf-11 and daf-21 mutants of Caenorhabditis elegans. *Genetics, 138*(2), 303-316. doi:10.1093/genetics/138.2.303
Waggoner, L. E., et al. (1998). Control of alternative behavioral states by serotonin in Caenorhabditis elegans. *Neuron, 21*(1), 203-214. doi:10.1016/s0896-6273(00)80527-9
Wakabayashi, T., et al. (2004). Neurons regulating the duration of forward locomotion in Caenorhabditis elegans. *Neurosci Res, 50*(1), 103-111. doi:10.1016/j.neures.2004.06.005

Ward, S. (1973). Chemotaxis by the nematode Caenorhabditis elegans: identification of attractants and analysis of the response by use of mutants. *Proc Natl Acad Sci U S A, 70*(3), 817-821. doi:10.1073/pnas.70.3.817
Ward, S., et al. (1975). Electron microscopical reconstruction of the anterior sensory anatomy of the nematode Caenorhabditis elegans.?2UU. *J Comp Neurol, 160*(3), 313-337. doi:10.1002/cne.901600305
Ware, R. W., et al. (1975). The nerve ring of the nematode Caenorhabditis elegans: sensory input and motor output. *Journal of Comparative Neurology, 162*(1), 71-110.
Wesson, D. W., et al. (2010). Olfactory dysfunction correlates with amyloid-beta burden in an Alzheimer's disease mouse model. *J Neurosci, 30*(2), 505-514. doi:10.1523/JNEUROSCI.4622-09.2010
White, J. G., et al. (1986). The structure of the nervous system of the nematode Caenorhabditis elegans. *Philos Trans R Soc Lond B Biol Sci, 314*(1165), 1-340. doi:10.1098/rstb.1986.0056
Wicher, D., et al. (2008). Drosophila odorant receptors are both ligand-gated and cyclic-nucleotide-activated cation channels. *Nature, 452*(7190), 1007-1011. doi:10.1038/nature06861
Yoshida, K., et al. (2012). Odour concentration-dependent olfactory preference change in C. elegans. *Nat Commun, 3*, 739. doi:10.1038/ncomms1750
Zagotta, W. N., et al. (1996). Structure and function of cyclic nucleotide-gated channels. *Annu Rev Neurosci, 19*, 235-263. doi:10.1146/annurev.ne.19.030196.001315
Zahratka, J. A., et al. (2015). Serotonin differentially modulates Ca2+ transients and depolarization in a C. elegans nociceptor. *J Neurophysiol, 113*(4), 1041-1050. doi:10.1152/jn.00665.2014
Zancanaro, C., et al. (2014). Neurobiology of Chemical Communication.
Zariwala, H. A., et al. (2003). Step response analysis of thermotaxis in Caenorhabditis elegans. *J Neurosci, 23*(10), 4369-4377. Retrieved from https://www.ncbi.nlm.nih.gov/pubmed/12764126
Zhang, Y., et al. (2005). Pathogenic bacteria induce aversive olfactory learning in Caenorhabditis elegans. *Nature, 438*(7065), 179-184. doi:10.1038/nature04216
Zwaal, R. R., et al. (1997). Two neuronal G proteins are involved in chemosensation of the Caenorhabditis elegans Dauer-inducing pheromone. *Genetics, 145*(3), 715-727. doi:10.1093/genetics/145.3.715

CHAPTER 2

A context-dependent response sign switch in a single sensory neuron type inverts olfactory preference behavior

CHAPTER 2

A context-dependent response sign switch in a single sensory neuron type inverts olfactory preference behavior

Munzareen Khan[1], Anna Hartmann[1,4], Michael P. O'Donnell[1,5], Madeline Piccione[1], Pin-Hao Chao[1], Noelle Dwyer[2], Cornelia I. Bargmann[3] and Piali Sengupta[1,7]

[1]Department of Biology, Brandeis University, Waltham, MA

[2]Department of Cell Biology, University of Virginia, Charlottesville, VA

[3]The Rockefeller University, New York, NY

[4]Current address: Department of Neurobiology, Harvard Medical School, Boston, MA

[5]Current address: Department of Molecular, Cell and Developmental Biology, Yale University, New Haven, CT

2. 1 Contributions to this work

This chapter is presented in the form of a manuscript written by PS and MK. The work relies on identification of the phenotype and initial experiments performed by AH with PC and is based on observations made by ND when in the lab of CIB. All experiments presented here were designed by PS and MK. MK and MP performed chemotaxis plate assay experiments. MK performed all additional experiments, including calcium imaging and microfluidics behavior, and curated and analyzed all data. MOD developed analysis scripts for microfluidics behavior and calcium imaging and helped with designing microfluidic chips.

2.2 Abstract

The valence and salience of individual odorants are not only modulated by an animal's innate preferences, learned associations, and internal state, but also by the context of odorant presentation. The mechanisms underlying context-dependent plasticity in odor valence are not fully understood. Here we show that the behavioral response of *C. elegans* to food-related medium-chain alcohols is switched from attraction to avoidance when presented in the background of a subset of additional attractive chemicals. This switch in odorant preference is driven by cell-autonomous inversion of the sign of the response to these alcohols in the single AWC olfactory neuron pair. While medium-chain alcohols inhibit the AWC olfactory neurons to drive attraction, when presented in the background of a second saturating AWC-sensed odorant, these alcohols instead activate AWC to promote avoidance. We show that these opposing responses are driven via odorant-mediated engagement of distinct downstream signal transduction pathways within AWC. Our results indicate that context-dependent recruitment of alternate intracellular signaling pathways within a single sensory neuron type is sufficient to convey opposite hedonic valences, thereby providing a robust mechanism for odorant encoding and discrimination at the periphery.

2.3 Introduction

Organisms live in complex and dynamic chemical environments. Animals continuously encounter heterogenous mixtures of multiple chemicals which fluctuate in their concentrations and provide information about the presence and location of food, mates, competitors, and predators (Baker et al., 2018; Laurent, 2002; Vickers, 2000).

To correctly decode these chemical inputs, chemosensory responses must not only be robust and sensitive, but must also be highly flexible (Grunwald Kadow, 2019; Kim et al., 2017; Stowers and Liberles, 2016). Experience and internal state modulate the salience of odorants and can even switch the valence of a specific chemical (eg. (Busto et al., 2010; Cho et al., 2016; Inagaki et al., 2014; Marella et al., 2012; Root et al., 2011; Saeki et al., 2001; Tomioka et al., 2006; Turner and Ray, 2009; Zhang et al., 2005)). The molecular and neuronal mechanisms that underlie plasticity in chemosensory behaviors remain to be fully described.

A critical task of the olfactory system is to discriminate among related chemical cues. Since chemicals that are structurally similar can nevertheless have distinct saliences for an organism (Bentley, 2006), these cues must be differentiated and identified in order to elicit the appropriate behavior. In particular, animals need to distinguish individual chemicals in a complex mixture or detect the presence of a new chemical in the background of a continuously present odorant [eg. (Badeke et al., 2016; Livermore and Laing, 1998; Riffell et al., 2014; Rokni et al., 2014)]. Context-dependent odorant discrimination can be driven via integration and processing of individual sensory inputs in central brain regions (Amin and Lin, 2019; Araneda et al., 2004; Groschner and Miesenbock, 2019; Hildebrand and Shepherd, 1997; Kadohisa and Wilson, 2006; Mohamed et al., 2019; Parnas et al., 2013; Saraiva et al., 2016; Stettler and Axel, 2009; Xia and Tully, 2007). However, mechanisms operating at the level of single sensory neuron types or sensilla in the periphery have also been implicated in this process (Duan et al., 2020; Inagaki et al., 2020; Kurahashi et al., 1994; Pfister et al., 2020; Reddy et al., 2018; Turner and Ray, 2009). In adult *Drosophila*, olfactory neurons in a

subset of sensilla generally express a single chemical receptor, and a single receptor can either excite or inhibit the sensory neuron in response to different odorants (Couto et al., 2005; Hallem and Carlson, 2006; Hallem et al., 2004). In the presence of a constant background of one chemical, the pattern of olfactory neuron response to a pulse of a second chemical is altered thereby permitting odorant discrimination by a single sensory neuron type (Cao et al., 2017; Su et al., 2011). Similarly, the tonic response of one of two sensory neurons in an individual sensillum in *Drosophila* or mosquitoes to a constant background odorant is modulated by a pulse of a different odorant sensed by the second sensory neuron via ephaptic coupling, thereby modulating behavioral responses to both chemicals (Su et al., 2012; Zhang et al., 2019). Whether additional mechanisms also operate in sensory neurons to enable odorant discrimination and drive olfactory behavioral plasticity is unclear.

C. elegans senses and navigates its complex chemical environment using a small subset of sensory neurons (Perkins et al., 1986; Ward et al., 1975; White et al., 1986). The valence of individual chemicals appears to be largely determined by the responding sensory neuron type, such that distinct subsets of chemosensory neurons drive either attraction or avoidance to different chemicals (Bargmann et al., 1993; Ferkey et al., 2021; Troemel et al., 1997; Wes and Bargmann, 2001). Each chemosensory neuron type in *C. elegans* expresses multiple receptors that are likely tuned to distinct odorants (Troemel et al., 1995; Vidal et al., 2018), raising the question of whether and how individual neurons discriminate between chemical cues. To address this question, animals have been tasked to navigate a gradient of one attractive odorant in the context of a uniform saturating concentration of a second attractive odorant

sensed by the same neuron (Bargmann et al., 1993). Failure to discriminate between the two odorants results in loss or reduced attraction, but importantly, not aversion, to the test attractant, presumably due to cross-saturation between the molecular signaling pathways within the neuron type (Bargmann et al., 1993). In contrast, aversion of a normally attractive chemical can occur as a consequence of modulation by experience and internal state. Association of an attractive chemical with starvation, or pairing with an aversive chemical, can result in subsequent avoidance or indifference to an initially attractive cue (Colbert and Bargmann, 1997; Ghosh et al., 2016; Ishihara et al., 2002; Nuttley et al., 2002; Rengarajan et al., 2019; Saeki et al., 2001; Tomioka et al., 2006). Experience- and state-dependent switches in the valence of a chemical appear to occur largely via integration and plasticity at the synaptic and circuit level (Ha et al., 2010; Jang et al., 2012; Kunitomo et al., 2013; Tsunozaki et al., 2008; Yoshida et al., 2012; Zhang et al., 2005), and have not been reported to be driven solely by plasticity in sensory neuron responses.

Here we report that inversion of the behavioral response of *C. elegans* to a subset of food-related odors can be driven by a context-dependent switch in the sign of the odorant response in a single sensory neuron type. We find that adult *C. elegans* hermaphrodites are attracted to low concentrations of medium chain alcohols such as 1-hexanol and 1-heptanol (henceforth referred to as hexanol and heptanol, respectively), but that worms are strongly repelled by these chemicals when presented in the context of a uniform saturating background of a subset of other attractive odorants. Using high resolution behavioral assays in microfluidics behavioral arenas, we show that while the AWC olfactory neuron pair drives attraction to hexanol in the absence of a background

saturating odorant, in saturating odorant conditions, this neuron type instead drives avoidance. Via quantification of stimulus-evoked changes in intracellular calcium dynamics, we find that while hexanol and heptanol inhibit AWC in non-saturating conditions, in saturating conditions, these chemicals activate AWC, correlating with the ability of AWC to drive either attraction or avoidance. We identify distinct downstream effectors that mediate the ability of this sensory neuron type to drive attraction to or avoidance of the same chemical in a context-dependent manner. Results described here indicate that context-dependent engagement of distinct intracellular signaling pathways within a single sensory neuron type is not only sufficient to discriminate between structurally related chemicals, but to also convey opposing hedonic valences.

2.4 Results

2.4.1 Medium-chain alcohols can either attract or repel *C. elegans* based on odorant context

Cross-saturation assays have previously been used as a measure of the ability of *C. elegans* to behaviorally discriminate between two volatile odorants (Bargmann et al., 1993). In these assays, animals are challenged with a point source of the test chemical in the presence of a uniform concentration of a second saturating chemical (Figure 1A). The ability to retain responses to the test chemical under these conditions suggests that the animal is able to discriminate between the test and saturating odorants.

The AWC olfactory neuron pair in *C. elegans* responds to low concentrations of a subset of bacterially produced attractive chemicals including benzaldehyde, isoamyl alcohol (IAA), and the short-chain alcohol 1-pentanol (Bargmann et al., 1993; Chalasani

et al., 2007; Choi et al., 2018; Yoshida et al., 2012). In the presence of a uniform background concentration of IAA, animals are indifferent to a point source of IAA (Figure 1A). However, as reported previously (Bargmann et al., 1993), saturating concentrations of IAA reduced but did not abolish the attractive response of *C. elegans* hermaphrodites to a point source of benzaldehyde, indicating that the AWC neurons are able to partly discriminate between these structurally distinct chemicals (Figure 1A). To investigate the extent to which AWC is able to discriminate among structurally related chemicals, we examined responses to point sources of the short-chain alcohols 1-butanol and 1-pentanol with or without saturating IAA. Attractive responses to different concentrations of these alcohols were reduced or abolished in saturating IAA indicating that animals are largely unable to discriminate between these chemicals (Figure 1B) (Bargmann et al., 1993). *C. elegans* is robustly repelled by long-chain alcohols such as 1-octanol (Bargmann et al., 1993); this response is mediated by integration of sensory inputs from multiple sensory neurons including AWC in a food-dependent manner (Chao et al., 2004; Summers et al., 2015; Troemel et al., 1995). However, saturating IAA had no effect on the avoidance of this chemical (Figure 1B). These observations indicate that in saturating IAA, AWC-driven attractive responses to a subset of related alcohols is decreased or abolished, but that long-range avoidance of alcohols driven by other sensory neurons is unaffected.

We noted that animals were also attracted to the medium-chain alcohols hexanol and heptanol at different concentrations (Figure 1B) (Bargmann et al., 1993). However, unlike the reduced attraction observed for 1-butanol and 1-pentanol in saturating IAA, animals instead strongly avoided both hexanol and heptanol under these conditions

(Figure 1B). In contrast, saturation with either hexanol or heptanol abolished attraction to a point source of IAA but did not result in avoidance (Figure 1C). To further characterize this behavioral plasticity, we examined chemotaxis towards different concentrations of hexanol. Many chemicals elicit distinct behaviors at different concentrations [eg. (Bargmann et al., 1993; Horio et al., 2019; Laing et al., 1978; Luo et al., 2008; Saraiva et al., 2016; Semmelhack and Wang, 2009; Stensmyr et al., 2003)]. Worms were attracted to low, but were weakly repelled by high, concentrations of hexanol (Figure 1D). Saturating IAA abolished attraction and shifted the response towards indifference of lower, and strong avoidance of higher, hexanol concentrations (Figure 1D). We infer that distinct underlying antagonistic neuronal pathways mediate attraction to, and avoidance of, hexanol at all concentrations, and that attraction predominates at lower, and avoidance at higher, hexanol concentration. Saturating IAA inhibits the attraction but not avoidance pathway. These results also indicate that animals are unable to discriminate between IAA and hexanol for attraction but are able to do so for avoidance.

2.4.2 The attraction-promoting AWC olfactory neurons instead drive hexanol avoidance in odorant saturation conditions

The ability of hexanol and IAA to cross-saturate for attraction suggested that hexanol attraction is mediated by AWC. The AWB, ASH and ADL sensory neuron pairs mediate avoidance of noxious alcohols including high concentrations of IAA (Bargmann et al., 1993; Bargmann and Horvitz, 1991; Duan et al., 2020; Ha et al., 2010; Jang et al., 2012; Troemel et al., 1997; Yoshida et al., 2012). We tested whether hexanol attraction

and avoidance requires AWC and one or more of the avoidance-mediating sensory neurons, respectively.

Since both attraction and avoidance of hexanol were somewhat variable in plate chemotaxis assays (Figure 1B), we sought to establish an assay that would allow us to more reliably characterize the contributions of different sensory neurons to hexanol attraction and avoidance behaviors. Microfluidics behavioral arenas (Figure 2A) that enable precise spatiotemporal control of stimulus delivery together with automated tracking of individual worm movement have been used previously to examine stimulus-evoked behaviors at high resolution (Albrecht and Bargmann, 2011). Animals were distributed throughout the microfluidics device in buffer alone but accumulated within a spatially restricted stripe of IAA under laminar flow over a 20 min period (Figure S1A,B). However, when a uniform concentration of 10^{-4} isoamyl alcohol also flowed throughout the device, animals were instead present both within and outside the central IAA stripe, indicating response saturation (Figure S1A,B). Consistent with hexanol being attractive at lower concentrations, the majority of wild-type animals were also present within a central stripe of 10^{-4} hexanol (Figure 2B,F, Movie S1). In IAA saturation conditions, animals avoided the central hexanol stripe and were present in regions containing buffer alone (Figure 2B,F, Movie S1). These observations establish that behaviors in microfluidics devices recapitulate the behavioral responses observed in plate chemotaxis assays, and can be used to assess the contributions of different sensory neurons to attraction and avoidance.

We found that animals in which AWC was genetically ablated or silenced via the expression of a gain-of function allele of the *unc-103* potassium channel (Reiner et al.,

2006), were no longer robustly attracted to hexanol but instead exhibited weak avoidance, indicating that AWC is necessary for hexanol attraction (Figure 2C,F, Figure S1C). We verified that AWC-ablated animals failed to be attracted to the AWC-sensed odorant benzaldehyde but noted that they were not repelled by this chemical (Bargmann et al., 1993) (Figure S1D). In saturating IAA, AWC-ablated or silenced animals continued to robustly avoid hexanol indicating that a neuron type other than AWC drives hexanol aversion under these conditions (Figure 2C,F, Figure S1C). Ablation of the nociceptive neuron type ASH had little effect on either attraction to, or avoidance of, hexanol in control or IAA-saturation conditions, respectively (Figure 2D,F), although these animals were defective in their ability to avoid high concentrations of the ASH-sensed chemical glycerol (Figure S1E). However, animals lacking both AWC and ASH were largely indifferent to hexanol regardless of conditions (Figure 2E,F). We conclude that while AWC drives attraction to hexanol, either AWC or ASH can mediate hexanol avoidance in saturating IAA. Thus, the typically attraction-mediating AWC sensory neurons are able to drive hexanol avoidance based on odorant context.

2.4.3 Saturation with AWC-sensed odorants cell-autonomously inverts the sign of the hexanol response in AWC

To investigate the mechanisms by which AWC mediates hexanol attraction or avoidance in a context-dependent manner, we next examined hexanol-evoked changes in intracellular calcium dynamics. Addition and removal of attractive odorants results in decreased and increased intracellular calcium levels in AWC, respectively (Chalasani et al., 2007; Zaslaver et al., 2015); these responses drive attraction (Chalasani et al.,

2007; Gordus et al., 2015). We first confirmed that the transgenic strain expressing the genetically encoded calcium indicator GCaMP3 in AWC exhibited behavioral responses to hexanol similar to those of wild-type animals (Figure S2A). We next assessed AWC calcium dynamics in animals immobilized in microfluidics imaging chips (Chronis et al., 2007) in response to hexanol and saturating IAA concentrations that elicited attraction and avoidance behaviors in microfluidics behavioral arenas.

AWC exhibits tonic activity that is decreased upon odorant addition (Chalasani et al., 2007; Chalasani et al., 2010). Consistently, a pulse of low IAA concentrations that robustly attracts wild-type animals decreased, and removal increased, intracellular calcium levels in AWC (Figure 3A) (Chalasani et al., 2007). However, in saturating IAA, a pulse of an additional 10^{-4} IAA failed to elicit a similar decrease in calcium levels in AWC (Figure 3A), correlating with loss of attraction to an IAA stripe in these conditions (Figure S1A,B). Addition of low hexanol concentrations that attracts wild-type animals also decreased calcium levels in AWC similar to observations with a pulse of low IAA concentrations (Figure 3B, Movie S2). However, when saturated with IAA, a pulse of hexanol instead increased intracellular calcium in AWC correlating with hexanol aversion under these conditions (Figure 3B, Movie S2). Animals also avoid heptanol in saturating IAA (Figure 1B); heptanol responses in AWC were also inverted in this context (Figure 3C). The AWC neuron pair exhibits bilateral response asymmetry to a subset of odorants and differential expression of a subset of chemoreceptors (Bauer Huang et al., 2007; Chalasani et al., 2007; Troemel et al., 1999; Vidal et al., 2018; Wes and Bargmann, 2001). Although we did not distinguish between the two neurons when examining hexanol- or heptanol-induced neuronal activity, ~90% of imaged AWC

neurons responded similarly to both hexanol and heptanol with and without saturating IAA (Figure 3B,C), implying that both AWC neurons are able to respond to these chemicals regardless of context. Hexanol-driven calcium increases and decreases in AWC were maintained in *unc-13* and *unc-31* mutants that lack synaptic and peptidergic transmission, respectively (Sieburth et al., 2007; Speese et al., 2007), indicating that these responses are mediated cell-autonomously (Figure S2B, Figure 3B).

We considered the possibility that upon saturation with IAA, addition of any AWC-sensed chemical also increases calcium levels in AWC. However, in IAA saturation conditions, a pulse of benzaldehyde again decreased calcium levels in AWC albeit with a significantly weaker amplitude than in control conditions (Figure 3D), consistent with decreased attraction, but not aversion, to a point source of benzaldehyde upon IAA saturation (Figure 1B). Similarly, upon saturation with hexanol, a pulse of IAA elicited variable responses of smaller amplitude but did not drive an inversion in the response sign, consistent with animals being indifferent to IAA in hexanol saturation conditions (Figure S2C, Figure S1A,B). Calcium levels were also robustly decreased by a pulse of the attractive chemical 2-methylpyrazine (Figure S2D). Upon saturation with IAA, this chemical again evoked variable responses of small amplitude but did not increase intracellular calcium levels in AWC (Figure S2D). Attraction to this chemical remained unaffected upon IAA saturation (Figure S2E), likely due to this behavior being driven by the AWA olfactory neuron pair which also responds to pyrazine but not IAA (Bargmann et al., 1993). These results indicate that odorant-mediated inhibition of AWC is not sufficient for any second AWC-sensed chemical to elicit an increase in intracellular calcium, and that the observed response sign switch

under these conditions may be restricted to specific odorants such as hexanol and heptanol.

We next tested whether saturation of AWC by an AWC-sensed odorant other than IAA would also result in hexanol-mediated activation and avoidance. Indeed, we found that saturation with benzaldehyde also resulted in hexanol-driven increases in calcium in AWC together with avoidance of hexanol (Figure 3E,F). If odorant saturation is permissive for the hexanol-driven rise in intracellular calcium, we would predict that addition of a mixture of hexanol and IAA would not be sufficient to evoke this response. Indeed, we found that a hexanol/IAA mixture reduced AWC calcium levels similar to the effects observed with hexanol or IAA alone (Figure 3G). Moreover, pre-exposure to saturating IAA was also not sufficient to increase calcium levels in AWC upon subsequent exposure to a hexanol pulse (Figure S2F). We conclude that while attractive chemicals typically decrease intracellular calcium in AWC, upon saturation with an AWC-sensed attractant, a pulse of medium-chain alcohols such as hexanol and heptanol instead increases intracellular calcium levels in AWC, and that this response is correlated with avoidance of these chemicals.

2.4.4 ASH responds similarly to hexanol in the absence or presence of a saturating odor

We next examined whether hexanol-evoked responses in ASH are also modulated by odorant context. We verified that the transgenic strain expressing GCaMP3 in ASH exhibited behavioral responses to hexanol similar to those of wild-type animals (Figure S3A). Similar to many chemical-evoked responses in ASH (Fukuto et al., 2004; Hilliard et al., 2004), hexanol elicited a robust phasic response in ASH

neurons with a rapid and transient rise upon hexanol addition (Figure 4A,B, Figure S3B). Response dynamics were similar in saturating IAA, although the response peak as well as the response baseline in the presence of hexanol were consistently higher as compared to the responses in control conditions (Figure 4A,B, Figure S3B). Responses rapidly returned to baseline upon hexanol removal in both the presence and absence of saturating IAA.

Hexanol responses in ASH in *unc-13* synaptic transmission mutants were similar to those in wild-type animals (Figure 4A,B, Figure S3C). However, in *unc-31* mutants defective in neuropeptidergic signaling (Ann et al., 1997; Sieburth et al., 2007; Speese et al., 2007), the dynamics of the hexanol response were altered such that the response appeared to be tonic in both control and IAA-saturated conditions (Figure 4B, Figure S3D). We tested whether peptidergic signaling from AWC might modulate hexanol response dynamics in ASH. Due to technical limitations, we could not assess hexanol responses in ASH in AWC-ablated animals. Sensory responses in AWC (including hexanol responses, see Figure 6A) are abolished in animals mutant for the *tax-4* cyclic nucleotide-gated channel (Bargmann et al., 1993; Komatsu et al., 1996). Hexanol responses in ASH in *tax-4* mutants resembled those in *unc-31* mutants (Figure S3E), suggesting that AWC may influence hexanol response dynamics in ASH in both control and IAA-saturated conditions. Together, these results indicate that unlike our observations in AWC, the sign of the hexanol response in ASH is unaltered in IAA-saturated conditions. However, while ASH responds cell-autonomously to hexanol, these responses may be modulated by AWC.

2.4.5 The ODR-3 Gα protein is necessary for the hexanol driven response sign switch in odorant saturation conditions

To probe the molecular mechanisms underlying the hexanol response sign switch in AWC, we tested the behaviors and hexanol responses of mutants previously implicated in AWC sensory signal transduction. Binding of odorants to their cognate receptors in AWC decreases intracellular cGMP levels either via inhibiting the activity of receptor guanylyl cyclases such as ODR-1 and DAF-11, and/or by promoting the activity of one or more phosphodiesterases, via heterotrimeric G proteins (Bargmann et al., 1993; Birnby et al., 2000; Ferkey et al., 2021; L'Etoile and Bargmann, 2000; Lans et al., 2004; Roayaie et al., 1998; Shidara et al., 2017). Reduced intracellular cGMP levels closes cGMP-gated channels, inhibits calcium influx, and promotes attraction (Figure 5A) (Chalasani et al., 2007; Coburn and Bargmann, 1996; Ferkey et al., 2021). While the identities of hexanol and IAA receptors in AWC are unknown, multiple Gα proteins are expressed in AWC and have been implicated in mediating odorant signal transduction in this neuron type (Ferkey et al., 2021; Jansen et al., 1999; Lans et al., 2004; Roayaie et al., 1998) (Figure 5A). The inversion in the hexanol response sign in AWC under control and saturating IAA conditions indicates that hexanol likely acts via distinct molecular mechanisms in AWC under different conditions to evoke a response.

We first examined the requirement of different G proteins in hexanol-evoked behaviors and responses in AWC. The ODR-3 $G\alpha_i$/$G\alpha_o$-like protein decreases although does not fully abolish attraction to multiple AWC-sensed chemicals including IAA (Kato et al., 2014; L'Etoile and Bargmann, 2000; Lans et al., 2004; Roayaie et al., 1998). We found that *odr-3* null mutants continued to be robustly attracted to hexanol, indicating

that this G protein is dispensable for this behavior (Figure 5B,C, Figure S4A). Animals mutant for the additional AWC-expressed nematode-specific Gα genes *gpa-2, gpa-3*, and *gpa-13*, as well as animals triply mutant for all three *gpa* genes, also retained the ability to be attracted to hexanol (Figure S4A). In contrast, *odr-3*, but not the *gpa* single or triple mutants, no longer avoided hexanol in saturating IAA, but were instead attracted, similar to the behavior of these animals under control conditions (Figure 5B,C, Figure S4A). *gpa-3 gpa-13 odr-3* triple mutants were also attracted to hexanol in saturating IAA (Figure S4A). Hexanol avoidance behavior was rescued upon expression of *odr-3* specifically in AWC (Figure 5B,C).

To correlate neuronal responses in AWC with behavior, we next examined hexanol-evoked intracellular calcium dynamics in *odr-3* animals. Under control conditions, a pulse of hexanol decreased intracellular calcium concentrations in AWC similarly in both wild-type and *odr-3* animals (Figure 5D,E). However, consistent with *odr-3* mutants retaining attraction to hexanol in saturating IAA, hexanol failed to increase calcium levels AWC in saturating conditions and instead continued to inhibit the neurons in these mutant animals (Figure 5D,E). Although this result implies that ODR-3 is necessary for hexanol to activate AWC in saturation conditions, a trivial explanation for the observed phenotype is that ODR-3 is required for IAA-mediated saturation in AWC, leading to similar hexanol-evoked responses in *odr-3* mutants in unsaturated and saturated conditions. ODR-3 has previously been shown to regulate rapid IAA-evoked calcium responses in AWC, such that in *odr-3* mutants, AWC retains the ability to respond to fluctuating IAA stimuli but on slower timescales, resulting in defective chemotaxis (Kato et al., 2014; Yoshida et al., 2012). Intracellular calcium

levels in AWC were decreased in response to a pulse of 10^{-4} IAA in *odr-3* mutants, indicating that consistent with previous observations, AWC is able to respond to this chemical (Figure S4B,C). However, the response amplitude as well as the number of responding neurons were decreased as compared to responses in wild-type animals (Figure S4B). We conclude that while hexanol attraction does not require ODR-3, ODR-3 is essential for the hexanol-mediated activation of AWC in odorant saturation conditions. However, we are unable to exclude the possibility that IAA does not fully saturate AWC in *odr-3* mutants, leading to a defect in hexanol-evoked activation of this neuron type.

2.4.6 Hexanol-mediated activation but not inhibition of AWC requires the ODR-1 receptor guanylyl cyclase

We next asked whether hexanol acts via distinct downstream effector pathways in AWC in the absence or presence of saturating IAA to decrease or increase intracellular calcium levels, respectively. Both activation and inhibition by hexanol were abolished in animals mutant for the *tax-4* cyclic nucleotide-gated channel, indicating that these responses require cGMP signaling (Figure 6A). Consistent with a demonstrated requirement for the ODR-1 receptor guanylyl cyclase in mediating odorant responses in AWC including responses to IAA (Bargmann et al., 1993; L'Etoile and Bargmann, 2000; Shidara et al., 2017), *odr-1* mutants failed to be attracted to hexanol and were instead weakly repelled (Figure 6B). However, *odr-1* mutant animals continued to robustly avoid hexanol in saturating IAA (Figure 6B), indicating that ODR-1 is dispensable for hexanol avoidance but is necessary for attraction.

Since ASH does not express *odr-1*, we tested the notion that AWC retains the ability to be activated but not inhibited by hexanol in *odr-1* mutants. Addition of IAA decreased intracellular calcium levels in AWC only to a minor extent in *odr-1* mutants (Figure S4B,C), consistent with the inability of these animals to be attracted to IAA in behavioral assays. Similarly, hexanol-evoked decreases in intracellular calcium in AWC in *odr-1* mutants were also significantly decreased (Figure 6C). However, in saturating IAA, hexanol robustly increased intracellular calcium levels AWC in *odr-1* mutants, correlated with these mutants retaining the ability to avoid hexanol (Figure 6C). These results indicate that while hexanol acts via ODR-1 to inhibit AWC in control conditions, in saturating IAA, hexanol acts via a distinct signaling pathway to activate these neurons.

2.5 Discussion

Animals assign valence to an odor based on innate preferences or learned association with positive or negative experiences (Knaden and Hansson, 2014; Li and Liberles, 2015; Mori and Sakano, 2021; Sachse and Beshel, 2016; Stowers and Kuo, 2015; Takahashi, 2014). However, even innate responses to a chemical are flexible, and can be extensively modified by experience and context (Grunwald Kadow, 2019; Stowers and Liberles, 2016). Here we show that the behavioral response of *C. elegans* to a food-related odor is inverted from attraction to avoidance in the continuous presence of a second background chemical. We find that this behavioral inversion is correlated with an inversion in the sign of the odorant response in a single olfactory neuron type. This response sign switch is affected by the engagement of different

intracellular signal transduction pathways in different chemical environments. Bidirectional responses of neurons such as parietal eye photoreceptors in lower vertebrates and olfactory neurons of *Drosophila* in response to different stimuli have been reported previously (Cao et al., 2017; Hallem and Carlson, 2006; Hallem et al., 2004; Solessio and Engbretson, 1993; Su et al., 2006). Inhibition or excitation of single sensory neuron types in these examples is mediated by distinct stimuli such as blue or green light, or different odors. In this work we describe a mechanism by which a single chemical evokes bidirectional sensory responses in a context-dependent manner in a single chemosensory neuron type, and suggest that related principles may underlie aspects of stimulus encoding and stimulus discrimination across sensory modalities.

Similar to other sensory neurons in *C. elegans*, the AWC neurons express multiple (>20) odorant receptors, Gα protein subunits, two transmembrane guanylyl receptor cyclases, several phosphodiesterases, as well as multiple subunits of cyclic nucleotide-gated sensory transduction channel (Ferkey et al., 2021). In control conditions, we propose that hexanol interacts with its cognate receptor(s) in AWC and Gα proteins other than or in addition to ODR-3 to inhibit the ODR-1 receptor guanylyl cyclase. The consequent decrease in intracellular cGMP levels closes the TAX-2/TAX-4 channels and decreases intracellular calcium concentrations (Chalasani et al., 2007) (Figure 7A). However, in the presence of saturating AWC-sensed chemicals, the hexanol receptor instead likely acts via the ODR-3 Gα protein to activate a receptor guanylyl cyclase other than ODR-1 or inhibit a phosphodiesterase to increase cGMP levels, open the TAX-2/TAX-4 channels and increase intracellular calcium to activate AWC (Figure 7A). The engagement of distinct signaling pathways in distinct odorant

contexts suggests that the observed increase in hexanol/heptanol-evoked intracellular calcium levels under odorant saturation conditions is unlikely to simply be due to disinhibition, but instead represents a stimulus-driven neuronal response. We propose that the hexanol-evoked inhibition of AWC overrides the response in ASH to drive robust hexanol attraction in control conditions. In contrast, in saturating odor, either activation of AWC or ASH is sufficient to drive hexanol avoidance (Figure 7B).

How might hexanol engage different downstream effector pathways under different odorant conditions? In one model, occupancy of a shared receptor by IAA may antagonize hexanol binding, and drive hexanol-mediated activation of a different signaling pathway via alternate AWC-expressed hexanol receptor(s). Antagonism of olfactory receptors by odorants in mixtures has now been extensively described and shown to play a role in stimulus encoding and odorant discrimination (Araneda et al., 2000; Araneda et al., 2004; Kurian et al., 2021; Oka et al., 2004; Pfister et al., 2020; Reddy et al., 2018; Xu et al., 2020; Zak et al., 2020). However, a mixture of IAA and hexanol does not activate AWC, and moreover, saturation with the structurally distinct chemical benzaldehyde is also sufficient to activate this neuron type. Although we are unable to exclude the possibility that AWC-sensed chemicals share a broadly tuned receptor that alters neuronal responses based on odorant context (MacWilliam et al., 2018; Turner and Ray, 2009), we instead favor the possibility that saturation with one chemical alters neuronal state in a manner that then dictates the differential usage of intracellular signaling pathways to elicit distinct sensory responses. The as yet unidentified hexanol (and heptanol) receptor(s) may be posttranslationally modified in a neuronal state-dependent manner to promote coupling to distinct effector pathways

upon ligand binding (Calebiro et al., 2021; Flock et al., 2017; Patwardhan et al., 2021). It is also possible that differential compartmentalization of signaling complexes within the AWC sensory cilia membrane promotes the usage of distinct signal transduction machinery in different neuronal conditions (Ellisdon and Halls, 2016; Hilgendorf et al., 2019; L'Etoile and Bargmann, 2000; Langeberg and Scott, 2015; Magalhaes et al., 2012; Polit et al., 2020). We note that this mechanism of odorant discrimination appears to be largely restricted to hexanol and heptanol among our tested odorants. Branched and straight-chain alcohols are produced by multiple bacteria that are food sources for *C. elegans* (Elgaali et al., 2002; Worthy et al., 2018). The ethological relevance of hexanol and heptanol-evoked avoidance in the presence of other AWC-sensed attractive chemicals remains to be determined.

State-dependent behavioral plasticity is a well-established phenomenon (Kim et al., 2017; Kong and Zweifel, 2021; Smith and Torregrossa, 2021; Stowers and Liberles, 2016). For instance, in *Drosophila*, starvation increases the palatability of food-related odors and decreases or switches the avoidance response to noxious stimuli (Devineni et al., 2019; Inagaki et al., 2012; LeDue et al., 2016; Root et al., 2011; Vogt et al., 2021). Attraction driven by AWC and other sensory neurons has also previously been shown to be markedly reduced or switched to avoidance in specific mutant backgrounds or upon association with starvation and odorant experience (Adachi et al., 2010; Cho et al., 2016; Colbert and Bargmann, 1995; L'Etoile et al., 2002; Ohno et al., 2014; Tomioka et al., 2006; Tsunozaki et al., 2008). However, unlike the mechanism described in this work, many of these forms of behavioral plasticity including those mediated by AWC, are regulated by modulation of synaptic transmission and downstream integration in the

circuit, with little to no changes in the primary sensory response. A potential advantage of differential usage of intracellular signaling pathways over modulation of sensory neuron synaptic output is the ability to discriminate between, and differentially respond to, each stimulus sensed by that neuron in a context-dependent manner. This mechanism may be particularly relevant for polymodal sensory neurons such as those in *C. elegans* (Ferkey et al., 2021) in which state-dependent engagement of different signaling molecules and pathways within a single sensory neuron type may fine-tune the response and allow animals to more effectively assess the salience of individual olfactory cues. Subsets of chemosensory neurons in *Drosophila* and *Aedes aegypti* have also now been reported to co-express chemosensory receptors and may also utilize similar principles for chemical coding and discrimination (McLaughlin et al., 2021; Task et al., 2020; Younger et al., 2020).

While hexanol responses in AWC are distinct in control and saturation conditions, the sign of the response in ASH is unaffected by odorant context. However, hexanol response dynamics in ASH may be modulated by AWC directly or indirectly (Duan et al., 2020; Ezcurra et al., 2016; Guo et al., 2015; Krzyzanowski et al., 2016; Leinwand and Chalasani, 2013; Wu et al., 2019) (Figure 7B). Chemicals are recognized by multiple receptors of different affinities expressed in different sensory neuron types and also in non-neuronal cells, and generally, each receptor also responds to multiple odorants (Ahn et al., 2017; Araneda et al., 2000; Duan et al., 2020; Liberles and Buck, 2006; Malnic et al., 1999; Nara et al., 2011; Oka et al., 2013; Saraiva et al., 2016; Yoshida et al., 2012). Population coding and integration of distinct patterns of combinatorial excitatory and inhibitory inputs from multiple chemosensory neuron

channels contribute to odor coding particularly of complex odor blends, and also permits additional state-dependent behavioral plasticity (Bell and Wilson, 2016; Cao et al., 2017; Dobosiewicz et al., 2019; Hukema et al., 2006; Inagaki et al., 2020; Jang et al., 2019; Knaden et al., 2012; Kreher et al., 2008; Kurian et al., 2021; MacWilliam et al., 2018; Reddy et al., 2018; Saraiva et al., 2016; Tumkaya et al., 2021; Xu et al., 2020; Zak et al., 2020). Chemical encoding strategies in *C. elegans* have largely been studied in response to monomolecular odorants. It will be important to expand this analysis to different odorant contexts and mixtures presented in different temporal sequences to more closely resemble environments that worms may encounter in the wild to more completely describe how chemical stimuli are represented and interpreted by the sensory nervous system of these animals.

Findings described here further highlight the remarkable flexibility of neuron and neuronal circuit functions. As the signaling content of sensory cells across different organisms is described more fully via single cell transcriptomics approaches (Kozma et al., 2020; McLaughlin et al., 2021; Taylor et al., 2021; van Giesen et al., 2020; Zheng et al., 2019), a challenging next step will be to assess how different intra- and intercellular pathways are used under different conditions, and how this response flexibility is translated through the circuit to drive adaptive behavioral responses.

2.6 Methods

2.6.1 Strains and growth conditions

All *C.elegans* strains were maintained on nematode growth medium (NGM) at 20°C. 5 days prior to behavioral assays, 10 L4 larvae per genotype were picked to 10 cm assay growth plates (day 1), and young adults were tested in behavioral and calcium imaging assays 4 days later (day 5). Animals were maintained under well-fed conditions at all times.

To standardize growth conditions, NGM plates were seeded with bacteria as follows: concentrated *Escherichia coli* OP50 was cultured by inoculating 10 µl of a starter OP50 culture (grown in LB for ~2 hr from a single colony) per 1L of SuperBroth media (3.2% w/v tryptone, 2.0% yeast extract, 0.5% NaCl). SuperBroth cultures grown overnight were treated with a low concentration of the antibiotic gentamicin (300 ng/ml; Sigma G1397) for ~4 hours, centrifuged for 20 minutes at 4°C, and the resulting pellets resuspended in 75 ml of S-Basal buffer. The concentrated bacterial food was stored at -80°C and thawed as needed to seed plates (1 ml/10cm plate).

All strains were constructed using standard genetic procedures. The presence of mutations was confirmed by PCR-based amplification and/or sequencing. *odr1*p*::odr-3::SL2::mCherry* (PSAB1269) plasmid was injected at 10 ng/µl together with the *unc-122*p*::gfp* co-injection marker at 50 ng/µl to generate transgenic rescue strains. Expression patterns and phenotypes were confirmed in initial experiments using multiple independent transgenic lines, and a single line was selected for additional analysis. A complete list of strains used in this work is provided in Table S1.

2.6.2 Molecular biology

An *odr-3* cDNA (Roayaie et al., 1998) was cloned into a worm expression plasmid containing ~1.0 kb upstream *odr1* regulatory sequences using standard restriction enzyme cloning (PSAB1269).

2.6.3 Plate chemotaxis assays

Chemotaxis assays were performed according to previously published protocols (Bargmann et al., 1993; Troemel et al., 1997). Assays were performed on 10 cm square or round plates with two 1 µl spots of odorant and the diluent ethanol at either end, together with 1µl of 1 M sodium azide at each spot to immobilize worms. Odorants were diluted freshly in ethanol as needed. Saturation assays were performed using the same protocol, except that the relevant odorant was added to the assay agar before pouring plates (1 µl diluted odorant /10ml agar). Animals were washed off growth plates with S-Basal and washed twice subsequently with S-Basal and once with Milli-Q water. Washed animals were placed at the center of the assay plate and allowed to move for an hour. The number of worms in two horizontal rows adjacent to the odor and ethanol spots was quantified at the end of the assay. Each assay was performed at least in duplicate each day; data are reported from biologically independent assays performed on at least 3 days.

2.6.4 Osmotic avoidance assay

Osmotic avoidance behavior assays were performed essentially as previously described (Cornils et al., 2016; Culotti and Russell, 1978). 10 young adult worms were

transferred without food to an agar plate and allowed to recover for at least 2 min. They were then placed in the center of an NGM plate with a ring of 8M glycerol containing bromophenol blue (Sigma B0126). The number of worms inside and outside of the ring was counted after 10 minutes.

2.6.5 Microfluidics behavioral assays

Microfluidics assays were performed following published protocols, using custom designed microfluidic devices (Albrecht and Bargmann, 2011). The assembled microfluidic device was degassed in a vacuum desiccator for ~30 minutes prior to loading a 5% w/v poloxamer surfactant (Sigma P5556) with 2% xylene cyanol (2 mg/ml) solution through the outlet port. These steps ensured that the arena was bubble-free prior to loading the worms and stimulus reservoirs. Buffer and stimulus flowed by gravity from elevated reservoirs and were controlled with manual Luer valves. 20-30 young adult animals were transferred to unseeded plates and flooded with S-Basal buffer to remove any residual bacteria. The worms were then transferred into a tube and gently loaded into the buffer-filled arena via syringe. After allowing the worms to disperse throughout the arena (~5 min), the flow of the odorant stimulus was started. 3 parallel stripes flowed through the stimulus; 2 outer stripes consisted of buffer and the central stripe contained the odorant. 2% xylene cyanol (2 mg/ml) was added to the odorant to allow visualization and tracking. For IAA saturation assays, in addition to the stimulus odorant in the middle stripe, 10^{-4} IAA was included in all buffer and stimulus reservoirs. Movies were recorded at 2 Hz on a PixelLink camera while worms were exposed to 20 minutes of constant odor. Following each experiment, the devices were flushed with

water and soaked in ethanol overnight to remove any residual odorant. Prior to using the devices for additional assays, the chip was rinsed in water and baked at 50°C for a minimum of 4 hours to evaporate any residual ethanol odor and liquid. The cleaning procedure was validated by buffer-buffer control assays, in which worms showed no spatial preference.

All movie acquisition, processing, and subsequent behavioral analysis was performed via custom MATLAB software modified from (Albrecht and Bargmann, 2011). Data visualization and figures were generated using RStudio (version 1.3.959). A minimum of 3 assays per condition were performed on multiple days, and mean relative residency and chemotaxis index in respect to spatial stimuli was calculated. Briefly, the *y*-position data were binned into 50 bins for each assay. Relative residence was calculated by counting the # of tracks in each of the 50 *y*-position bins, and dividing each of these counts by the average # of counts across all 50 bins. Average residency histograms show the average of these residency values for each *y*-position bin over 3 assays/condition. Chemotaxis index was calculated as (normalized # of tracks within the odorant – normalized # of tracks in buffer)/total # of normalized tracks. Track numbers were normalized by calculating the # tracks X (total length of arena/ length of respective buffer or odorant region). Stripe boundaries containing the odorant were determined using luminance data using xylene cyanol dye. To account for variable luminance across the device, luminance values were normalized using a linear regression fit. Boundaries were identified as the first and second sign switch of luminance values using the normalized luminance data.

2.6.6 Calcium imaging

Calcium imaging was performed as previously described, using custom microfluidic devices (Chronis et al., 2007; Neal et al., 2015). Imaging was conducted on an Olympus BX52WI microscope with a 40X oil objective and Hamamatsu Orca CCD camera. Recordings were performed at 4 Hz. All odorants were diluted in S-Basal buffer and 1 µl of 20 µM fluorescein was added to one of the channels to confirm correct fluid flow. IAA saturation assays included IAA (1:10,000) in all channels, including the worm loading buffer. 1 mM (-)-tetramisole hydrochloride (Sigma L9756) was added to the S-Basal buffer to paralyze body wall muscles and keep animals stationary. To prevent the chip from clogging, poloxamer surfactant (Sigma P5556) was also added to S-Basal while loading the worms. Odor evoked calcium transients in AWC and ASH sensory neurons were similar in the presence or absence of these chemicals. AWC and ASH neurons were imaged for one cycle of 30s buffer/30s odor/30s buffer stimulus. Imaging was also performed in the presence of buffer only each imaging day to ensure that observed neuronal responses were to the odor stimulus and not artefactual. Recorded image stacks were aligned with Fiji using the Template Matching plugin, and cropped to a region containing the cell body. The region of interest (ROI) was defined by outlining the desired cell body; background subtracted fluorescence intensity of the ROI was used for subsequent analysis. To correct for photobleaching, an exponential decay was fit to fluorescence intensity values for the first 30s and the last 20s of imaging (prior and post stimulus). The resulting curve was subtracted from original intensity values. Amplitude was calculated as maximum change in fluorescence ($F-F_0$) in the 10s following odor addition; F_0 was set to the average $\Delta F/F$ value for 5s before odor onset.

Data visualization and figures were generated using RStudio (version 1.3.959). Reported data were collected from biologically independent experiments over at least 2 days.

2.6.7 Statistical analyses

Excel (Microsoft) and GraphPad Prism version 9.0.2 (www.graphpadpad.com) were used to generate all chemotaxis plate assay data. Plate chemotaxis index and peak $\Delta F/F_0$ amplitude data were analyzed using the Mann Whitney Wilcoxon or Kruskal-Wallis tests followed by the posthoc pairwise Wilcoxon test and Benjamini-Hochberg method for p-value correction. Chemotaxis index data derived from microfluidics behavioral assays were analyzed using one-way or two-way ANOVA followed by Bonferroni's multiple comparison test. All statistical analyses were performed in R (https://www.R-project.org/) and RStudio (http://www.rstudio.com), and GraphPad Prism version 9.0.2 (www.graphpadpad.com). The tests used are indicated in the corresponding Figure Legends.

2.7 Acknowledgements

We are grateful to the *Caenorhabditis* Genetics Center and Steven Flavell, Yun Zhang, and Gert Jansen for providing strains, and the Brandeis Materials Research Science and Engineering Center (MRSEC) for access to the microfabrication facility. We thank members of the Sengupta lab for critical comments on the manuscript. This work was supported in part by the NSF (IOS 165518 and IOS 20142100 – P.S., MRSEC 2011846), and the NIH (F31 DC015186 - A.H.).

2. 8 Figure legends

Figure 1. Animals avoid normally attractive medium-chain alcohols in saturating IAA.

A) (Left) Cartoon of assay setup (see Methods). Filled circles: location of 1 µl each of the test odorant; open circles: location of 1 µl each of the ethanol diluent. Positive and negative chemotaxis indices indicate attraction and avoidance, respectively. (Right) Behaviors of wild-type animals on control or IAA-saturated plates. Test odorants used were 1:200 dilution of benzaldehyde (BZ) or 1:1000 dilution of IAA.

B) Behaviors of wild-type animals on control and IAA-saturated plates containing undiluted (left) or 1:10 dilution (right) of the indicated alcohols as the test odorant.

C) Behaviors of wild-type animals on control plates or plates saturated with either hexanol or 1-heptanol. A 1:1000 dilution of IAA was used as the test odorant.

D) Behaviors of wild-type animals on control or IAA-saturated plates to the indicated concentrations of hexanol.

In **A-C**, each dot represents the chemotaxis index of a single assay plate containing ~100-200 adult hermaphrodites. Long horizontal bars indicate the mean; errors are SEM. In **D),** each dot represents the average chemotaxis index of 3-4 independent assays of ~100-200 animals each. Errors are SEM. Assays were performed in duplicate over at least 3 days. Odorant saturation was performed using 1 µl of 10^{-4} dilution of the indicated odorant per 10 ml of agar. **, *** - different from indicated control **(A-C)** or respective control at that concentration **(D)** at $P<0.01$ and 0.001, respectively (Kruskal-Wallis with posthoc pairwise Wilcoxon test followed by Benjamini-Hochberg method for p-value correction); ns: not significant.

Figure 2. The AWC neurons drive attraction or avoidance in the absence or presence of saturating IAA.

A) Schematic of the microfluidics behavioral device used in behavioral assays. The test odorant together with a visible dye is presented in a stripe through the center of the device. Adapted from (Albrecht and Bargmann, 2011).

B-E) Average histograms showing mean relative residence (relative to spatial odor pattern) of animals of the indicated genotypes over 20 minutes in devices with a central stripe of 10^{-4} hexanol without (left), or with, a uniform concentration of 10^{-4} IAA (right) in the device. Mean relative residence >1 or <1 (dashed vertical line) indicate attraction and avoidance, respectively. Corresponding heat maps show the density of tracks in the *y*-position for each individual assay. n=20-30 animals per assay.

F) Chemotaxis indices calculated from behavioral assays shown in **B-E**. Each dot represents the chemotaxis index from a single assay in behavior chips. Long horizontal bars indicate the mean; errors are SEM. *** - different from indicated control at $P<0.001$ (two-way ANOVA followed by Bonferroni's multiple comparison test); ns: not significant. Also see Figure S1.

Figure 3. Hexanol-mediated inhibition of AWC is switched to activation in saturating odor conditions.

A-E, G) (Left) Average changes in GCaMP3 fluorescence in AWC in response to a 30s pulse of 10^{-4} dilution of the indicated odorant (solid line). The presence of saturating chemicals in the imaging chip at 10^{-4} dilution is indicated by a dashed line. Shaded regions indicate SEM. Corresponding heatmaps of changes in fluorescence intensity

are shown to the right **(A,B,G)** or below **(C-E).** Each row in the heatmaps shows responses from a single AWC neuron from different animals; n = ≥15 each. (Right) Quantification of peak fluorescence intensity changes upon odorant onset under non-saturated or saturated conditions. Each dot represents the response from a single neuron. Wild-type hexanol response data were interleaved with experimental data in **B, E**, and **G** and are repeated. Control wild-type IAA response data were interleaved with experimental data in **A** and Figure **S2C** and are repeated. Alleles used in **B** were *unc-13(e51)* and *unc-31(e928)*. Long horizontal bars indicate the mean; errors are SEM. **, *** indicate different between indicated at *P* <0.01 and 0.001 and, respectively (**A, C-E**: Mann Whitney Wilcoxon test; **B**: Kruskal-Wallis with posthoc pairwise Wilcoxon test followed by Benjamini-Hochberg method for p-value correction); ns – not significant. Average traces and heatmaps of responses in *unc-13* and *unc-31* mutants are shown in Figure S2B.

F) Behavioral responses of animals to a point source of undiluted hexanol on plates with or without saturating benzaldehyde at 10^{-4} dilution. Each dot represents the chemotaxis index of a single assay plate containing ~100-200 adult hermaphrodites. Thick horizontal bars indicate the mean; errors are SEM. Assays were performed in duplicate over at least 3 days. Errors are SEM. *** - different from indicated control at *P*<0.001 (Mann Whitney Wilcoxon test followed by Benjamini-Hochberg method for p-value correction); ns – not significant.

HEX – 1-hexanol, HEPT- 1-heptanol, BZ - benzaldehyde. Also see Figure S2.

Figure 4. The ASH neurons are activated by hexanol in the absence of presence of saturating IAA.

A) Average changes in GCaMP3 fluorescence in ASH in response to a 30s pulse of 10^{-4} dilution of hexanol (solid line). The presence of saturating IAA in the imaging chip at 10^{-4} dilution is indicated by a dashed line. Shaded regions indicate SEM. Corresponding heatmaps of changes in fluorescence intensity are shown below. Each row in the heatmaps shows responses from a single ASH neuron from different animals ordered by the time of the first response; n = ≥15 each.

B) Quantification of peak fluorescence intensity changes upon hexanol odor onset under non-saturated or IAA-saturated conditions. Each dot represents the response from a single neuron. Alleles used were *unc-13(e51)* and *unc-31(e928)*. Long horizontal bars indicate the mean; errors are SEM. *, ** indicate different between indicated at *P*<0.05 and 0.01, respectively (Kruskal-Wallis with posthoc pairwise Wilcoxon test followed by Benjamini-Hochberg method for p-value correction); ns- not significant. Average traces and heatmaps of responses in *unc-13* and *unc-31* mutants are shown in Figure S3B.

Figure 5. The ODR-3 Gα protein is required for hexanol-mediated activation of AWC in saturating IAA.

A) Cartoon of the olfactory signal transduction pathway in AWC. Odorant binding to cognate receptors decreases intracellular cGMP via Gα protein-mediated inhibition of receptor guanylyl cyclases such as ODR-1 (and/or activation of multiple phosphodiesterases), closes cyclic nucleotide-gated channels encoded by *tax-2* and

tax-4, and decreases intracellular calcium. Odorant-mediated inhibition of AWC drives attraction.

B) Average histograms showing mean relative residence (relative to spatial odor pattern) of animals of the indicated genotypes over 20 minutes in devices with a central stripe of 10^{-4} hexanol without (left), or with, a uniform concentration of 10^{-4} IAA (right) in the device. Mean relative residence >1 or <1 (dashed vertical line) indicate attraction and avoidance, respectively. Corresponding heat maps show the density of tracks in the *y*-position for each individual assay. n=20-30 animals per assay. An *odr-3* cDNA was expressed in AWC under the *odr-1* promoter. **C)** Chemotaxis indices calculated from behavioral assays shown in **B.** Each dot represents the chemotaxis index from a single assay in behavior chips. Long horizontal bars indicate the mean; errors are SEM. *** - different from indicated at $P<0.001$ (two-way ANOVA followed by Bonferroni's multiple comparison test); ns: not significant.

D) (Left) Average changes in GCaMP3 fluorescence in AWC in wild-type and *odr-3(n2150)* mutants in response to a 30s pulse of 10^{-4} dilution of hexanol (solid line). The presence of saturating IAA in the imaging chip at 10^{-4} dilution is indicated by a dashed line. Shaded regions indicate SEM. (Right) Corresponding heatmaps of changes in fluorescence intensity. Each row in the heatmaps shows responses from a single AWC neuron from different animals; n = ≥15 each. Wild-type hexanol response data under IAA saturation conditions were interleaved with experimental data in Figure 6C, and are repeated.

E) Quantification of fluorescence intensity changes upon hexanol odorant onset under non-saturated or saturated conditions from data shown in **D**. Each dot represents the

response from a single neuron. Long horizontal bars indicate the mean; errors are SEM. *, *** - different from indicated at *P*<0.05 and 0.001, respectively (Kruskal-Wallis with posthoc pairwise Wilcoxon test followed by Benjamini-Hochberg method for p-value correction); ns – not significant.

Also see Figure S4.

Figure 6. The ODR-1 receptor guanylyl cyclase is required for hexanol-evoked inhibition but not activation of AWC.

A, C) (Left) Average changes in GCaMP3 fluorescence in AWC in response to 30s pulse of 10^{-4} dilution of hexanol without (solid line) or with saturating IAA (dashed line) in the imaging chip at 10^{-4} dilution in wild-type and *tax-4(p678)* **(A)** and *odr-1(n1936)* **(C)** animals. Corresponding heatmaps of changes in fluorescence intensity are shown below. Each row in the heatmaps shows responses from a single AWC neuron from different animals; n = ≥15 each. Shaded regions indicate SEM. (Right) Quantification of fluorescence intensity changes upon hexanol onset and offset under non-saturated or saturated conditions. Each dot represents the response from a single neuron. Thick horizontal bars indicate the mean; errors are SEM. *, *** - different from indicated at *P*<0.05 and 0.001, respectively (Kruskal-Wallis with posthoc pairwise Wilcoxon test followed by Benjamini-Hochberg method for p-value correction); ns – not significant.

B) Behavioral responses of animals to a point source of 1:10 dilution of hexanol on plates with or without saturating IAA at 10^{-4} dilution. Each dot represents the chemotaxis index of a single assay plate containing ~100-200 adult hermaphrodites. Long horizontal bars indicate the mean; errors are SEM. Assays were performed in duplicate over at

least 3 days. Errors are SEM. *** - different from indicated control at *P*<0.001 (Kruskal-Wallis with posthoc pairwise Wilcoxon test followed by Benjamini-Hochberg method for p-value correction).

Also see Figure S4.

Figure 7. Model of intracellular signaling and neuronal mechanisms driving context-dependent plasticity in hexanol responses.

A) In non-saturated conditions, hexanol inhibits the ODR-1 receptor guanylyl cyclase via Gα proteins other than or in addition to ODR-3 to decrease intracellular cGMP, close the TAX-2/TAX-4 cGMP-gated channels and inhibit AWC. In odor saturation conditions, hexanol instead acts via the ODR-3 Gα protein to activate a receptor guanylyl cyclase other than ODR-1, or inhibits a phosphodiesterase(s), to increase intracellular cGMP and activate AWC.

B) Hexanol inhibits or activates AWC and ASH, respectively in non-saturated conditions. AWC-driven attraction predominates over ASH-driven avoidance. When AWC is inhibited by saturating odors, hexanol activates both AWC and ASH. Either AWC or ASH can drive avoidance of hexanol in odorant saturation conditions. AWC may modulate ASH hexanol responses via peptidergic signaling (gray dashed arrow).

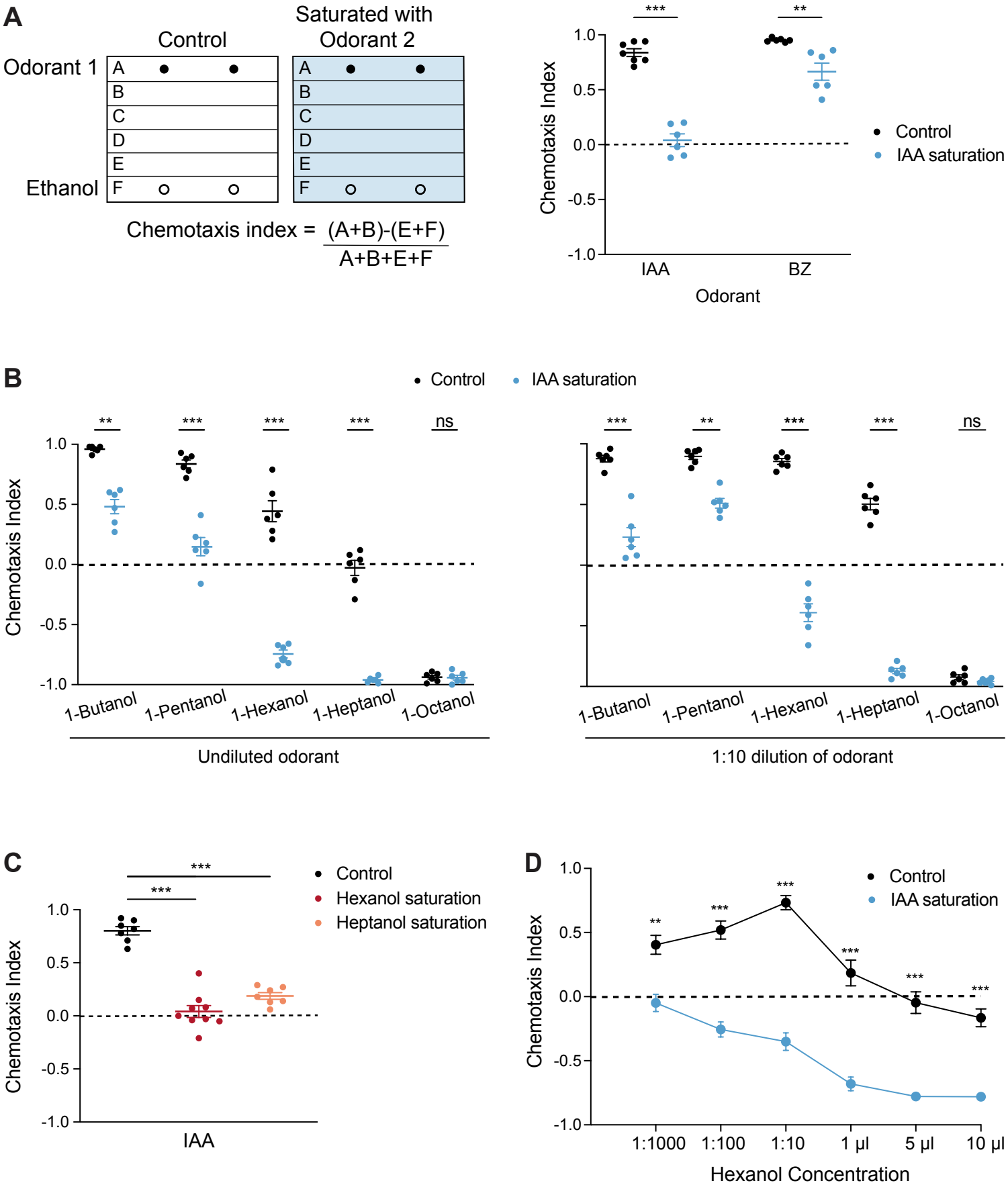

Khan et al., Figure 1

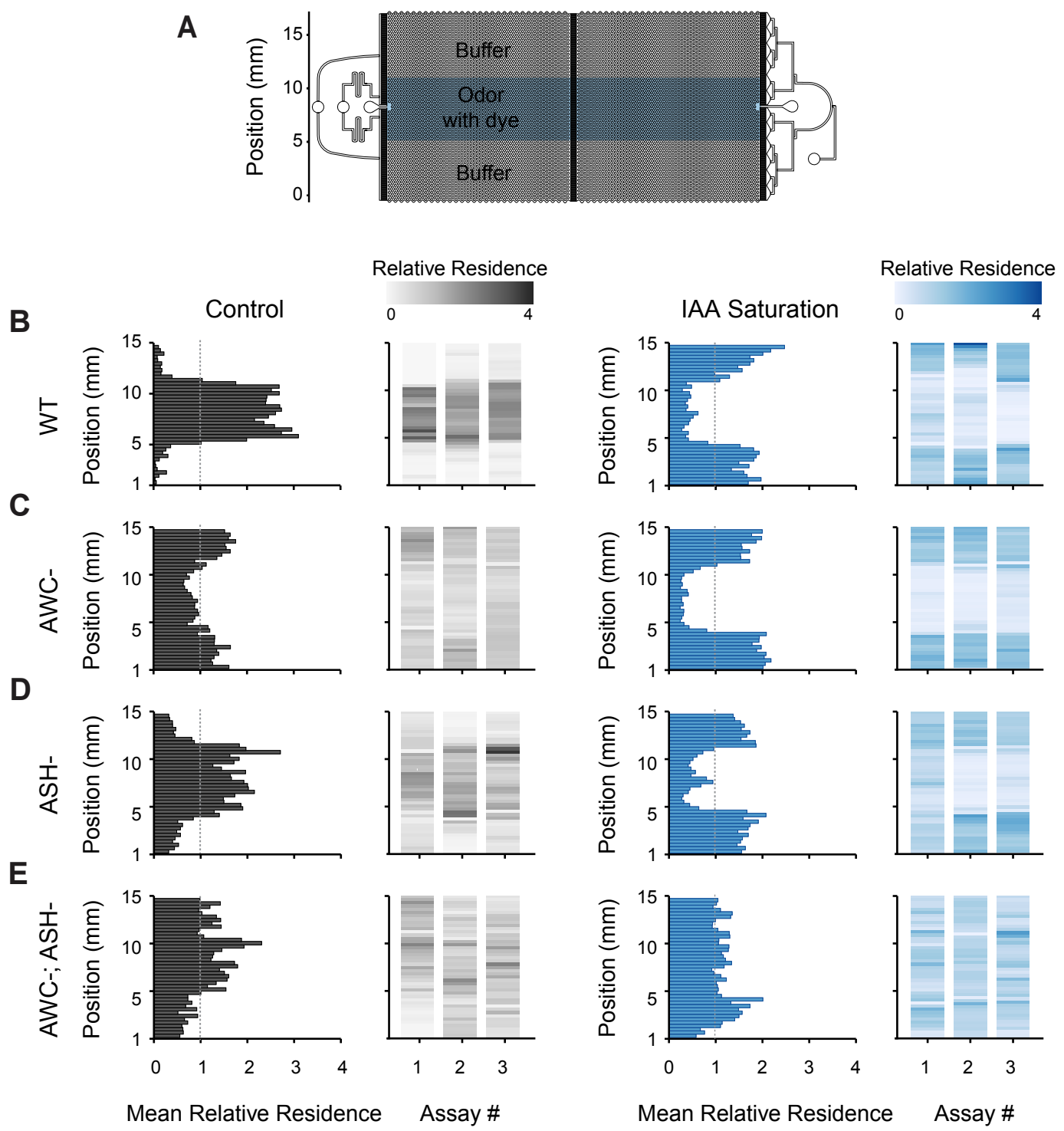

Khan et al., Figure 2

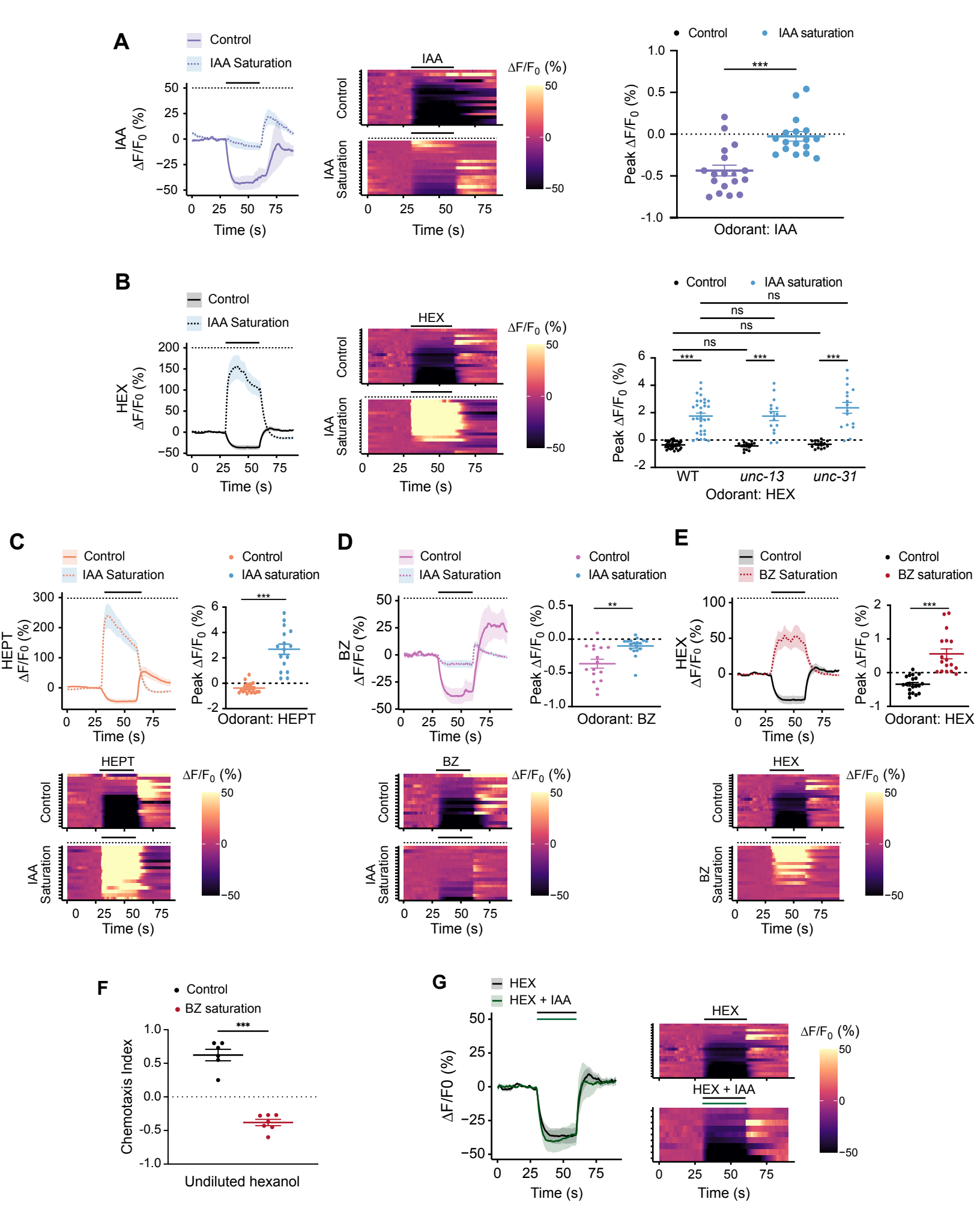

Khan et al., Figure 3

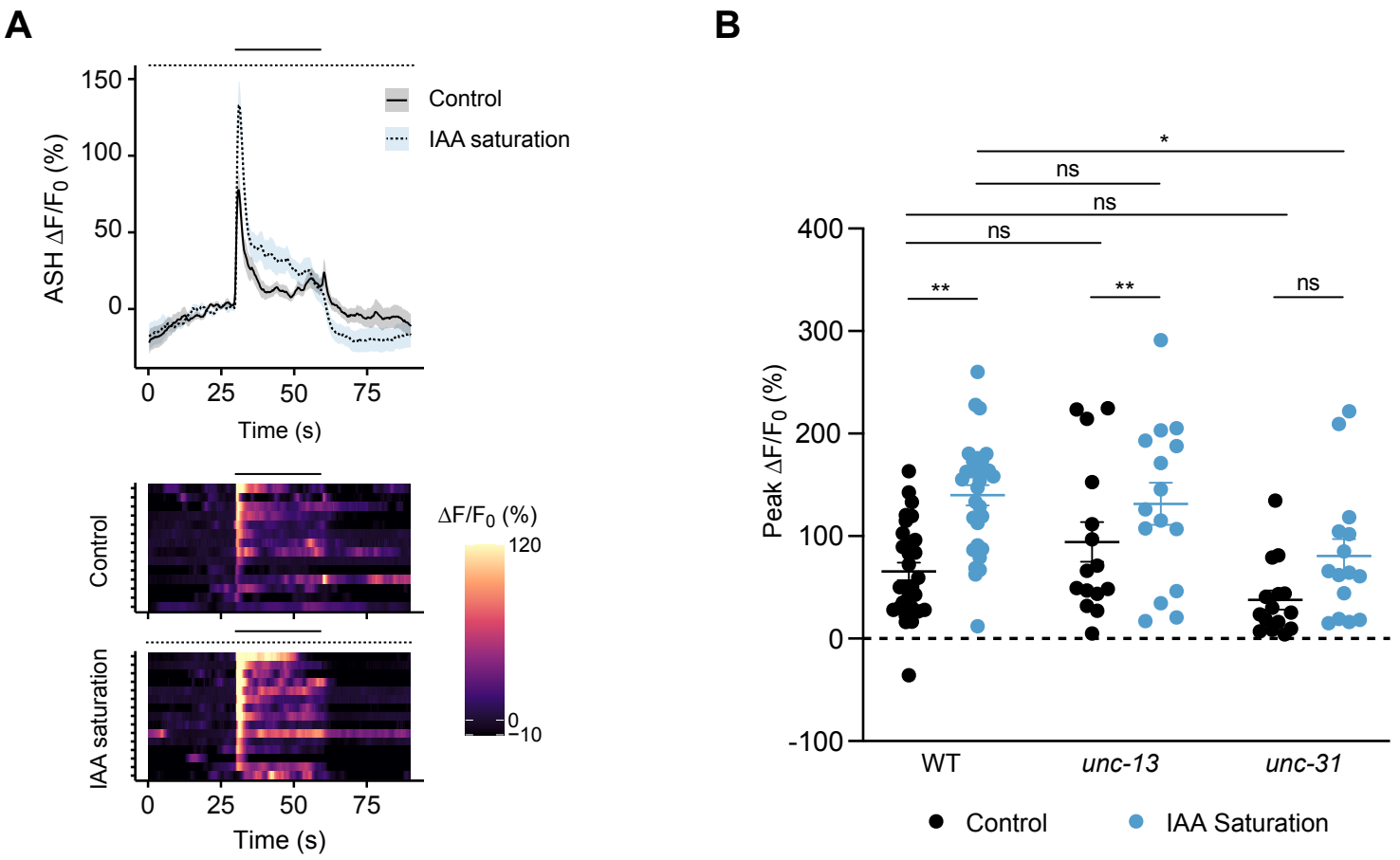

Khan et al., Figure 4

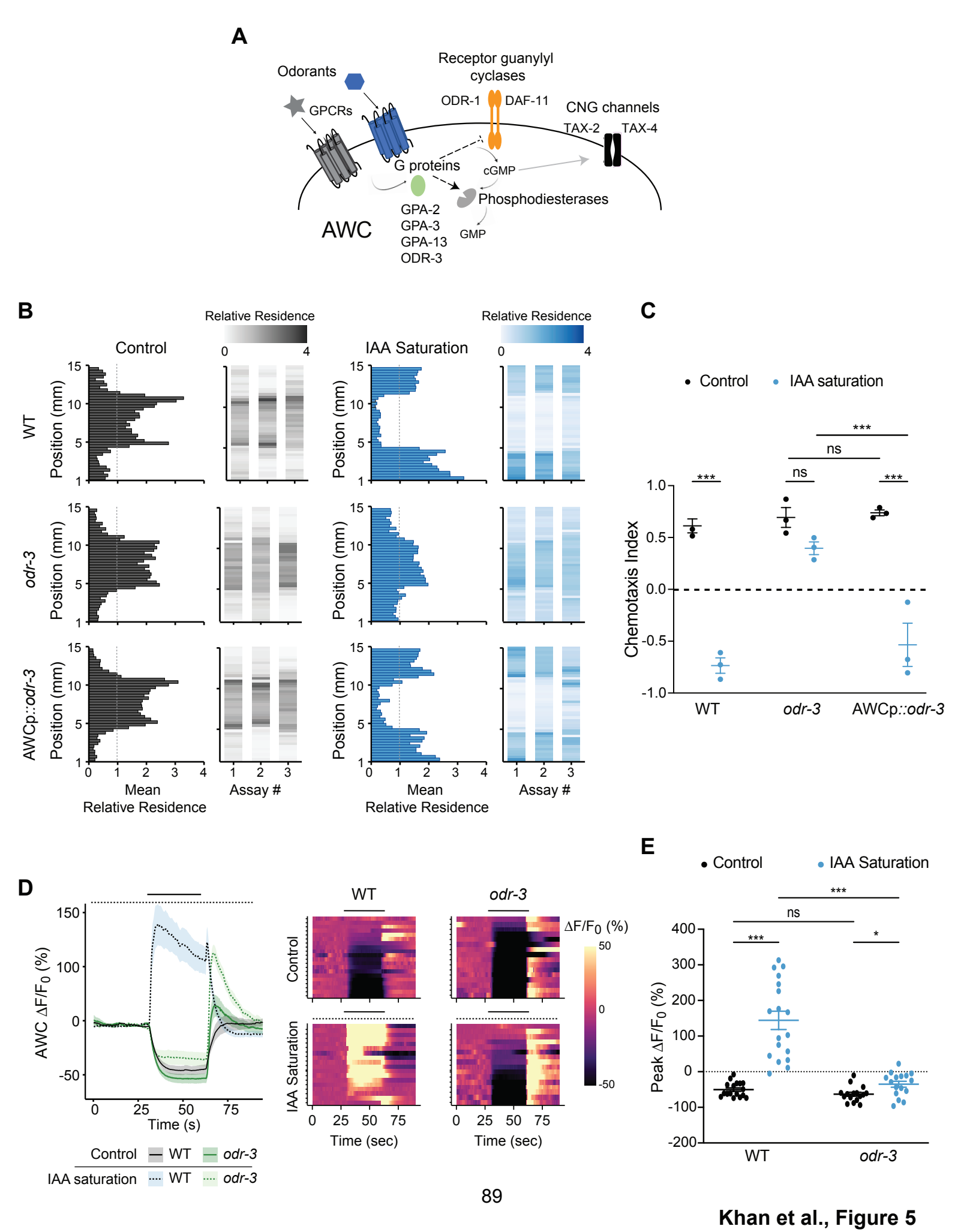

Khan et al., Figure 5

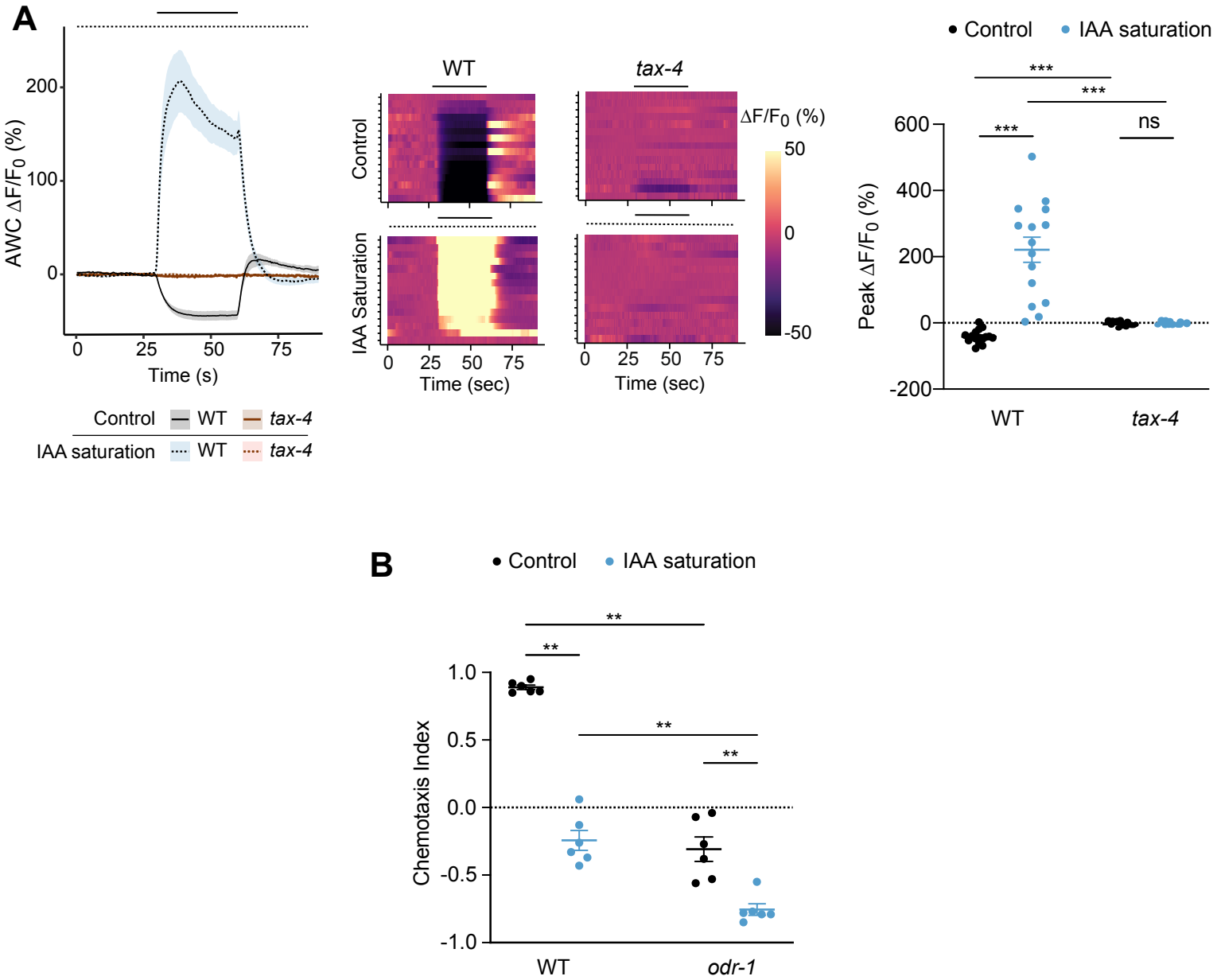
A
AWC ΔF/F0 (%)
Time (s)
Control WT tax-4
IAA saturation WT tax-4
WT
tax-4
Control
IAA Saturation
ΔF/F0 (%)
Time (sec)
Control
IAA saturation
Peak ΔF/F0 (%)
ns
WT
tax-4
B
Chemotaxis Index
WT
odr-1
C
AWC ΔF/F0 (%)
Time (s)
Control WT odr-1
IAA saturation WT odr-1
WT
odr-1
Peak ΔF/F0 (%)

A

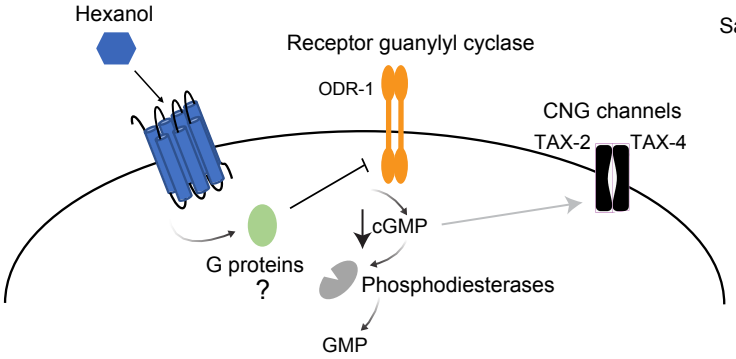

Decreased intracelullar Ca^{2+}: neuronal inhibition
Attraction

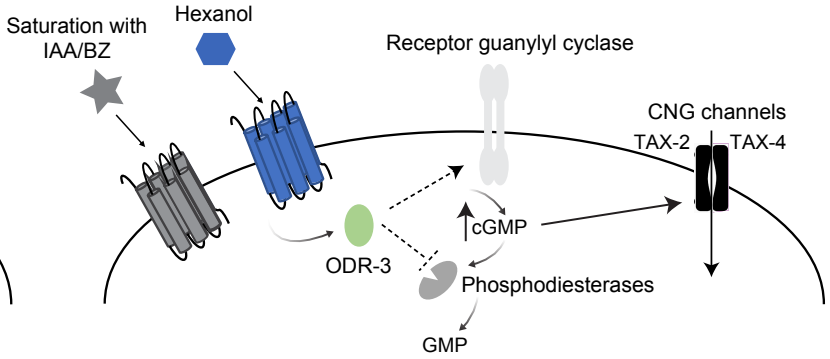

Increased intracellular Ca^{2+}: neuronal activation
Avoidance

B

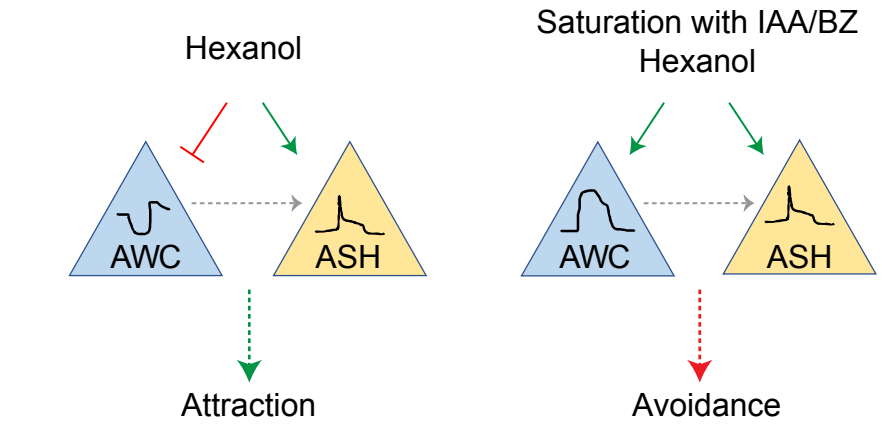

Khan et al.,

Fig. 7

2.8 Supplemental figure legends

Figure S1 related to Figure 2. The AWC sensory neurons are required for attraction to hexanol.

A) Average histograms showing mean relative residence (relative to spatial odor pattern) of wild-type animals over 20 minutes in devices containing buffer alone (left), a central stripe of 10^{-4} IAA (center), and a central stripe of 1:8000 dilution of IAA with a uniform concentration of 10^{-4} IAA (right) in the device. Mean relative residence >1 or <1 (dashed vertical line) indicate attraction and avoidance, respectively. Corresponding heat maps show the density of tracks in the *y*-position for each individual assay. n=20-30 animals per assay.

B) Chemotaxis indices calculated from behavioral assays shown in **A**. Each dot represents the chemotaxis index from a single assay in behavior chips.

C) Behaviors of animals of the indicated genotypes on control or IAA-saturated plates to undiluted hexanol. The *odr-1* promoter was used to drive *unc-103(gf)* in AWC (Yeon et al., 2021).

D) Behaviors of animals of the indicated genotypes to a 1:200 dilution of benzaldehyde.

E) Shown is the percentage of animals of the indicated genotypes that escaped a ring of 8M glycerol.

In **C,D**, each dot represents the chemotaxis index of a single assay plate containing ~100-200 adult hermaphrodites. In **E**, each dot represents a single osmotic avoidance assay of ~20 animals. Assays were performed in duplicate over at least 3 days. Long horizontal bars indicate the mean; errors are SEM. *, ** and *** are different between indicated at $P<0.05$, 0.01 and $P<0.001$, respectively (**B:** one-way ANOVA followed by

Bonferroni's multiple comparison test; **C**: Kruskal-Wallis with posthoc pairwise Wilcoxon test followed by Benjamini-Hochberg method for p-value correction ; **D,E**: Mann Whitney Wilcoxon test followed by Benjamini-Hochberg method for p-value correction)

Figure S2 related to Figure 3. Hexanol but not other odorants evokes an ON response in AWC under odorant saturation conditions.

A) Behaviors of wild-type or a strain expression GCaMP3 under the *odr-1* promoter in AWC to a point source of 1:10 dilution of hexanol on plates with or without saturating IAA at 10^{-4} dilution. Each dot represents the chemotaxis index of a single assay plate containing ~100-200 adult hermaphrodites. Long horizontal bars indicate the mean; errors are SEM. Assays were performed in duplicate over at least 3 days. *** - different from indicated control at $P<0.001$ (Kruskal-Wallis with posthoc pairwise Wilcoxon test followed by Benjamini-Hochberg method for p-value correction); ns – not significant.

B-D,F) Average changes in GCaMP3 fluorescence in AWC in response to a 30s pulse of 10^{-4} dilution of hexanol **(B,F)** or the indicated odorants **(C,D)** (solid line). The presence of saturating odorant in the imaging chip at 10^{-4} dilution is indicated by a dashed line. In **F**, animals were pre-exposed to a 10^{-4} dilution of IAA (see Methods). Shaded regions indicate SEM. Corresponding heatmaps of changes in fluorescence intensity are shown below **(B)** or to the right **(C,D,F).** Each row in the heatmaps shows responses from a single AWC neuron from different animals; n = ≥14 each. (Right in **C,D**) Quantification of peak fluorescence intensity changes upon odorant onset under non-saturated or saturated conditions. Each dot represents the response from a single neuron. Alleles used in **B** were *unc-13(e51)* and *unc-31(e928)*. Long horizontal bars

indicate the mean; errors are SEM. **, *** indicates different between indicated at *P*<0.01 and 0.001, respectively (Mann Whitney Wilcoxon test followed by Benjamini-Hochberg method for p-value correction). Quantification of responses in **B** are shown in Figure 3B. PYR – 2-methyl-1-pyrazine.

E) Behavioral responses of animals to a point source of 1 µl of 10 mg/ml dilution of 2-methylpyrazine (PYR) on plates with or without saturating IAA at 10^{-4} dilution. Each dot represents the chemotaxis index of a single assay plate containing ~100-200 adult hermaphrodites. Thick horizontal bars indicate the mean; errors are SEM. Assays were performed in duplicate over at least 3 days. ns – not significant.

Figure S3 related to Figure 4. ASH responds partly cell-autonomously to hexanol.

A) Behaviors of wild-type or a strain expressing GCaMP3 in ASH under the *sra-6* promoter to a point source of undiluted hexanol on plates without or with saturating IAA at 10^{-4} dilution. Each dot represents the chemotaxis index of a single assay plate containing ~100-200 adult hermaphrodites. Long horizontal bars indicate the mean; errors are SEM. Assays were performed in duplicate over at least 3 days. *** - different from indicated at *P*<0.001 (Kruskal-Wallis with posthoc pairwise Wilcoxon test followed by Benjamini-Hochberg method for p-value correction); ns – not significant.

B-E) Average changes in GCaMP3 fluorescence in ASH in response to a 30s pulse of 10^{-4} dilution of hexanol (solid line) in animals of the indicated genetic backgrounds. The presence of saturating IAA in the imaging chip at 10^{-4} dilution is indicated by a dashed line. Shaded regions indicate SEM. Corresponding heatmaps of changes in fluorescence intensity are shown below**.** Each row in the heatmaps shows responses

from a single ASH neuron from different animals ordered by the time of the first response; n = 10 (*tax-4*), 15 (all other genotypes). Alleles used were *unc-13(e51), unc-31(e928),* and *tax-4(p678)*. Quantification of peak response amplitudes are shown in Figure 4B.

Figure S4 related to Figures 5 and 6. Hexanol acts via distinct signaling pathways to inhibit or activate AWC in a context-dependent manner.

A) Behaviors of animals of the indicated genotypes (see Table S1) to a point source of 1:10 dilution of hexanol on plates with or without saturating IAA at 10^{-4} dilution. Each dot represents the chemotaxis index of a single assay plate containing ~100-200 adult hermaphrodites. Long horizontal bars indicate the mean; errors are SEM. Assays were performed in duplicate over at least 3 days. *** - different from indicated control at $P<0.001$ (Kruskal-Wallis with posthoc pairwise Wilcoxon test followed by Benjamini-Hochberg method for p-value correction); ns – not significant.

B) Average changes in GCaMP3 fluorescence in AWC in response to a 30s pulse of 10^{-4} dilution of IAA (solid line) in animals of the indicated genetic backgrounds. Alleles used were *odr-1(n1936)* and *odr-3(n2150).* Shaded regions are SEM. Corresponding heatmaps of changes in fluorescence intensity are shown at right**.** Each row in the heatmaps shows responses from a single AWC neuron from different animals; n = ≥15 each.

C) Quantification of peak response amplitudes from data shown in **B**. Long horizontal bars indicate the mean; errors are SEM. *, ** indicates different between indicated at

P<0.05 and 0.001, respectively (Kruskal-Wallis with posthoc pairwise Wilcoxon test followed by Benjamini-Hochberg method for p-value correction); ns – not significant.

Table S1. Strains used in this work.

Strain	Genotype	Source/parent strains	Relevant Figure(s)
WT	N2 (Bristol)	CGC	1A, 1B, 1C, 1D, 2B, 2F, 3F, 5B, 5C, 6B, S1A, S1B, S1C, S1D, S1E, S2A, S2E, S3A, S4A
PY7502	*oyIs85[ceh-36Δp::TU813(recCaspase), ceh-36Δp::TU814(recCaspase), unc-122p::dsRed, srtx-1p::gfp]*	(Beverly et al., 2011; Hawk et al., 2018)(Beverly et al., 2011; Hawk et al., 2018)	2C, 2F, S1D
PY12217	*oyEx677[odr-1p::unc-103(gf)::SL2::mCherry, unc-122p::gfp]* Line 1	(Yeon et al., 2021)	S1C
JN1713	*peIs1713[sra-6p::mCasp1, unc122p::mCherry]*	CGC	2D, 2F, S1E
PY10515	*oyIs85[ceh-36Δp::TU813(recCaspase), ceh-36Δp::TU814(recCaspase), unc-122p::dsRed, srtx-1p::gfp]; peIs1713 [sra-6p::mCasp1, unc-122p::mCherry]* Line 1	PY7502, JN1713	2E, 2F
PY12005	*kyIs602[sra-6p::GCaMP3, unc-122p::gfp]*	CX15030	4A, 4B, S3A, S3B
PY10511	*unc-13(e51); kyIs602[sra-6p::GCaMP3, unc-122p::gfp]* Line 1	MT7929, PY12005	4B, S3C
PY10513	*unc-31(e928); kyIs602[sra-6p::GCaMP3.0, unc-122p::gfp]* Line 1	CB928; PY12005	4B, S3D
PY10501	*oyIs91[odr-1p::GCaMP3, srsx-3p::mScarlet, unc-122p::dsRed]*	PY11610	3A, 3B, 3C, 3D, 3E, 3G 5D, 5E, 5F,

			6A, 6C, S2A, S2B, S2C, S2D, S2F, S4B
PY10505	*unc-31(e928); oyIs91[odr-1*p*::GCaMP3, srsx-3*p*::mScarlet, unc-122*p*::dsRed]* Line 1	CB928, PY10501	3B, S2B
PY10507	*unc-13(e51); oyIs91[odr-1*p*::GCaMP3, srsx-3*p*::mScarlet, unc-122*p*::dsRed]* Line 1	MT7929, PY10501	3B, S2B
CX2065	*odr-1(n1936)*	CGC	6B
PY10510	*odr-1(n1936); oyIs91[odr-1*p*::GCaMP3, srsx-3*p*::mScarlet, unc-122*p*::dsRed]*	CX2065, PY10501	6C
CX3222	*odr-3(n1605)*	CGC	5B, 5C, S4A
NL334	*gpa-2(pk16)*	CGC	S4A
NL335	*gpa-3(pk35)*	CGC	S4A
NL2330	*gpa-13(pk1270)*	CGC	S4A
GJ006	*gpa-3(pk35) gpa-13 (pk1270); gpa-2(pk16)*	Gert Jansen	S4A
GJ041	*gpa-3(pk35) gpa-13(pk1270) odr-3(n1605)*	Gert Jansen	S4A
PY10520	*odr-3(n1605);oyEx680 [odr1*p*::odr-3::SL2::mCherry, unc-122*p*::gfp)]* Line 3	PSAB1269 injected into CX3222	5B, 5C
PY10509	*odr-3(n1605); oyIs91[odr-1*p*::GCaMP, srsx-3*p*::mScarlet, unc-122*p*::dsRed]*	CX3222, PY10501	5D, 5E, 5F
PY10522	*tax-4 (p678); kyIs602[sra-6*p*::GCaMP3.0, unc-122*p*::gfp]*	PR678, PY12005	S3E
PY10518	*tax-4 (p678); oyIs91[odr-1*p*::GCaMP, srsx-3*p*::mScarlet, unc-122*p*::dsRed]*	PR678, PY10501	6A

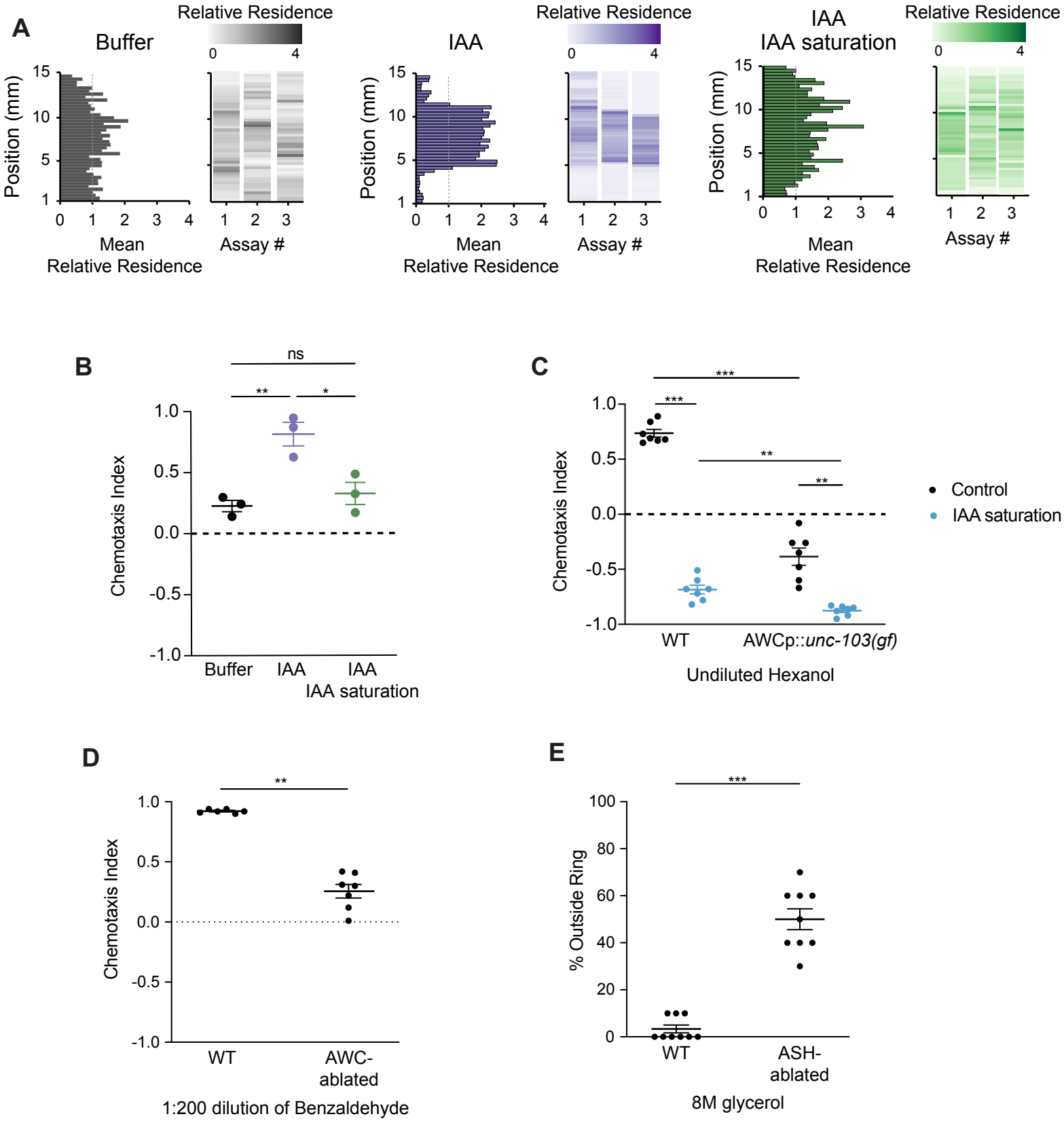

Khan et al., Figure S1

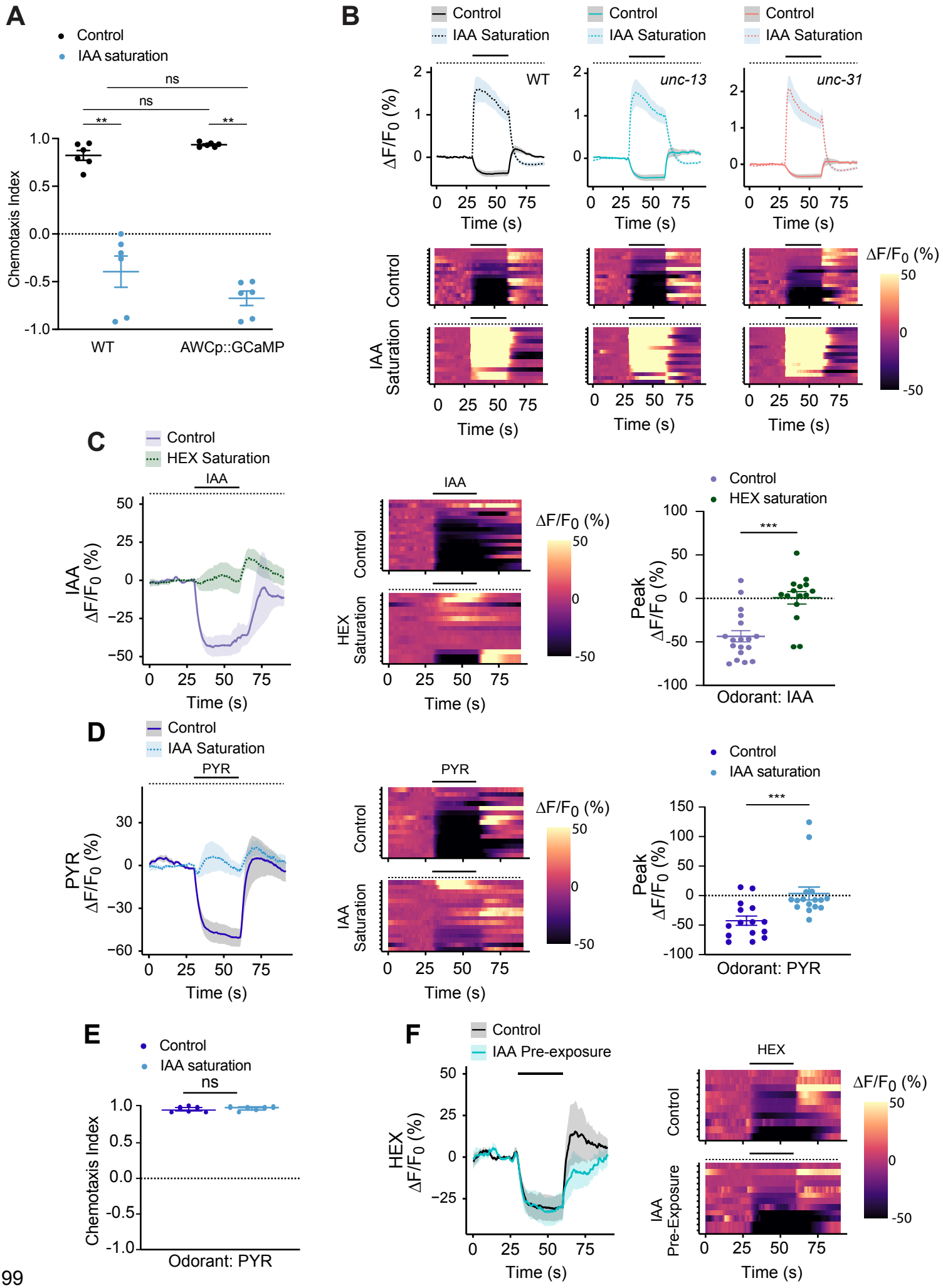
A
Control
IAA saturation
ns
ns
**
**
Chemotaxis Index
1.0
0.5
0.0
-0.5
-1.0
WT
AWCp::GCaMP
B
Control
IAA Saturation
WT
unc-13
unc-31
ΔF/F0 (%)
Time (s)
Control
IAA Saturation
ΔF/F0 (%)
50
0
-50
C
Control
HEX Saturation
IAA
IAA ΔF/F0 (%)
Time (s)
HEX Saturation
Control
HEX saturation
***
Peak ΔF/F0 (%)
Odorant: IAA
D
Control
IAA Saturation
PYR
PYR ΔF/F0 (%)
Time (s)
IAA Saturation
Control
IAA saturation
***
Peak ΔF/F0 (%)
Odorant: PYR
E
Control
IAA saturation
ns
Chemotaxis Index
Odorant: PYR
F
Control
IAA Pre-exposure
HEX
HEX ΔF/F0 (%)
Time (s)
IAA Pre-Exposure

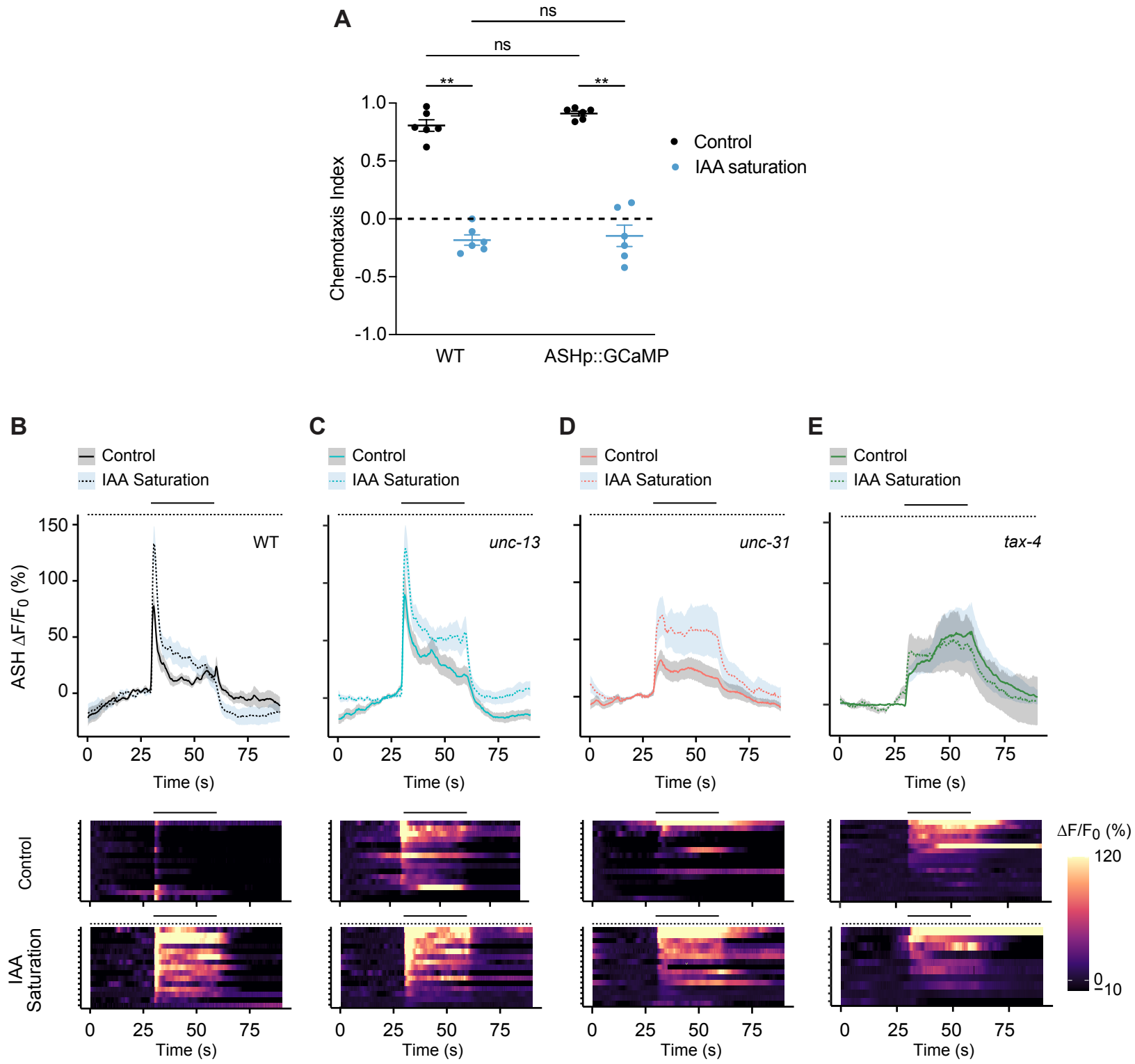

Khan et al., Figure S3

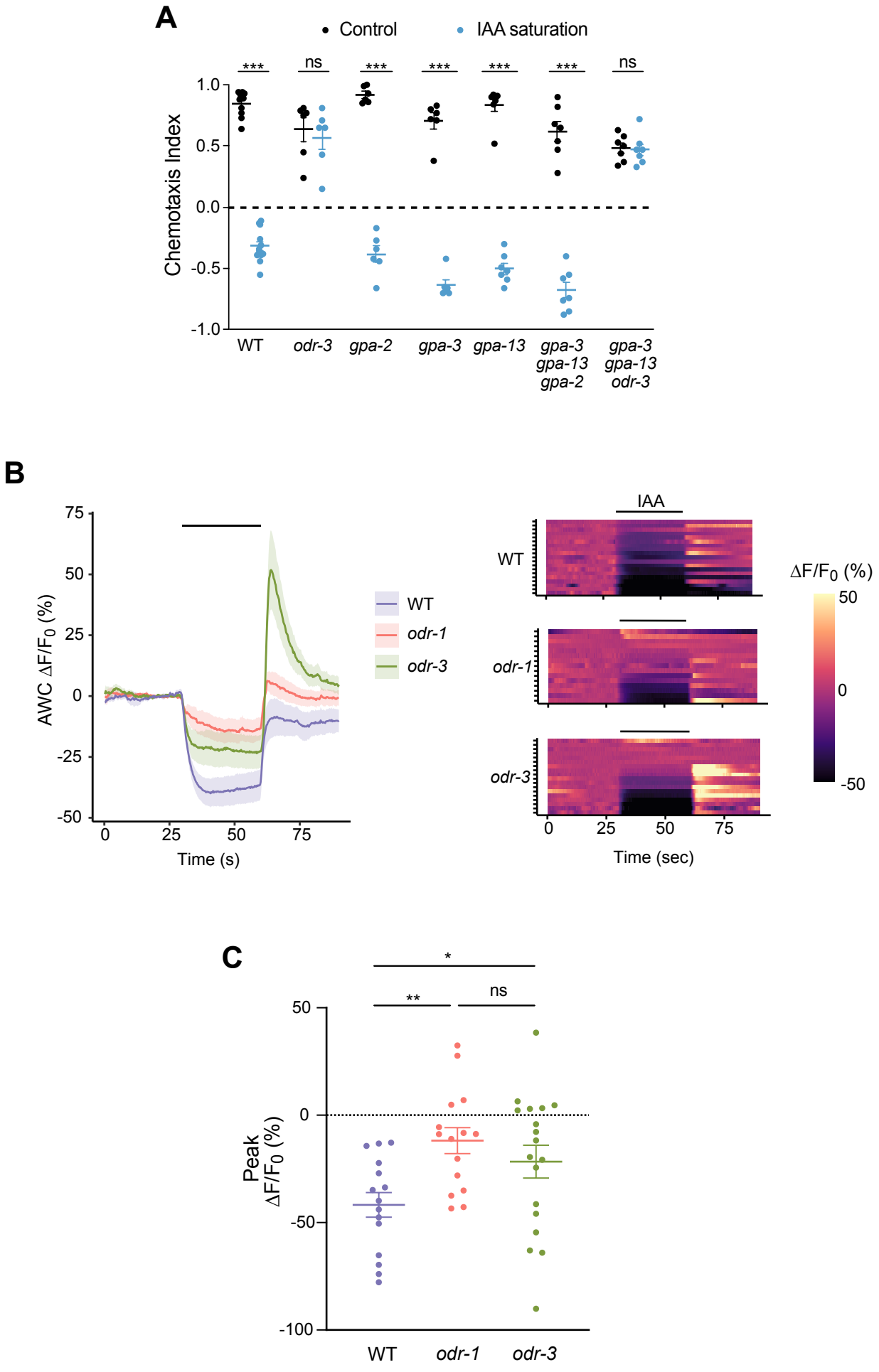

Khan et al., Figure S4

REFERENCES

Adachi, T., Kunitomo, H., Tomioka, M., Ohno, H., Okochi, Y., Mori, I., and Iino, Y. (2010). Reversal of salt preference is directed by the insulin/PI3K and Gq/PKC signaling in Caenorhabditis elegans. Genetics *186*, 1309-1319.

Ahn, J.E., Chen, Y., and Amrein, H. (2017). Molecular basis of fatty acid taste in Drosophila. Elife *6*.

Albrecht, D.R., and Bargmann, C.I. (2011). High-content behavioral analysis of *Caenorhabditis elegans* in precise spatiotemporal chemical environments. Nat Methods *8*, 599-605.

Amin, H., and Lin, A.C. (2019). Neuronal mechanisms underlying innate and learned olfactory processing in Drosophila. Curr Opin Insect Sci *36*, 9-17.

Ann, K., Kowalchyk, J.A., Loyet, K.M., and Martin, T.F. (1997). Novel Ca2+-binding protein (CAPS) related to UNC-31 required for Ca2+-activated exocytosis. J Biol Chem *272*, 19637-19640.

Araneda, R.C., Kini, A.D., and Firestein, S. (2000). The molecular receptive range of an odorant receptor. Nat Neurosci *3*, 1248-1255.

Araneda, R.C., Peterlin, Z., Zhang, X., Chesler, A., and Firestein, S. (2004). A pharmacological profile of the aldehyde receptor repertoire in rat olfactory epithelium. J Physiol *555*, 743-756.

Badeke, E., Haverkamp, A., Hansson, B.S., and Sachse, S. (2016). A Challenge for a Male Noctuid Moth? Discerning the Female Sex Pheromone against the Background of Plant Volatiles. Front Physiol *7*, 143.

Baker, K.L., Dickinson, M., Findley, T.M., Gire, D.H., Louis, M., Suver, M.P., Verhagen, J.V., Nagel, K.I., and Smear, M.C. (2018). Algorithms for Olfactory Search across Species. J Neurosci *38*, 9383-9389.

Bargmann, C.I., Hartwieg, E., and Horvitz, H.R. (1993). Odorant-selective genes and neurons mediate olfaction in *C. elegans*. Cell *74*, 515-527.

Bargmann, C.I., and Horvitz, H.R. (1991). Chemosensory neurons with overlapping functions direct chemotaxis to multiple chemicals in C. elegans. Neuron *7*, 729-742.

Bauer Huang, S.L., Saheki, Y., VanHoven, M.K., Torayama, I., Ishihara, T., Katsura, I., van der Linden, A., Sengupta, P., and Bargmann, C.I. (2007). Left-right olfactory asymmetry results from antagonistic functions of voltage-activated calcium channels and the Raw repeat protein OLRN-1 in C. elegans. Neural Dev *2*, 24.

Bell, J.S., and Wilson, R.I. (2016). Behavior Reveals Selective Summation and Max Pooling among Olfactory Processing Channels. Neuron *91*, 425-438.

Bentley, R. (2006). The nose as a stereochemist. Enantiomers and odor. Chem Rev *106*, 4099-4112.

Beverly, M., Anbil, S., and Sengupta, P. (2011). Degeneracy and signaling within a sensory circuit contributes to robustness in thermosensory behaviors in *C. elegans*. J Neurosci *31*, 11718-11727.

Birnby, D.A., Link, E.A., Vowels, J.J., Tian, H., Colacurcio, P.L., and Thomas, J.H. (2000). A transmembrane guanylyl cyclase (DAF-11) and Hsp90 (DAF-21) regulate a common set of chemosensory behaviors in *C. elegans*. Genetics *in press*.

Busto, G.U., Cervantes-Sandoval, I., and Davis, R.L. (2010). Olfactory learning in Drosophila. Physiology (Bethesda) *25*, 338-346.
Calebiro, D., Koszegi, Z., Lanoiselee, Y., Miljus, T., and O'Brien, S. (2021). G protein-coupled receptor-G protein interactions: a single-molecule perspective. Physiol Rev *101*, 857-906.
Cao, L.H., Yang, D., Wu, W., Zeng, X., Jing, B.Y., Li, M.T., Qin, S., Tang, C., Tu, Y., and Luo, D.G. (2017). Odor-evoked inhibition of olfactory sensory neurons drives olfactory perception in Drosophila. Nat Commun *8*, 1357.
Chalasani, S.H., Chronis, N., Tsunozaki, M., Gray, J.M., Ramot, D., Goodman, M.B., and Bargmann, C.I. (2007). Dissecting a neural circuit for food-seeking behavior in *Caenorhabditis elegans*. Nature *450*, 63-70.
Chalasani, S.H., Kato, S., Albrecht, D.R., Nakagawa, T., Abbott, L.F., and Bargmann, C.I. (2010). Neuropeptide feedback modifies odor-evoked dynamics in Caenorhabditis elegans olfactory neurons. Nat Neurosci *13*, 615-621.
Chao, M.Y., Komatsu, H., Fukuto, H.S., Dionne, H.M., and Hart, A.C. (2004). Feeding status and serotonin rapidly and reversibly modulate a Caenorhabditis elegans chemosensory circuit. Proc Natl Acad Sci U S A *101*, 15512-15517.
Cho, C.E., Brueggemann, C., L'Etoile, N.D., and Bargmann, C.I. (2016). Parallel encoding of sensory history and behavioral preference during *Caenorhabditis elegans* olfactory learning. Elife *5*, e14000.
Choi, J.I., Lee, H.K., Kim, H.S., Park, S.Y., Lee, T.Y., Yoon, K.H., and Lee, J.I. (2018). Odor-dependent temporal dynamics in Caenorhabitis elegans adaptation and aversive learning behavior. PeerJ *6*, e4956.
Chronis, N., Zimmer, M., and Bargmann, C.I. (2007). Microfluidics for in vivo imaging of neuronal and behavioral activity in Caenorhabditis elegans. Nat Methods *4*, 727-731.
Coburn, C.M., and Bargmann, C.I. (1996). A putative cyclic nucleotide-gated channel is required for sensory development and function in C. elegans. Neuron *17*, 695-706.
Colbert, H.A., and Bargmann, C.I. (1995). Odorant-specific adaptation pathways generate olfactory plasticity in *C. elegans*. Neuron *14*, 803-812.
Colbert, H.A., and Bargmann, C.I. (1997). Environmental signals modulate olfactory acuity, discrimination, and memory in Caenorhabditis elegans. Learn Mem *4*, 179-191.
Cornils, A., Maurya, A.K., Tereshko, L., Kennedy, J., Brear, A.G., Prahlad, V., Blacque, O.E., and Sengupta, P. (2016). Structural and Functional Recovery of Sensory Cilia in C. elegans IFT Mutants upon Aging. PLoS Genet *12*, e1006325.
Couto, A., Alenius, M., and Dickson, B.J. (2005). Molecular, anatomical, and functional organization of the Drosophila olfactory system. Curr Biol *15*, 1535-1547.
Culotti, J.G., and Russell, R.L. (1978). Osmotic avoidance defective mutants of the nematode Caenorhabditis elegans. Genetics *90*, 243-256.
Devineni, A.V., Sun, B., Zhukovskaya, A., and Axel, R. (2019). Acetic acid activates distinct taste pathways in *Drosophila* to elicit opposing, state-dependent feeding responses. Elife *8*, e47677.
Dobosiewicz, M., Liu, Q., and Bargmann, C.I. (2019). Reliability of an interneuron response depends on an integrated sensory state. Elife *8*, e50566.

Duan, D., Zhang, H., Yue, X., Fan, Y., Xue, Y., Shao, J., Ding, G., Chen, D., Li, S., Cheng, H.*, et al.* (2020). Sensory Glia Detect Repulsive Odorants and Drive Olfactory Adaptation. Neuron *108*, 707-721 e708.

Elgaali, H., Hamilton-Kemp, T.R., Newman, M.C., Collins, R.W., Yu, K., and Archbold, D.D. (2002). Comparison of long-chain alcohols and other volatile compounds emitted from food-borne and related Gram positive and Gram negative bacteria. J Basic Microbiol *42*, 373-380.

Ellisdon, A.M., and Halls, M.L. (2016). Compartmentalization of GPCR signalling controls unique cellular responses. Biochem Soc Trans *44*, 562-567.

Ezcurra, M., Walker, D.S., Beets, I., Swoboda, P., and Schafer, W.R. (2016). Neuropeptidergic Signaling and Active Feeding State Inhibit Nociception in Caenorhabditis elegans. J Neurosci *36*, 3157-3169.

Ferkey, D.M., Sengupta, P., and L'Etoile, N.D. (2021). Chemosensory signal transduction in Caenorhabditis elegans. Genetics *217*.

Flock, T., Hauser, A.S., Lund, N., Gloriam, D.E., Balaji, S., and Babu, M.M. (2017). Selectivity determinants of GPCR-G-protein binding. Nature *545*, 317-322.

Fukuto, H.S., Ferkey, D.M., Apicella, A.J., Lans, H., Sharmeen, T., Chen, W., Lefkowitz, R.J., Jansen, G., Schafer, W.R., and Hart, A.C. (2004). G protein-coupled receptor kinase function is essential for chemosensation in C. elegans. Neuron *42*, 581-593.

Ghosh, D.D., Sanders, T., Hong, S., McCurdy, L.Y., Chase, D.L., Cohen, N., Koelle, M.R., and Nitabach, M.N. (2016). Neural architecture of hunger-dependent multisensory decision making in *C. elegans*. Neuron *92*, 1049-1062.

Gordus, A., Pokala, N., Levy, S., Flavell, S.W., and Bargmann, C.I. (2015). Feedback from network states generates variability in a probabilistic olfactory circuit. Cell *161*, 215-227.

Groschner, L.N., and Miesenbock, G. (2019). Mechanisms of Sensory Discrimination: Insights from Drosophila Olfaction. Annu Rev Biophys *48*, 209-229.

Grunwald Kadow, I.C. (2019). State-dependent plasticity of innate behavior in fruit flies. Curr Opin Neurobiol *54*, 60-65.

Guo, M., Wu, T.H., Song, Y.X., Ge, M.H., Su, C.M., Niu, W.P., Li, L.L., Xu, Z.J., Ge, C.L., Al-Mhanawi, M.T.*, et al.* (2015). Reciprocal inhibition between sensory ASH and ASI neurons modulates nociception and avoidance in Caenorhabditis elegans. Nat Commun *6*, 5655.

Ha, H.I., Hendricks, M., Shen, Y., Gabel, C.V., Fang-Yen, C., Qin, Y., Colon-Ramos, D., Shen, K., Samuel, A.D., and Zhang, Y. (2010). Functional organization of a neural network for aversive olfactory learning in *Caenorhabditis elegans*. Neuron *68*, 1173-1186.

Hallem, E.A., and Carlson, J.R. (2006). Coding of odors by a receptor repertoire. Cell *125*, 143-160.

Hallem, E.A., Ho, M.G., and Carlson, J.R. (2004). The molecular basis of odor coding in the Drosophila antenna. Cell *117*, 965-979.

Hawk, J.D., Calvo, A.C., Liu, P., Almoril-Porras, A., Aljobeh, A., Torruella-Suarez, M.L., Ren, I., Cook, N., Greenwood, J., Luo, L.*, et al.* (2018). Integration of plasticity mechanisms within a single sensory neuron of *C. elegans* actuates a memory. Neuron *97*, 356-367

Hildebrand, J.G., and Shepherd, G.M. (1997). Mechanisms of olfactory discrimination: converging evidence for common principles across phyla. Annu Rev Neurosci *20*, 595-631.
Hilgendorf, K.I., Johnson, C.T., Mezger, A., Rice, S.L., Norris, A.M., Demeter, J., Greenleaf, W.J., Reiter, J.F., Kopinke, D., and Jackson, P.K. (2019). Omega-3 Fatty Acids Activate Ciliary FFAR4 to Control Adipogenesis. Cell *179*, 1289-1305 e1221.
Hilliard, M.A., Bergamasco, C., Arbucci, S., Plasterk, R.H., and Bazzicalupo, P. (2004). Worms taste bitter: ASH neurons, QUI-1, GPA-3 and ODR-3 mediate quinine avoidance in Caenorhabditis elegans. Embo J *23*, 1101-1111.
Horio, N., Murata, K., Yoshikawa, K., Yoshihara, Y., and Touhara, K. (2019). Contribution of individual olfactory receptors to odor-induced attractive or aversive behavior in mice. Nat Commun *10*, 209.
Hukema, R.K., Rademakers, S., Dekkers, M.P., Burghoorn, J., and Jansen, G. (2006). Antagonistic sensory cues generate gustatory plasticity in Caenorhabditis elegans. Embo J *25*, 312-322.
Inagaki, H.K., Ben-Tabou de-Leon, S., Wong, A.M., Jagadish, S., Ishimoto, H., Barnea, G., Kitamoto, T., Axel, R., and Anderson, D.J. (2012). Visualizing neuromodulation in vivo: TANGO-mapping of dopamine signaling reveals appetite control of sugar sensing. Cell *148*, 583-595.
Inagaki, H.K., Panse, K.M., and Anderson, D.J. (2014). Independent, reciprocal neuromodulatory control of sweet and bitter taste sensitivity during starvation in *Drosophila*. Neuron *84*, 806-820.
Inagaki, S., Iwata, R., Iwamoto, M., and Imai, T. (2020). Widespread Inhibition, Antagonism, and Synergy in Mouse Olfactory Sensory Neurons In Vivo. Cell Rep *31*, 107814.
Ishihara, T., Iino, Y., Mohri, A., Mori, I., Gengyo-Ando, K., Mitani, S., and Katsura, I. (2002). HEN-1, a secretory protein with an LDL receptor motif, regulates sensory integration and learning in Caenorhabditis elegans. Cell *109*, 639-649.
Jang, H., Kim, K., Neal, S.J., Macosko, E., Kim, D., Butcher, R.A., Zeiger, D.M., Bargmann, C.I., and Sengupta, P. (2012). Neuromodulatory state and sex specify alternative behaviors through antagonistic synaptic pathways in C. elegans. Neuron *75*, 585-592.
Jang, M.S., Y., T., Tomioka, M., Kunitomo, H., and Iino, Y. (2019). Multiple sensory neurons mediate starvation-dependent aversive navigation in Caenorhabditis elegans. Proc Natl Acad Sci USA *116*, 18673-18683.
Jansen, G., Thijssen, K.L., Werner, P., van der Horst, M., Hazendonk, E., and Plasterk, R.H. (1999). The complete family of genes encoding G proteins of Caenorhabditis elegans. Nat Genet *21*, 414-419.
Kadohisa, M., and Wilson, D.A. (2006). Olfactory cortical adaptation facilitates detection of odors against background. J Neurophysiol *95*, 1888-1896.
Kato, S., Xu, Y., Cho, C.E., Abbott, L.F., and Bargmann, C.I. (2014). Temporal responses of C. elegans chemosensory neurons are preserved in behavioral dynamics. Neuron *81*, 616-628.
Kim, S.M., Su, C.Y., and Wang, J.W. (2017). Neuromodulation of innate behaviors in *Drosophila*. Annu Rev Neurosci *40*, 327-348.

Knaden, M., and Hansson, B.S. (2014). Mapping odor valence in the brain of flies and mice. Curr Opin Neurobiol *24*, 34-38.
Knaden, M., Strutz, A., Ahsan, J., Sachse, S., and Hansson, B.S. (2012). Spatial representation of odorant valence in an insect brain. Cell Rep *1*, 392-399.
Komatsu, H., Mori, I., and Ohshima, Y. (1996). Mutations in a cyclic nucleotide-gated channel lead to abnormal thermosensation and chemosensation in C. elegans. Neuron *17*, 707-718.
Kong, M.S., and Zweifel, L.S. (2021). Central amygdala circuits in valence and salience processing. Behav Brain Res *410*, 113355.
Kozma, M.T., Ngo-Vu, H., Rump, M.T., Bobkov, Y.V., Ache, B.W., and Derby, C.D. (2020). Single cell transcriptomes reveal expression patterns of chemoreceptor genes in olfactory sensory neurons of the Caribbean spiny lobster, Panulirus argus. BMC Genomics *21*, 649.
Kreher, S.A., Mathew, D., Kim, J., and Carlson, J.R. (2008). Translation of sensory input into behavioral output via an olfactory system. Neuron *59*, 110-124.
Krzyzanowski, M.C., Woldemariam, S., Wood, J.F., Chaubey, A.H., Brueggemann, C., Bowitch, A., Bethke, M., L'Etoile, N.D., and Ferkey, D.M. (2016). Aversive Behavior in the Nematode C. elegans Is Modulated by cGMP and a Neuronal Gap Junction Network. PLoS Genet *12*, e1006153.
Kunitomo, H., Sato, H., Iwata, R., Satoh, Y., Ohno, H., Yamada, K., and Iino, Y. (2013). Concentration memory-dependent synaptic plasticity of a taste circuit regulates salt concentration chemotaxis in Caenorhabditis elegans. Nat Commun *4*, 2210.
Kurahashi, T., Lowe, G., and Gold, G.H. (1994). Suppression of odorant responses by odorants in olfactory receptor cells. Science *265*, 118-120.
Kurian, S.M., Naressi, R.G., Manoel, D., Barwich, A.S., Malnic, B., and Saraiva, L.R. (2021). Odor coding in the mammalian olfactory epithelium. Cell Tissue Res *383*, 445-456.
L'Etoile, N.D., and Bargmann, C.I. (2000). Olfaction and odor discrimination are mediated by the C. elegans guanylyl cyclase ODR-1. Neuron *25*, 575-586.
L'Etoile, N.D., Coburn, C.M., Eastham, J., Kistler, A., Gallegos, G., and Bargmann, C.I. (2002). The cyclic GMP-dependent protein kinase EGL-4 regulates olfactory adaptation in C. elegans. Neuron *36*, 1079-1089.
Laing, D.G., Panhuber, H., and Baxter, R.I. (1978). Olfactory properties of amines and n-butanol. Chem Senses *3*.
Langeberg, L.K., and Scott, J.D. (2015). Signalling scaffolds and local organization of cellular behaviour. Nat Rev Mol Cell Biol *16*, 232-244.
Lans, H., Rademakers, S., and Jansen, G. (2004). A network of stimulatory and inhibitory Galpha-subunits regulates olfaction in Caenorhabditis elegans. Genetics *167*, 1677-1687.
Laurent, G. (2002). Olfactory network dynamics and the coding of multidimensional signals. Nat Rev Neurosci *3*, 884-895.
LeDue, E.E., Mann, K., Koch, E., Chu, B., Dakin, R., and Gordon, M.D. (2016). Starvation-Induced Depotentiation of Bitter Taste in Drosophila. Curr Biol *26*, 2854-2861.

Leinwand, S.G., and Chalasani, S.H. (2013). Neuropeptide signaling remodels chemosensory circuit composition in Caenorhabditis elegans. Nat Neurosci *16*, 1461-1467.
Li, Q., and Liberles, S.D. (2015). Aversion and attraction through olfaction. Curr Biol *25*, R120-129.
Liberles, S.D., and Buck, L.B. (2006). A second class of chemosensory receptors in the olfactory epithelium. Nature *442*, 645-650.
Livermore, A., and Laing, D.G. (1998). The influence of odor type on the discrimination and identification of odorants in multicomponent odor mixtures. Physiol Behav *65*, 311-320.
Luo, L., Gabel, C.V., Ha, H.I., Zhang, Y., and Samuel, A.D. (2008). Olfactory behavior of swimming C. elegans analyzed by measuring motile responses to temporal variations of odorants. J Neurophysiol *99*, 2617-2625.
MacWilliam, D., Kowalewski, J., Kumar, A., Pontrello, C., and Ray, A. (2018). Signaling Mode of the Broad-Spectrum Conserved CO2 Receptor Is One of the Important Determinants of Odor Valence in Drosophila. Neuron *97*, 1153-1167 e1154.
Magalhaes, A.C., Dunn, H., and Ferguson, S.S. (2012). Regulation of GPCR activity, trafficking and localization by GPCR-interacting proteins. Br J Pharmacol *165*, 1717-1736.
Malnic, B., Hirono, J., Sato, T., and Buck, L.B. (1999). Combinatorial receptor codes for odors. Cell *96*, 713-723.
Marella, S., Mann, K., and Scott, K. (2012). Dopaminergic modulation of sucrose acceptance behavior in *Drosophila*. Neuron *73*, 941-950.
McLaughlin, C.N., Brbic, M., Xie, Q., Li, T., Horns, F., Kolluru, S.S., Kebschull, J.M., Vacek, D., Xie, A., Li, J.*, et al.* (2021). Single-cell transcriptomes of developing and adult olfactory receptor neurons in Drosophila. Elife *10*.
Mohamed, A.A.M., Retzke, T., Das Chakraborty, S., Fabian, B., Hansson, B.S., Knaden, M., and Sachse, S. (2019). Odor mixtures of opposing valence unveil inter-glomerular crosstalk in the Drosophila antennal lobe. Nat Commun *10*, 1201.
Mori, K., and Sakano, H. (2021). Olfactory Circuitry and Behavioral Decisions. Annu Rev Physiol *83*, 231-256.
Nara, K., Saraiva, L.R., Ye, X., and Buck, L.B. (2011). A large-scale analysis of odor coding in the olfactory epithelium. J Neurosci *31*, 9179-9191.
Neal, S.J., Takeishi, A., O'Donnell, M.P., Park, J., Hong, M., Butcher, R.A., Kim, K., and Sengupta, P. (2015). Feeding state-dependent regulation of developmental plasticity via CaMKI and neuroendocrine signaling. Elife *4*.
Nuttley, W.M., Atkinson-Leadbeater, K.P., and Van Der Kooy, D. (2002). Serotonin mediates food-odor associative learning in the nematode Caenorhabditiselegans. Proc Natl Acad Sci U S A *99*, 12449-12454.
Ohno, H., Kato, S., Naito, Y., Kunitomo, H., Tomioka, M., and Iino, Y. (2014). Role of synaptic phosphatidylinositol 3-kinase in a behavioral learning response in C. elegans. Science *345*, 313-317.
Oka, Y., Butnaru, M., von Buchholtz, L., Ryba, N.J., and Zuker, C.S. (2013). High salt recruits aversive taste pathways. Nature *494*, 472-475.
Oka, Y., Omura, M., Kataoka, H., and Touhara, K. (2004). Olfactory receptor antagonism between odorants. Embo J *23*, 120-126.

Parnas, M., Lin, A.C., Huetteroth, W., and Miesenbock, G. (2013). Odor discrimination in Drosophila: from neural population codes to behavior. Neuron *79*, 932-944.
Patwardhan, A., Cheng, N., and Trejo, J. (2021). Post-Translational Modifications of G Protein-Coupled Receptors Control Cellular Signaling Dynamics in Space and Time. Pharmacol Rev *73*, 120-151.
Perkins, L.A., Hedgecock, E.M., Thomson, J.N., and Culotti, J.G. (1986). Mutant sensory cilia in the nematode *Caenorhabditis elegans*. Dev Biol *117*, 456-487.
Pfister, P., Smith, B.C., Evans, B.J., Brann, J.H., Trimmer, C., Sheikh, M., Arroyave, R., Reddy, G., Jeong, H.Y., Raps, D.A.*, et al.* (2020). Odorant Receptor Inhibition Is Fundamental to Odor Encoding. Curr Biol *30*, 2574-2587 e2576.
Polit, A., Rysiewicz, B., Mystek, P., Blasiak, E., and Dziedzicka-Wasylewska, M. (2020). The Galphai protein subclass selectivity to the dopamine D2 receptor is also decided by their location at the cell membrane. Cell Commun Signal *18*, 189.
Reddy, G., Zak, J.D., Vergassola, M., and Murthy, V.N. (2018). Antagonism in olfactory receptor neurons and its implications for the perception of odor mixtures. Elife *7*.
Reiner, D.J., Weinshenker, D., Tian, H., Thomas, J.H., Nishiwaki, K., Miwa, J., Gruninger, T., Leboeuf, B., and Garcia, L.R. (2006). Behavioral genetics of *Caenorhabditis elegans unc-103*-encoded erg-like K(+) channel. J Neurogenet *20*, 41-66.
Rengarajan, S., Yankura, K.A., Guillermin, M.L., Fung, W., and Hallem, E.A. (2019). Feeding state sculpts a circuit for sensory valence in *Caenorhabditis elegans*. Proc Natl Acad Sci USA *116*, 1776-1781.
Riffell, J.A., Shlizerman, E., Sanders, E., Abrell, L., Medina, B., Hinterwirth, A.J., and Kutz, J.N. (2014). Sensory biology. Flower discrimination by pollinators in a dynamic chemical environment. Science *344*, 1515-1518.
Roayaie, K., Crump, J.G., Sagasti, A., and Bargmann, C.I. (1998). The Ga protein ODR-3 mediates olfactory and nociceptive function and controls cilium morphogenesis in *C. elegans* olfactory neurons. Neuron *20*, 55-67.
Rokni, D., Hemmelder, V., Kapoor, V., and Murthy, V.N. (2014). An olfactory cocktail party: figure-ground segregation of odorants in rodents. Nat Neurosci *17*, 1225-1232.
Root, C.M., Ko, K.I., Jafari, A., and Wang, J.W. (2011). Presynaptic facilitation by neuropeptide signaling mediates odor-driven food search. Cell *145*, 133-144.
Sachse, S., and Beshel, J. (2016). The good, the bad, and the hungry: how the central brain codes odor valence to facilitate food approach in Drosophila. Curr Opin Neurobiol *40*, 53-58.
Saeki, S., Yamamoto, M., and Iino, Y. (2001). Plasticity of chemotaxis revealed by paired presentation of a chemoattractant and starvation in the nematode *Caenorhabditis elegans*. J. Exp. Biol. *204*, 1757-1764.
Saraiva, L.R., Kondoh, K., Ye, X., Yoon, K.H., Hernandez, M., and Buck, L.B. (2016). Combinatorial effects of odorants on mouse behavior. Proc Natl Acad Sci U S A *113*, E3300-3306.
Semmelhack, J.L., and Wang, J.W. (2009). Select Drosophila glomeruli mediate innate olfactory attraction and aversion. Nature *459*, 218-223.
Shidara, H., Hotta, K., and Oka, K. (2017). Compartmentalized cGMP Responses of Olfactory Sensory Neurons in Caenorhabditis elegans. J Neurosci *37*, 3753-3763.

Sieburth, D., Madison, J.M., and Kaplan, J.M. (2007). PKC-1 regulates secretion of neuropeptides. Nat Neurosci *10*, 49-57.
Smith, D.M., and Torregrossa, M.M. (2021). Valence encoding in the amygdala influences motivated behavior. Behav Brain Res *411*, 113370.
Solessio, E., and Engbretson, G.A. (1993). Antagonistic chromatic mechanisms in photoreceptors of the parietal eye of lizards. Nature *364*, 442-445.
Speese, S., Petrie, M., Schuske, K., Ailion, M., Ann, K., Iwasaki, K., Jorgensen, E.M., and Martin, T.F. (2007). UNC-31 (CAPS) is required for dense-core vesicle but not synaptic vesicle exocytosis in Caenorhabditis elegans. J Neurosci *27*, 6150-6162.
Stensmyr, M.C., Giordano, E., Balloi, A., Angioy, A.M., and Hansson, B.S. (2003). Novel natural ligands for Drosophila olfactory receptor neurones. J Exp Biol *206*, 715-724.
Stettler, D.D., and Axel, R. (2009). Representations of odor in the piriform cortex. Neuron *63*, 854-864.
Stowers, L., and Kuo, T.H. (2015). Mammalian pheromones: emerging properties and mechanisms of detection. Curr Opin Neurobiol *34*, 103-109.
Stowers, L., and Liberles, S.D. (2016). State-dependent responses to sex pheromones in mouse. Curr Opin Neurobiol *38*, 74-79.
Su, C.Y., Luo, D.G., Terakita, A., Shichida, Y., Liao, H.W., Kazmi, M.A., Sakmar, T.P., and Yau, K.W. (2006). Parietal-eye phototransduction components and their potential evolutionary implications. Science *311*, 1617-1621.
Su, C.Y., Martelli, C., Emonet, T., and Carlson, J.R. (2011). Temporal coding of odor mixtures in an olfactory receptor neuron. Proc Natl Acad Sci U S A *108*, 5075-5080.
Su, C.Y., Menuz, K., Reisert, J., and Carlson, J.R. (2012). Non-synaptic inhibition between grouped neurons in an olfactory circuit. Nature *492*, 66-71.
Summers, P.J., Layne, R.M., Ortega, A.C., Harris, G.P., Bamber, B.A., and Komuniecki, R.W. (2015). Multiple sensory inputs Are extensively integrated to modulate nociception in C. elegans. J Neurosci *35*, 10331-10342.
Takahashi, L.K. (2014). Olfactory systems and neural circuits that modulate predator odor fear. Front Behav Neurosci *8*, 72.
Task, D., Lin, C.-C., Vulpe, A., Afify, A., Ballou, S., Brbic, M., Schlegel, P., Jefferis, G.S.X.E., Li, H., Menuz, K.*, et al.* (2020). Chemoreceptor co-expression in Drosophila olfactory neurons. bioRxiv *doi.org/10.1101/2020.11.07.355651*
Taylor, S.R., Santpere, G., Weinreb, A., Barrett, A., Reilly, M.B., Xu, C., Varol, E., Oikonomou, P., Glenwinkel, L., McWhirter, R.*, et al.* (2021). Molecular topography of an entire nervous system. Cell *184*, 4329-4347 e4323.
Tomioka, M., Adachi, T., Suzuki, H., Kunitomo, H., Schafer, W.R., and Iino, Y. (2006). The insulin/PI 3-kinase pathway regulates salt chemotaxis learning in *Caenorhabditis elegans*. Neuron *51*, 613-625.
Troemel, E.R., Chou, J.H., Dwyer, N.D., Colbert, H.A., and Bargmann, C.I. (1995). Divergent seven transmembrane receptors are candidate chemosensory receptors in *C. elegans*. Cell *83*, 207-218.

Troemel, E.R., Kimmel, B.E., and Bargmann, C.I. (1997). Reprogramming chemotaxis responses: sensory neurons define olfactory preferences in C. elegans. Cell *91*, 161-169.
Troemel, E.R., Sagasti, A., and Bargmann, C.I. (1999). Lateral signaling mediated by axon contact and calcium entry regulates asymmetric odorant receptor expression in *C. elegans*. Cell *99*, 387-398.
Tsunozaki, M., Chalasani, S.H., and Bargmann, C.I. (2008). A behavioral switch: cGMP and PKC signaling in olfactory neurons reverses odor preference in *C. elegans*. Neuron *59*, 959-971.
Tumkaya, T., Burhanudin, S., Khalilnezhad, A., Stewart, J.A., Choi, H., and Claridge-Chang, A. (2021). Most primary olfactory neurons have individually neutral effects on behavior. bioRxiv *doi: https://doi.org/10.1101/2021.06.10.447838*
Turner, S.L., and Ray, A. (2009). Modification of CO2 avoidance behaviour in Drosophila by inhibitory odorants. Nature *461*, 277-281.
van Giesen, L., Kilian, P.B., Allard, C.A.H., and Bellono, N.W. (2020). Molecular Basis of Chemotactile Sensation in Octopus. Cell *183*, 594-604 e514.
Vickers, N.J. (2000). Mechanisms of animal navigation in odor plumes. Biol Bull *198*, 203-212.
Vidal, B., Aghayeva, U., Sun, H., Wang, C., Glenwinkel, L., Bayer, E.A., and Hobert, O. (2018). An atlas of Caenorhabditis elegans chemoreceptor expression. PLoS Biol *16*, e2004218.
Vogt, K., Zimmerman, D.M., Schlichting, M., Hernandez-Nunez, L., Qin, S., Malacon, K., Rosbash, M., Pehlevan, C., A., C., and A.D.T., S. (2021). Internal state configures olfactory behavior and early sensory processing in *Drosophila* larva. Sci Adv *7*, eabd6900.
Ward, S., Thomson, N., White, J.G., and Brenner, S. (1975). Electron microscopical reconstruction of the anterior sensory anatomy of the nematode *Caenorhabditis elegans.* J. Comp. Neurol. *160*, 313-337.
Wes, P.D., and Bargmann, C.I. (2001). C. elegans odour discrimination requires asymmetric 12
Worthy, S.E., Haynes, L., Chambers, M., Bethune, D., Kan, E., Chung, K., Ota, R., Taylor, C.J., and Glater, E.E. (2018). Identification of attractive odorants released by preferred bacterial food found in the natural habitats of C. elegans. PLoS One *13*, e0201158.
Wu, T., Duan, F., Yang, W., Liu, H., Caballero, A., Fernandes de Abreu, D.A., Dar, A.R., Alcedo, J., Ch'ng, Q., Butcher, R.A.*, et al.* (2019). Pheromones Modulate Learning by Regulating the Balanced Signals of Two Insulin-like Peptides. Neuron *104*, 1095-1109 e1095.
Xia, S., and Tully, T. (2007). Segregation of odor identity and intensity during odor discrimination in Drosophila mushroom body. PLoS Biol *5*, e264.
Xu, L., Li, W., Voleti, V., Zou, D.J., Hillman, E.M.C., and Firestein, S. (2020). Widespread receptor-driven modulation in peripheral olfactory coding. Science *368*.
Yeon, J., Takeishi, A., and Sengupta, P. (2021). Chronic vs acute manipulations reveal degeneracy in a thermosensory neuron network. MicroPubl Biol *2021*, 10.17912.

Yoshida, K., Hirotsu, T., Tagawa, T., Oda, S., Wakabayashi, T., Iino, Y., and Ishihara, T. (2012). Odour concentration-dependent olfactory preference change in C. elegans. Nat Commun *3*, 739.

Younger, M.A., Herre, M., Ehrlich, A.R., Gong, Z., Gilbert, Z.N., Rahiel, S., Matthws, B.J., and Vosshall, L.B. (2020). Non-canonical odor coding ensures unbreakable mosquito attraction to humans. bioRxiv *doi.org/10.1101/2020.11.07.368720*

Zak, J.D., Reddy, G., Vergassola, M., and Murthy, V.N. (2020). Antagonistic odor interactions in olfactory sensory neurons are widespread in freely breathing mice. Nat Commun *11*, 3350.

Zaslaver, A., Liani, I., Shtangel, O., Ginzburg, S., Yee, L., and Sternberg, P.W. (2015). Hierarchical sparse coding in the sensory system of Caenorhabditis elegans. Proc Natl Acad Sci U S A *112*, 1185-1189.

Zhang, Y., Lu, H., and Bargmann, C.I. (2005). Pathogenic bacteria induce aversive olfactory learning in Caenorhabditis elegans. Nature *438*, 179-184.

Zheng, Y., Liu, P., Bai, L., Trimmer, J.S., Bean, B.P., and Ginty, D.D. (2019). Deep Sequencing of Somatosensory Neurons Reveals Molecular Determinants of Intrinsic Physiological Properties. Neuron *103*, 598-616 e597.

CHAPTER 3

Antagonistic neuronal circuits drive concentration-dependent changes in olfactory cue valence

Antagonistic neuronal circuits drive concentration-dependent changes in olfactory cue valence

Munzareen Khan, Madeline Piccione, and Piali Sengupta

3.1 Contributions to this work

This chapter includes unpublished data that derived from the experiments shown in Chapter 2. MK and MP performed all chemotaxis experiments. MK performed calcium imaging experiments, curated, and analyzed all data and wrote this chapter. PS acquired funding and supervised the project.

3.2 Abstract

Organisms rely on olfactory signals to find food and mates, avoid predators, and extract other ecologically important information from the environment. However, odor environments are dynamic and complex- chemosensory stimuli will frequently undergo concentration changes, and concentration changes can in turn induce changes in olfactory preference. Behavioral preference can change as a result of changes in sensory neuron responses and/or changes in synaptic output. A central problem in olfactory processing is understanding how the system can respond to the same odorant at different concentrations and drive relevant behavioral output. Here we show that *C. elegans* is normally attracted to low concentrations of the straight-chain alcohol 1-hexanol and avoids high concentrations of the odorant. Genetic ablation and mutant analyses indicate that distinct combinations of sensory neurons respond to different concentrations of the odorant. The AWC sensory neurons drive attraction to low concentrations of hexanol. ASH and AWB sensory neurons drive repulsion to high concentrations of the chemical in a non-redundant manner. We also find that there is crosstalk between the two arms of the circuit and the weighted response of the distinct subsets of neuron drives concentration-dependent behavioral responses.

3.3 Introduction

Olfactory systems can detect and discriminate among a large repertoire of odorants, including a wide range of concentrations of the same odorant. Previous studies have shown that in many organisms, including in humans, olfactory preference to the same odorant can change depending on concentration (Laing, et al.,1978; Charro

et al.,1994; Poucher, 1974; Yoshida et al., 2012). For example, in *Drosophila,* apple cider vinegar, a food odor, is attractive at lower concentrations but repulsive at higher concentrations (Semmelhack & Wang, 2009; Yoshida et al., 2012). Moreover, indole, an aromatic odorant, has a floral smell in low concentrations, but is repulsive at high concentrations to humans (Poucher, 1974; Yoshida et al.,2012). The ability to discriminate odorants at different concentrations while recognizing the same odor across same concentrations can serve evolutionary, nutritional, reproductive, and safety purposes, allowing animals to make appropriate behavioral decisions and ensure survival. Modulation of responses by odor concentration may involve plasticity at the sensory neuron level or their synaptic output, but it could also arise from changes in downstream circuit properties. How information of odor concentration in encoded in olfactory circuits and how changes in odor concentration drive behavioral preference switch are not well understood.

The nematode *C. elegans* serves as an excellent model system in which to probe these questions since the connectivity pattern of all chemosensory neurons have been well described and the roles of these neurons in detecting various odorants have been broadly characterized (Bargmann, 2006). *C. elegans* senses and navigates its complex chemosensory environment using a relatively small subset of sensory neurons (Perkins et al., 1986; Ward et al., 1975). The assigned valence of individual chemicals is largely determined by the responding sensory neuron type, such that distinct subsets of chemosensory neurons drive either attraction or avoidance to different odorants (Bargmann et al., 1993; Ferkey et al., 2021; Troemel et al., 1997; Wes & Bargmann, 2001). As discussed in Chapter 1, in general, the ASE neurons detect soluble

attractants, whereas the AWC and AWA neurons detect volatile attractants (Bargmann et al., 1993). The ASH, ADL, and AWB neurons have been shown to detect volatile repellants (Chao et al., 2004; Troemel et al., 1997). Despite this general classification into attraction- and avoidance-driving neurons, it is also known that each chemosensory neuron in *C. elegans* expresses multiple olfactory receptors and some neurons have been shown to respond to the same odorants, but at different intensities (Bargmann et al., 1993; Chalasani et al., 2007; Troemel et al., 1995; Yoshida et al., 2012, Duan et al., 2020). Additionally, it has also been shown that glia can detect odorants at high concentrations and can drive repulsion independently of sensory neurons, thereby serving as bona fide odorant receptor cells (Duan et al., 2020). However, it remains unclear how olfactory neurons of diverse functionality ultimately assign concentration-dependent valence to chemical stimuli and influence downstream circuit to generate appropriate behavioral responses.

In the wild, *C. elegans* live on rotten fruit and plant matter and they largely depend on their chemosensory system to differentiate among predators, competitors, and vectors (Brenner, 1974; Felix & Braendle, 2010; Frezal & Felix, 2015; Haber et al., 2005; Hodgkin & Doniach, 1997; Norhave et al., 2012; Samuel et al., 2016; Schulenburg & Felix, 2017; Troemel et al., 2008). In addition, *C. elegans* feed on bacteria and use their chemosensory system to discriminate between good, bad, and neutral food sources (Bargmann et al., 1993; Harris et al., 2014; Zhang et al., 2005). Previous studies have shown that bacteria can produce alcohols as metabolites (Worthy, Haynes, et al., 2018) (Worthy, Rojas, et al., 2018) and worms are attracted to short-chain alcohols but avoid long-chain alcohols (Bargmann et al., 1993). Responses

to medium chain alcohols such as 1-hexanol have not been extensively characterized but appear to induce both attraction and avoidance based on context (Bargmann et al., 1993) (Chapter 2).

In this study, we show that olfactory preference of *C. elegans* to hexanol changes based on concentration. We find that *C. elegans* is normally attracted to low (diluted and 1µl undiluted) concentrations of the straight-chain alcohol 1-hexanol. However, they display mild avoidance to high concentrations (>1µl undiluted) of hexanol. Genetic ablation and mutant analyses indicate that distinct combinations of sensory neurons respond to different concentrations of the odorant. The AWC sensory neurons drives attraction to low concentrations of hexanol. ASH and AWB sensory neurons drive repulsion to high concentrations of the chemical and they are not redundant in their response to high concentrations of hexanol- both neurons are required in the circuit to drive repulsion. In the absence of either ASH or AWB neurons, animals are unable to avoid this chemical. We also found that perturbing the function of the attractive arm of the circuit promotes stronger repulsion, and *vice versa*. Therefore, data in this chapter suggest that *C. elegans* chemosensory circuits may represent an opposing components motif, where neurons of diverse functionality serve to coordinate, regulate, and assign concentration-dependent valence to chemical stimuli. Specifically, our results demonstrate that the behavioral response to hexanol is driven by the balanced output of two opposing sensory pathways, revealing a previously uncharacterized mechanism of concentration-dependent olfactory plasticity.

3.4 Results

3.4.1 Hexanol is attractive at low concentrations (diluted and 1µl undiluted) and repulsive at high concentrations (>1µl undiluted)

To characterize behavioral responses of worms to different concentrations of hexanol, we used plate chemotaxis assays to calculate a preference index (Bargmann et al., 1993). Briefly, these plates had a single point source of varying concentrations of hexanol at one end of the plate and ethanol at the other end. The number of worms in odor and ethanol spots was quantified at the end of 1 hour. We found that animals had a concentration-dependent behavioral preference towards hexanol. Animals were attracted to 1µl of diluted and undiluted hexanol but displayed mildly repulsive behaviors to >1µl undiluted hexanol (henceforth referred to as low and high concentrations of hexanol, respectively) (Figure 3.1).

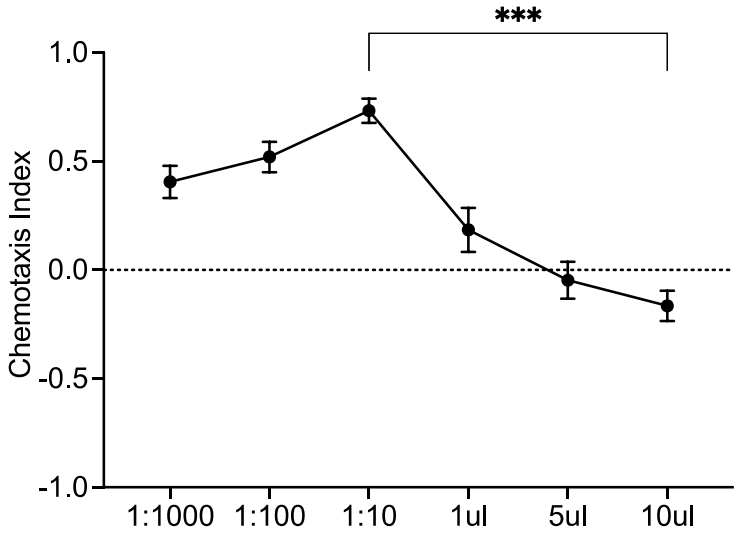

Fig. 3.1. Chemotaxis responses of wild-type worms to the indicated concentrations of hexanol. Each dot represents the average chemotaxis index of 3-4 independent assays of ~100-200 animals each. Errors are SEM. Assays were performed in duplicate over at least 3 days. ***p<0.001 comparing most attractive index with least attractive index. Data were analyzed using one-way ANOVA with Tukey's post hoc test for multiple comparisons. A variation of this figure is also shown in Chapter 2, Figure 1D.

This result indicates that behavioral preference of *C. elegans* to hexanol is not constant- the chemical can drive attraction or repulsion based on the concentration, consistent with previous reports that high concentrations of several odorants caused avoidance behavior (Bargmann et al,1993; Luo et al, 2008; Troemel et al, 1995).

3.4.2 AWC sensory neurons respond and drive attraction to low concentrations of hexanol

To identify neurons that drive behavioral responses to hexanol, we tested animals mutant for sensory transduction genes known to affect the responses of specific sensory neuron subsets. A major signal transduction cation channel in a subset of chemosensory neurons is the TAX-4 cyclic nucleotide-gated (CNG) channel. This CNG channel is expressed in ASE, ASG, ASI, ASJ, ASK, AWB, and AWC chemosensory neurons (Coburn & Bargmann, 1996; Komatsu et al., 1996). ASH, ADL, and AWA chemosensory neurons use the TRPV channel subunits OCR-2/OSM-9 (Colbert et al., 1997; Tobin et al., 2002). We found that unlike wild-type animals, *tax-4* mutants failed to exhibit attraction to 10^{-1} (1:10) dilution of hexanol (Figure 3.2A), the concentration at which wild-type animals display the strongest attraction (Figure 3.1). *ocr-2* mutants retained the ability to be attracted to hexanol (Figure 3.2A).

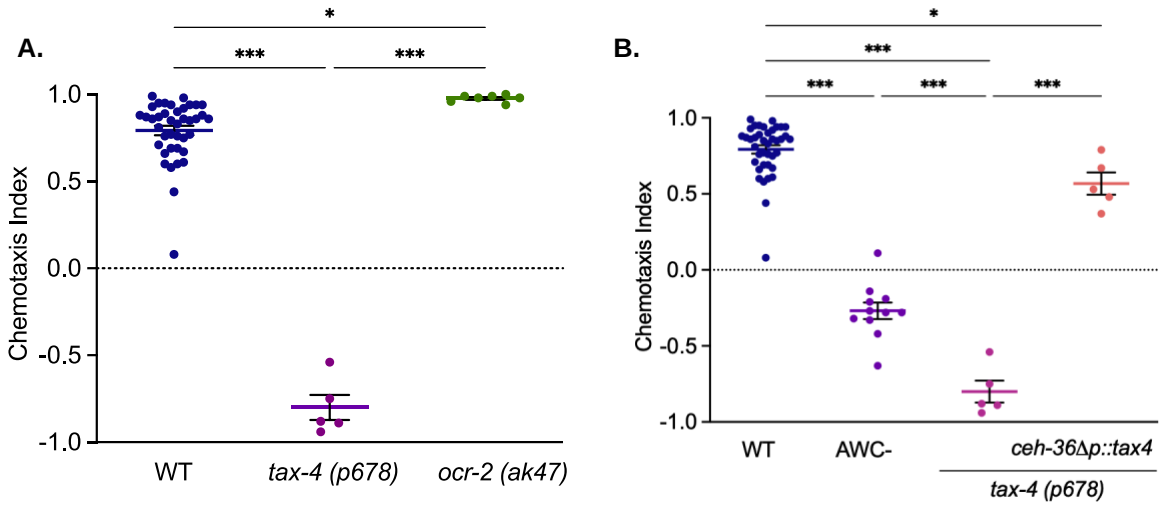

Fig. 3.2. **(A)** Chemotaxis responses of wild-type, channel mutants, and **(B)** mutant and rescue strains in response to 10^{-1} hexanol. Each dot represents the chemotaxis index of a single assay plate containing ~100-200 adult hermaphrodites. Thick horizontal bars indicate the mean; errors are SEM. ***p<0.001, *p<0.05 data were analyzed using one-way ANOVA with Tukey's post hoc test for multiple comparisons.

Next, we wanted to identify the neuron where TAX-4 function is required to mediate attraction. As discussed in detail in Chapter 2, the AWC olfactory neuron pair in *C. elegans* has previously been shown to drive attraction to low concentrations of alcohols including isoamyl alcohol (IAA) and the short-chain alcohol 1-pentanol (Bargmann et al., 1993; Chalasani et al., 2007; Choi et al., 2018; Yoshida et al., 2012). It has also been shown that sensory responses in AWC are abolished in animals mutant for the *tax-4* cyclic nucleotide-gated channel (Bargmann et al., 1993; Komatsu et al., 1996). Thus, we tested whether attraction to hexanol requires the function of AWC neurons by performing chemotaxis assays with animals in which AWC was genetically ablated. We found that AWC ablated animals were no longer robustly attracted to hexanol but instead exhibited avoidance, indicating that AWC is necessary for hexanol attraction (Figure 3.2B, also shown in Chapter 2 Figure 2). We also found that expression of *tax-4* under the AWC-specific promoter *ceh-36Δ* (Kim et al., 2010),

rescued attraction to hexanol (Figure 3.2B), further confirming the role of AWC in driving attraction to low hexanol concentrations. Furthermore, in Chapter 2, we have shown that calcium responses in AWC neuron to hexanol were abolished in animals mutant for the *tax-4* cyclic nucleotide-gated channel, indicating that these responses require cGMP signaling (a variation of Chapter 2 Figure 6A shown below). Taken together with the chemotaxis data shown in Figure 3.2A, these results indicate that signaling through the TAX-4 CNG channel in AWC olfactory neuron drives attraction to low concentrations of hexanol.

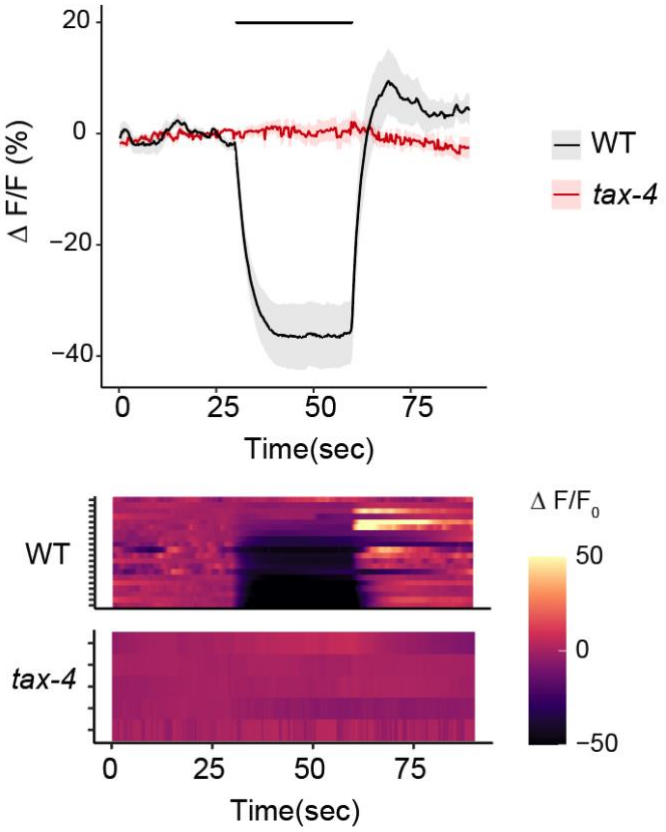

Fig. 3.3. Average changes in GCaMP3 fluorescence in AWC in response to 30s pulse of 10^{-4} dilution of hexanol in wild-type (black) and *tax-4* mutants (red). Corresponding heatmaps of changes in fluorescence intensity are shown below. Each row in the heatmaps shows responses from a single AWC neuron from different animals; n = 15 for WT and 5 for *tax-4* mutants. Shaded regions indicate SEM. A variation of this figure is also shown in Chapter 2, Figure 6A

3.4.3 AWB and ASH sensory neurons drive repulsion to high concentrations of hexanol

We then asked what neurons function to promote avoidance of high concentrations of hexanol. ASH, ADL, and AWB are the major chemosensory neurons that have been previously reported to mediate responses to repellents including high concentrations of isoamyl alcohol (Bargmann et al., 1993; Chao et al., 2004; Troemel et al., 1997; Duan et al., 2020). Additionally, it has also been shown that the amhid sheath glial cells (AMsh glia), a sheath for multiple sensory neurons including ASH, can cell-autonomously respond to aversive odorants (Duan et al., 2020). First, we tested whether repulsion to high concentration of hexanol requires ASH, ADL, and/or AWB by performing chemotaxis assays with animals in which each of these neurons was genetically ablated. We found that AWC and ADL-ablated animals phenocopied wild-type animals and displayed avoidance of 10µl hexanol (Figure 3.4A), the concentration at which wild-type animals display the strongest repulsion (Figure 3.1). Surprisingly, both ASH and AWB ablated worms were strongly attracted to high concentrations of the odorant (Figure 3.4A), indicating that these neurons drive repulsion to high concentrations of hexanol. They likely function together to drive the behavioral response towards repulsion, since in the absence of one neuron, the other neuron is unable to drive repulsion (Figure 3.4A).

We next examined calcium responses in ASH and AWB neurons in response to hexanol. Due to technical limitations and solubility issues, microfluidic calcium imaging cannot be performed with undiluted odorants. Therefore, we investigated whether ASH and AWB neurons respond to low concentrations of hexanol. As shown in Chapter 2,

upon imaging calcium responses in ASH to 10^{-4} hexanol, we found that ASH responds to the same low concentration of hexanol as AWC (Figure 3.4B, also shown in Chapter 2 Figure 4A), but it is likely that it may respond more robustly to higher concentrations of the chemical. Few animals displayed negligible responses to hexanol in AWB, with most of the animals not responding (Figure 3.4B). This may suggest that the hexanol receptor(s) in AWB are more tightly tuned and perhaps only respond to and drive repulsion to higher concentrations of the chemical as shown in Figure 3.4A. Taken together, these data suggest that more than one sensory neuron can respond to hexanol, however, the hexanol receptors that are expressed in these neurons are likely tuned to different sensitivities. Furthermore, we also conclude that dedicated subsets of sensory neurons in *C. elegans* drive concentration-dependent olfactory preference of hexanol.

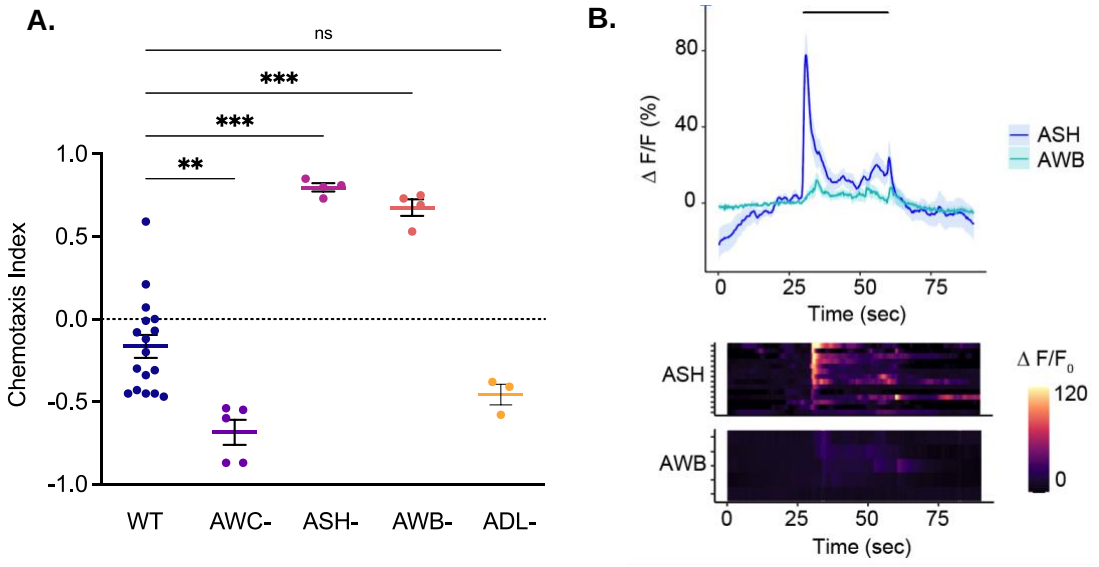

Fig. 3.4.**(A)** Chemotaxis responses of wild-type and ablation strains in response to 10µl hexanol. Each dot represents the chemotaxis index of a single assay plate containing ~100-200 adult hermaphrodites. Thick horizontal bars indicate the mean; errors are SEM.***p<0.001,*p<0.05, ns- not significant. Data were analyzed using one-way ANOVA with Tukey's post hoc test for multiple comparisons. **(B)** Average changes in GCaMP3 fluorescence in ASH and AWB neurons in response to 30s pulse of 10^{-4} dilution of hexanol. Corresponding heatmaps of changes in fluorescence intensity are shown below. Each row in the heatmaps shows responses from a single neuron from different animals ordered by the time of the first response; n = 15 for ASH and 5 for AWB. Shaded regions indicate SEM. ASH calcium data also shown in Chapter 2, Figure 4A

3.4.4 Weighting between two antagonist sensory pathways drives behavioral plasticity in response to different concentrations of the same chemical

It is evident from both the chemotaxis and calcium imaging data that more than one sensory neuron can respond to hexanol, and the response varies depending on the concentration. We have identified distinct sets of neurons either driving attraction or repulsion to the same chemical. But, is this olfactory circuit entirely segregated or do the two arms of the circuit communicate with each other? We noticed that there was enhanced attraction to 1µl undiluted hexanol in ASH and AWB ablated animals, compared to wild-type animals (Figure 3.5). In addition, we also noticed that AWC-ablated animals displayed a stronger repulsion to a high concentration of hexanol, compared to wild type (Figure 3.4A). In Chapter 2 we have shown that hexanol responses in ASH in *tax-4* mutants resembled those in *unc-31* peptidergic neurotransmission mutants (Figure S3E), suggesting that AWC may influence hexanol response dynamics in ASH. Taken together, our data suggest that these distinct subsets of neurons do not operate entirely in parallel- there is crosstalk between them. Mutants that take away the function of the attractive arm of the circuit promotes stronger repulsion, and vice versa (Figure 3.4A, Figure 3.5). This crosstalk, either directly between the sensory neurons, or via downstream overlapping target neurons, can allow for fine-tuning and regulation of appropriate behavioral responses in response to changing concentrations of olfactory stimuli.

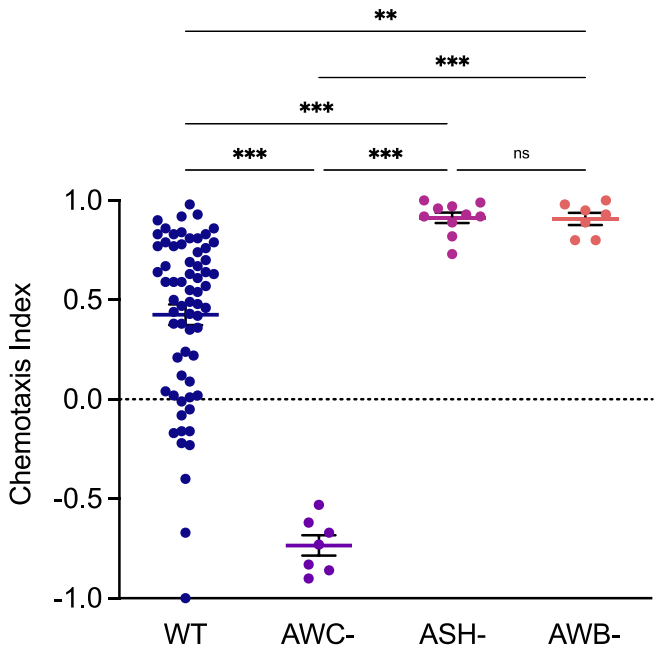

Fig. 3.5. Chemotaxis responses of wild-type and ablation strains in response to 1µl hexanol. Each dot represents the chemotaxis index of a single assay plate containing ~100-200 adult hermaphrodites. Thick horizontal bars indicate the mean; errors are SEM. ***p<0.001,**p<0.01 data were analyzed using one-way ANOVA with Tukey's post hoc test for multiple comparisons.

3.5 Discussion

Although changes in odor concentration have been empirically known to change the behavioral preference to an odor, the mechanisms guiding such changes at the sensory neuron level are not well understood. In this chapter, we show that *C. elegans'* behavioral response to hexanol can be strong attraction or repulsion based on concentration (Figure 3.1). As shown before for IAA (Yoshida et al., 2012), our results indicate that the odor concentration information in *C. elegans* is modulated at the sensory neuron level. Specifically, we found that distinct sensory neurons are responsible for mediating attraction and avoidance of the chemical. AWC-mediated signaling is required for attraction to low concentrations of hexanol (Figures 3.2, 3.3), whereas repulsion to high concentration of the chemical is mediated by both ASH and

AWB neurons (Figure 3.4). We have also shown that the AWC-mediated attraction to hexanol is dependent on signaling through the TAX-4 CNG channels and rescuing *tax-4* in AWC was sufficient to rescue the attraction phenotype (Figure 3.2). Thus, data in this chapter indicate that the olfactory system of *C. elegans* recruits additional neurons to respond to high concentrations of odorants as shown before (Yoshida et al., 2012), much akin to the mammalian olfactory system, where additional neurons and glomeruli are recruited in response to increasing odorant concentration (Fried et al., 2002; Jiang et al., 2015; Khan et al., 2010; Rubin & Katz, 1999; Wilson et al., 2017). However, although we have established that differential recruitment of sensory neurons influence the behavioral preference to different concentrations of hexanol, we cannot rule out whether the behavioral change is also a result of altered signaling in downstream interneurons.

C. elegans has a relatively compact olfactory system- with about only ~32 chemosensory neurons, worms can detect and discriminate hundreds of chemicals and in varying concentrations (Bargmann et al., 1993; Chou et al., 1996; L'Etoile & Bargmann, 2000). How can such a relatively small chemosensory circuit have such a large repertoire of chemosensory responses? From both the calcium imaging and chemotaxis behavior data shown in this chapter, it is evident that multiple sensory neurons have receptors that can respond to the same chemical. However, it is possible that they are tuned differently- ASH and AWC respond to the same concentration of hexanol, but our data also shows that ASH can drive repulsive responses to high concentrations of the chemical. This may suggest that (1) hexanol receptor(s) in ASH is broadly tuned and that it can respond to both low and high concentrations of the

chemical or (2) it is also possible that ASH expresses more than one hexanol receptor, each responding to different concentration ranges of the odorant. Moreover, calcium imaging data in Figure 3.4B also suggests that AWB is weakly tuned for low concentrations of hexanol. However, AWB ablated mutants are unable to avoid high concentrations of hexanol (Figure 3.4A), suggesting that HEX receptor in AWB responds to high concentrations of the chemical. Recent work has shown that distinct receptors expressed in different cells can drive distinct responses to the same concentration of a chemical. For example, the AMsh glia and ASH neurons express distinct GPCRs as IAA receptors and respond to aversive concentrations of IAA (Duan et al., 2020). However, the activation threshold and response kinetics to aversive concentrations of IAA varied between the two cells (Duan et al., 2020).

In both mammals and *Drosophila*, it has previously been shown that chemicals can bind to multiple odorant receptors with different affinities and in turn activate them with different efficacies (Fried et al., 2002; Jiang et al., 2015; Khan et al., 2010; Rubin & Katz, 1999; Saberi & Seyed-Allaei, 2016; Wilson et al., 2017). For example, odorant receptor response pattern to a citrus ordor broadens with concentration; some highly sensitive receptors respond to only a low concentration of the odor but in others, the response is directly proportional to the concentration (McClintock et al., 2020). Data in this chapter indicate that olfactory neurons in *C. elegans* can exhibit different response thresholds to hexanol and this variation of threshold essentially results in a “tuning curve”, such that different subsets of neurons respond and drive behavioral preferences to different concentrations of hexanol. Similar olfactory coding strategy has also been shown for the chemical diacetyl. ODR-10, the first identified olfactory receptor in *C.*

elegans, is expressed in the AWA neurons and responds and drives attraction to low concentrations of diacetyl (Sengupta, 1996). Diacetyl elicits aversive responses at high concentrations, and it was later found that the chemoreceptor SRI-14 mediates this detection in the ASH neuron (Taniguchi et al., 2014). Furthermore, it has also been shown that downstream integration of coordinated dose-dependent activity from multiple chemosensory neurons can encode valence of diacetyl (Dobosiewicz, et al., 2019). Reliable responses in the AIA interneuron requires integration of two sensory inputs: activation of the AWA olfactory neurons that are activated by diacetyl, and inhibition of one or more chemosensory neurons that are inhibited by diacetyl (Dobosiewicz, et al., 2019). It is perhaps this combinatorial encoding strategy that enables the olfactory system of *C. elegans* to efficiently respond to changes in chemical concentrations despite its relatively small size.

We have shown that two distinct arms of the chemosensory circuit drive attraction or repulsion to HEX depending on the concentration. But is there any crosstalk between them? *C. elegans'* olfactory system has long been described with the label-lined hypothesis (Yoshida et al., 2012) – that distinct sets of sensory neurons and their downstream targets are dedicated to driving attraction or repulsion to olfactory stimulus (Yoshida et al., 2012). The functional goal of a label-lined circuit is to separate streams of sensory stimuli according to their valence and drive appropriate behavioral responses. Algorithmically, the advantage of such system is that it is fast and robust. However, without crosstalk between the two streams of information, the circuit is unable to generate a weighted response and loses flexibility. Although we find that the olfactory neurons driving attraction and repulsion are distinct, our data suggest that

there is crosstalk between the two circuits. Mutants that take away the function of the attractive arm of the circuit promotes stronger repulsion, and vice versa. Sensory context-dependent remodeling of neural circuit composition has been shown previously in a salt-sensing circuit in *C. elegans* (Leinwand & Chalasani, 2014). The primary salt detectors, ASE sensory neurons, releases an insulin-like peptide in response to large but not small changes in external salt stimuli. This peptidergic signaling functionally switches the AWC olfactory neuron into an interneuron in the salt circuit, thereby increasing the dynamic range of the salt circuit and preventing behavioral responses from saturating at high salt level (Leinwand & Chalasani, 2014).

Previous studies and results in this chapter show that *C. elegans* chemosensory neural circuits are flexible and their composition can be modified by sensory context. Specifically, data shown in this chapter suggest that behavioral responses to hexanol are likely to be regulated by an opposing-components circuit/push-pull mechanism, based on two antagonistic chemical signals, where the weighted sensory neuron responses from both attraction and repulsion mediating neurons determine the animal's behavioral response to the chemical. This type of circuitry often involves opposing signals synapsing onto the same downstream effector cells (Tye, 2018). Thus, it is likely that AWC, AWB, and ASH responses to hexanol converges into overlapping interneurons which then relay the information to motor neurons to drive appropriate behavioral output. The net balance between the strengths of the AWC attraction neuron and AWB/ASH repulsive neurons can shift the operating point of the circuit in a concentration-dependent manner. The advantages of this neural circuit motif include flexibility and regulation of competing valence stimuli. However, how signals from

sensory neurons are integrated downstream in the circuit and ultimately drives concentration dependent preference of the chemical remains yet to be identified.

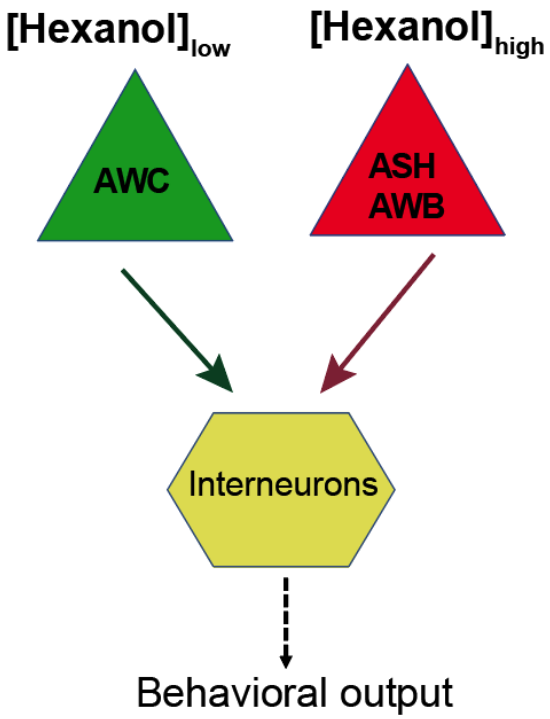

Fig. 3.6 Model of opposing-components olfactory circuit driving behavioral response to different concentrations of hexanol.

3.6 Methods

3.6.1 Strains and growth conditions

Table 3.1 List of strains used in this chapter

Strain	Genotype	Source/parent strains[a]	Relevant Figure(s) (3.X)
WT	N2 (Bristol)	CGC	1, 2, 4, 5
PY7502	*oyIs85[ceh-36∆p::TU813(recCaspase), ceh-36∆p::TU814(recCaspase), unc-122p::dsRed, srtx-1p::gfp]*	(Beverly et al., 2011)	1, 2, 4, 5
PR678	*tax-4(p678)*	CGC	2
PY7513	*tax-4(p678);Ex[ceh-36∆p::tax-4, unc-122p::dsRed] Line 2*	(Beverly et al., 2011)	2
JN1713	*peIs1713[sra-6p::mCasp1, unc122p::mCherry]*	CGC	4, 5
CX4544	*ocr-2(ak47)*	CGC	2
JN1715	*peIs1715 [str-1p::mCasp-1 + unc-122p::GFP]*	CGC	4, 5
PY10501	*oyIs91[odr-1*p*::GCaMP3, srsx-3*p*::mScarlet, unc-122*p*::dsRed]*	PY11610	3
PY12005	*kyIs602[sra-6*p*::GCaMP3, unc-122*p*::gfp]*	CX15030	5
PY9735	oyEx[str-1p::GCaMP 3]	(Takeishi et al., 2016)	5
PY10518	*tax-4 (p678); oyIs91[odr-1*p*::GCaMP, srsx-3*p*::mScarlet, unc-122*p*::dsRed]*	PR678, PY10501	3
Not available	Ex[srh281p::mCasp1 + myo-3p::GFP]	UR1106; (Luo & Portman, 2021)	4

[a]CGC- *Caenorhabditis* Genetics Center

All *C. elegans* strains were maintained on nematode growth medium (NGM) at 20 °C, and hermaphrodites were used for all experiments. 5 days prior to assays, 10 L4 larvae per genotype were picked to 10cm assay growth plates (day 1), and young adults were tested in behavioral and calcium imaging assays 4 days later (day 5). To reduce variability between assays, the growth plates were seeded with standardized bacteria as follows: concentrated *Escherichia coli* OP50-1 was cultured by inoculating 10µl of starter OP50 culture (grown in LB for ~2hr from a single colony) per 1L of Superbroth media (3.2%w/v tryptone, 2.0% yeast extract, 0.5% NaCl). After allowing Superbroth cultures to grow overnight, they were treated with the antibiotic gentamicin (300ng/ml) (Sigma G1397) for ~4 hours, centrifuged for 20 minutes at 4 °C, and resulting pellets were resuspended in 75 mL of S-Basal buffer. The concentrated food was stored at -80°C and thawed as needed to seed plates (1mL/10cm plate).

3.6.2 Plate chemotaxis assays

Chemotaxis assays were performed according to previously published protocols (Bargmann et al., 1993; Troemel et al., 1997). Assays were performed on 10cm square plates with 1µl spot of odorant at one end and 1ul control spot of ethanol at the other end, together with 1µl of 1 M sodium azide. When necessary, the odorant was diluted in ethanol. The number of worms in two horizontal rows adjacent to the odor and ethanol spots was quantified at the end of 1 hour. Chemotaxis index = [(A+B) – (E+F)(A+B+E+F)].

3.6.3 Calcium imaging

Calcium imaging was performed as previously described, using custom microfluidic devices (Chronis et al., 2007; Neal et al., 2015). Imaging was conducted on an Olympus BX52WI microscope with a 40X oil objective and Hamamatsu Orca CCD camera. Recordings were performed at 4 Hz. All odorants were diluted in S-Basal buffer and 1 µl of 20 µM fluorescein was added to one of the channels to confirm correct fluid flow. 1 mM (-)-tetramisole hydrochloride (Sigma L9756) was added to the S-Basal buffer to paralyze body wall muscles and keep animals stationary. To prevent the chip from clogging, poloxamer surfactant (Sigma P5556) was also added to S-Basal while loading the worms. Odor evoked calcium transients in the sensory neurons were similar in the presence or absence of these chemicals. Neurons were imaged for one cycle of 30s buffer/30s odor/30s buffer stimulus. Recorded image stacks were aligned with Fiji using the Template Matching plugin and cropped to a region containing the cell body. The region of interest (ROI) was defined by outlining the desired cell body; background subtracted fluorescence intensity of the ROI was used for subsequent analysis. To correct for photobleaching, an exponential decay was fit to fluorescence intensity values for the first 20s and the last 15s of imaging (prior and post stimulus). The resulting curve was subtracted from original intensity values. Data visualization and figures were generated using RStudio (version 1.3.959).

3.6.4 Statistical analyses

Excel (Microsoft) and GraphPad Prism version 9.0.2 (www.graphpadpad.com) were used to generate all chemotaxis plate assay data. Chemotaxis index data were

analyzed using one-way ANOVA followed by Tukey's multiple comparison test using GraphPad Prism (version 9.0.2).

References

Bargmann, C. I. (2006). Chemosensation in C. elegans. *WormBook*, 1-29. doi:10.1895/wormbook.1.123.1

Bargmann, C. I., et al. (1993). Odorant-selective genes and neurons mediate olfaction in C. elegans. *Cell, 74*(3), 515-527. doi:10.1016/0092-8674(93)80053-h

Beverly, M., et al. (2011). Degeneracy and signaling within a sensory circuit contributes to robustness in thermosensory behaviors in *C. elegans*. *J Neurosci, 31*, 11718-11727.

Brenner, S. (1974). The genetics of Caenorhabditis elegans. *Genetics, 77*(1), 71-94. doi:10.1093/genetics/77.1.71

Chalasani, S. H., et al. (2007). Dissecting a circuit for olfactory behaviour in Caenorhabditis elegans. *Nature, 450*(7166), 63-70. doi:10.1038/nature06292

Chao, M. Y., et al. (2004). Feeding status and serotonin rapidly and reversibly modulate a Caenorhabditis elegans chemosensory circuit. *Proc Natl Acad Sci U S A, 101*(43), 15512-15517. doi:10.1073/pnas.0403369101

Choi, J. I., et al. (2018). Odor-dependent temporal dynamics in Caenorhabitis elegans adaptation and aversive learning behavior. *PeerJ, 6*, e4956. doi:10.7717/peerj.4956

Chou, J. H., et al. (1996). Olfactory recognition and discrimination in Caenorhabditis elegans. *Cold Spring Harb Symp Quant Biol, 61*, 157-164. Retrieved from https://www.ncbi.nlm.nih.gov/pubmed/9246444

Chronis, N., et al. (2007). Microfluidics for in vivo imaging of neuronal and behavioral activity in Caenorhabditis elegans. *Nat Methods, 4*(9), 727-731. doi:10.1038/nmeth1075

Coburn, C. M., et al. (1996). A putative cyclic nucleotide-gated channel is required for sensory development and function in C. elegans. *Neuron, 17*(4), 695-706. doi:10.1016/s0896-6273(00)80201-9

Colbert, H. A., et al. (1997). OSM-9, a novel protein with structural similarity to channels, is required for olfaction, mechanosensation, and olfactory adaptation in Caenorhabditis elegans. *J Neurosci, 17*(21), 8259-8269. Retrieved from https://www.ncbi.nlm.nih.gov/pubmed/9334401

Correction for Zaslaver et al., Hierarchical sparse coding in the sensory system of Caenorhabditis elegans. (2015). *Proc Natl Acad Sci U S A, 112*(13), E1688-1689. doi:10.1073/pnas.1504344112

Felix, M. A., et al. (2010). The natural history of Caenorhabditis elegans. *Curr Biol, 20*(22), R965-969. doi:10.1016/j.cub.2010.09.050

Ferkey, D. M., et al. (2021). Chemosensory signal transduction in Caenorhabditis elegans. *Genetics, 217*(3). doi:10.1093/genetics/iyab004

Frezal, L., et al. (2015). C. elegans outside the Petri dish. *Elife, 4*. doi:10.7554/eLife.05849

Fried, H. U., et al. (2002). Selective imaging of presynaptic activity in the mouse olfactory bulb shows concentration and structure dependence of odor responses in identified glomeruli. *Proc Natl Acad Sci U S A, 99*(5), 3222-3227. doi:10.1073/pnas.052658399

Haber, M., et al. (2005). Evolutionary history of Caenorhabditis elegans inferred from microsatellites: evidence for spatial and temporal genetic differentiation and the occurrence of outbreeding. *Mol Biol Evol, 22*(1), 160-173. doi:10.1093/molbev/msh264
Harris, G., et al. (2014). Dissecting the signaling mechanisms underlying recognition and preference of food odors. *J Neurosci, 34*(28), 9389-9403. doi:10.1523/JNEUROSCI.0012-14.2014
Hodgkin, J., et al. (1997). Natural variation and copulatory plug formation in Caenorhabditis elegans. *Genetics, 146*(1), 149-164. doi:10.1093/genetics/146.1.149
Jiang, Y., et al. (2015). Molecular profiling of activated olfactory neurons identifies odorant receptors for odors in vivo. *Nat Neurosci, 18*(10), 1446-1454. doi:10.1038/nn.4104
Khan, A. G., et al. (2010). Odor representations in the mammalian olfactory bulb. *Wiley Interdiscip Rev Syst Biol Med, 2*(5), 603-611. doi:10.1002/wsbm.85
Kim, K., et al. (2010). The HMX/NKX homeodomain protein MLS-2 specifies the identity of the AWC sensory neuron type via regulation of the ceh-36 Otx gene in C. elegans. *Development, 137*(6), 963-974. doi:10.1242/dev.044719
Komatsu, H., et al. (1996). Mutations in a cyclic nucleotide-gated channel lead to abnormal thermosensation and chemosensation in C. elegans. *Neuron, 17*(4), 707-718. doi:10.1016/s0896-6273(00)80202-0
L'Etoile, N. D., et al. (2000). Olfaction and odor discrimination are mediated by the C. elegans guanylyl cyclase ODR-1. *Neuron, 25*(3), 575-586. doi:10.1016/s0896-6273(00)81061-2
Luo, J., et al. (2021). Sex-specific, pdfr-1-dependent modulation of pheromone avoidance by food abundance enables flexibility in C. elegans foraging behavior. *Curr Biol*. doi:10.1016/j.cub.2021.07.069
McClintock, T. S., et al. (2020). Mixture and concentration effects on odorant receptor response patterns in vivo. *Chem Senses*. doi:10.1093/chemse/bjaa032
Neal, S. J., et al. (2015). Feeding state-dependent regulation of developmental plasticity via CaMKI and neuroendocrine signaling. *Elife, 4*. doi:10.7554/eLife.10110
Norhave, N. J., et al. (2012). How does growth temperature affect cadmium toxicity measured on different life history traits in the soil nematode Caenorhabditis elegans? *Environ Toxicol Chem, 31*(4), 787-793. doi:10.1002/etc.1746
Perkins, L. A., et al. (1986). Mutant sensory cilia in the nematode Caenorhabditis elegans. *Dev Biol, 117*(2), 456-487. doi:10.1016/0012-1606(86)90314-3
Rubin, B. D., et al. (1999). Optical imaging of odorant representations in the mammalian olfactory bulb. *Neuron, 23*(3), 499-511. doi:10.1016/s0896-6273(00)80803-x
Saberi, M., et al. (2016). Odorant receptors of Drosophila are sensitive to the molecular volume of odorants. *Sci Rep, 6*, 25103. doi:10.1038/srep25103
Samuel, B. S., et al. (2016). Caenorhabditis elegans responses to bacteria from its natural habitats. *Proc Natl Acad Sci U S A, 113*(27), E3941-3949. doi:10.1073/pnas.1607183113
Schulenburg, H., et al. (2017). The Natural Biotic Environment of Caenorhabditis elegans. *Genetics, 206*(1), 55-86. doi:10.1534/genetics.116.195511

Semmelhack, J. L., et al. (2009). Select Drosophila glomeruli mediate innate olfactory attraction and aversion. *Nature, 459*(7244), 218-223. doi:10.1038/nature07983
Takeishi, A., et al. (2016). Receptor-type Guanylyl Cyclases Confer Thermosensory Responses in C. elegans. *Neuron, 90*(2), 235-244. doi:10.1016/j.neuron.2016.03.002
Tobin, D. M., et al. (2002). Combinatorial expression of TRPV channel proteins defines their sensory functions and subcellular localization in C. elegans neurons. *Neuron, 35*(2), 307-318. doi:10.1016/s0896-6273(02)00757-2
Troemel, E. R., et al. (1995). Divergent seven transmembrane receptors are candidate chemosensory receptors in C. elegans. *Cell, 83*(2), 207-218. doi:10.1016/0092-8674(95)90162-0
Troemel, E. R., et al. (2008). Microsporidia are natural intracellular parasites of the nematode Caenorhabditis elegans. *PLoS Biol, 6*(12), 2736-2752. doi:10.1371/journal.pbio.0060309
Troemel, E. R., et al. (1997). Reprogramming chemotaxis responses: sensory neurons define olfactory preferences in C. elegans. *Cell, 91*(2), 161-169. doi:10.1016/s0092-8674(00)80399-2
Ward, S., et al. (1975). Electron microscopical reconstruction of the anterior sensory anatomy of the nematode Caenorhabditis elegans.?2UU. *J Comp Neurol, 160*(3), 313-337. doi:10.1002/cne.901600305
Wes, P. D., et al. (2001). C. elegans odour discrimination requires asymmetric diversity in olfactory neurons. *Nature, 410*(6829), 698-701. doi:10.1038/35070581
Wilson, C. D., et al. (2017). A primacy code for odor identity. *Nat Commun, 8*(1), 1477. doi:10.1038/s41467-017-01432-4
Worthy, S. E., et al. (2018). Identification of attractive odorants released by preferred bacterial food found in the natural habitats of C. elegans. *PLoS One, 13*(7), e0201158. doi:10.1371/journal.pone.0201158
Worthy, S. E., et al. (2018). Identification of Odor Blend Used by Caenorhabditis elegans for Pathogen Recognition. *Chem Senses, 43*(3), 169-180. doi:10.1093/chemse/bjy001
Yoshida, K., et al. (2012). Odour concentration-dependent olfactory preference change in C. elegans. *Nat Commun, 3*, 739. doi:10.1038/ncomms1750
Zhang, Y., et al. (2005). Pathogenic bacteria induce aversive olfactory learning in Caenorhabditis elegans. *Nature, 438*(7065), 179-184. doi:10.1038/nature04216

CHAPTER 4

General Discussion

4.1 Impact of this work

Sensory plasticity allows organisms to make appropriate behavioral decisions to maximize their fitness. Our sensory environments are rich, complex, and constantly changing. Thus, to correctly decode sensory stimuli, neuronal responses must not only be sensitive and robust, but they must also be flexible. Decades of research have investigated plasticity mechanisms that allow the nervous system to generate flexible and adaptive behavioral responses to sensory stimuli. However, our understanding of how the nervous system assigns context-dependent hedonic valence to sensory stimuli remains unclear. In this dissertation, I have described novel molecular and neuronal mechanisms driving context (Chapter 2) and concentration-dependent olfactory plasticity to hexanol (Chapter 3).

Hexanol and heptanol medium-chain alcohols, that are likely to be food-related odor to *C. elegans*, are attractive at low concentrations and repulsive at high concentrations (Chapter 3). However, in Chapter 2, I show that the behavioral response of *C. elegans* to low concentrations of hexanol is inverted from attraction to avoidance in the continuous presence of second background chemicals, including isoamyl alcohol (IAA) and benzaldehyde (BZ). Specifically, I identified that a context-dependent response sign switch in a single sensory neuron inverts olfactory preference behavior to hexanol. This response sign switch is driven by distinct intracellular signaling pathways under different odorant contexts. I have also shown that the response sign switch is not limited to hexanol; AWC also exhibits increase in calcium in response to heptanol under IAA saturation conditions. It is possible that this context-dependent odor discrimination strategy applies broadly to all medium-chain alcohols and suggest that similar principles

may underlie aspects of stimulus encoding and stimulus discrimination across sensory modalities. Bidirectional responses in neurons to multiple types of stimuli have been described before (Cao et al., 2017; Hallem & Carlson, 2006; Hallem et al., 2004; Solessio & Engbretson, 1993; Su et al., 2006). However, context-dependent bidirectional responses in a single sensory neuron to the same stimulus has not been reported previously.

In Chapter 3, I describe a push-pull opposing components olfactory circuit that drives changes in behavioral valence to varying concentrations of hexanol. A single chemosensory neuron, AWC, drives attraction to low concentrations/undiluted hexanol. Repulsion of high concentrations of the odorant are driven by recruitment of additional neurons, AWB and ASH, in the circuit. The net balance from the combinatorial responses of both attraction and repulsion neurons allows the circuit to respond to varying concentrations of hexanol. The neural circuits underlying the context-and concentration-dependent behavior in response to hexanol have overlapping chemosensory neurons. I have shown that functional reorganization and differential compartmentalization of signaling complexes within a single neuron, can increase the functionality of the olfactory circuit and enable encoding of context.

4.2 Future directions

Similar to other organisms, chemoreception in *C. elegans* is mediated by seven transmembrane G protein-coupled receptors (Troemel et al., 1995) . These receptors mediate the first step in signal transduction of olfactory stimuli, conferring stimulus specificity. In Chapter 2, we have identified a context-dependent circuit that mediates

responses to hexanol. We have shown that AWC and ASH neurons are able to respond to and drive olfactory preference towards the same concentration of hexanol. However, the receptor(s) for hexanol still remain to be identified. Upon comparing single-cell transcriptional profiling datasets on *C. elegans* Neuronal Gene Expression Map & Network (CeNGEN), [http://www.cengen.org, (Hammarlund et al., 2018)], we have identified three overlapping odorant receptor genes, *sra-37, srr-4,* and *srh-271* that are expressed in ASH and the AWC neuron pair. Future experiments can look into these genes to identify the receptor(s) that mediates responses to hexanol.

Unlike mammalian and insect olfactory neurons which express a single type of odorant receptor (Buck & Axel, 1991), *C. elegans* expresses multiple types of odorant receptors in a single chemosensory neuron (Chen et al., 2005; Colosimo et al., 2004; McCarroll et al., 2005; Troemel et al., 1995). Additionally, the *C. elegans* genome encodes a variety of G protein subunits, and each chemosensory neuron is capable of expressing multiple subunits in a single neuron. This allows for increased chemoreception repertoire of the system and allows for odor discrimination. Indeed, we have shown that responses to hexanol under control and IAA saturation conditions is divergent at the G protein level. Responses to hexanol under IAA saturation condition is transduced by the ODR-3 G protein, yet this G protein is not necessary to drive responses to hexanol under control conditions. Specifically, we found that unlike wild-type animals, in *odr-3* mutants, hexanol responses under IAA saturation condition continued to induce hyperpolarization of AWC, consistent with these animals retaining attraction to hexanol. What are the different ways ODR-3 and other G-proteins can gate the activity and produce bidirectional responses in a single neuron? As discussed in

Chapter 1, cGMP plays a crucial role as a second messenger in the regulation of sensory signal transduction in AWC (Bargmann et al., 1993). Intracellular cGMP concentrations are regulated by the activity of rGCs and PDEs, which synehtisze and hydrolyze cGMP, respectively (Bargmann et al., 1993; Birnby et al., 2000; Ferkey et al., 2021; L'Etoile & Bargmann, 2000; Lans et al., 2004; Roayaie et al., 1998; Shidara et al., 2017). Calcium influx through the CNG-gated channels in AWC in response to hexanol/ heptanol under IAA/BZ saturation conditions is a result of increase in cGMP. Thus, ODR-3 can either activate rGCs and/or inhibits PDEs to regulate the net cGMP levels, thereby gating the activity of the neuron. However, it is currently unclear whether ODR-3 positively or negatively regulates intracellular cGMP concentrations.

Unlike wild-type animals, tonic activity of AWC seemed to not be fully silenced upon IAA saturation in *odr-3* mutants, and under these conditions, hexanol continued to elicit hyperpolarization of AWC. Thus, the pre-stimulus neuronal state seems to be a contributing factor to the response sign switch. How can we precisely measure the tonic activity and get a readout of the neuronal state at rest? The neuronal response data shared in this thesis was collected via calcium imaging in neurons expressing the genetically encoded calcium indicator GCaMP. It is important to note that calcium imaging measures a change in fluorescence of the indicator, thereby reflecting a change in intracellular calcium concentrations. However, it fails to provide information on the absolute calcium levels at rest and therefore, we cannot conclude whether an observed change in the magnitude of GCaMP response stems from a change in baseline activity (Akerboom et al., 2012; Tian et al., 2009; Wei et al., 2020). The most direct way of monitoring neuronal activity is by quantifying its electrical activity or the

membrane voltage, which is upstream to calcium changes and neurotransmitter release. Thus, future work may require electrophysiology or the use of genetically encoded voltage sensors to directly assess neuronal state (Flytzanis et al., 2014).

Context-dependent change in behavioral preference to odorants may involve plasticity throughout different levels of the circuit. It can arise from changes in sensory neuron responses and their synaptic output, but it can also be a result of alterations in downstream circuit properties. AWC and ASH sensory neurons are directly presynaptic to the AIA, AIB, AVA, and RIA interneurons (White et al., 1986). ASH and AWC have inhibitory connections onto AIA, while both neurons activate AIB. The two interneurons play opposing roles in regulating motor movements, with AIA suppressing and AIB promoting turns, respectively (Gray et al., 2005; Iino & Yoshida, 2009; Luo et al., 2014; Piggott et al., 2011). These interneurons have been studied in the context of several olfactory circuits, and their activities have been shown to drive distinct behavioral outputs (Gray et al., 2005; Iino & Yoshida, 2009; Larsch et al., 2015; Tsalik & Hobert, 2003). Therefore, context-dependent changes in behavior to hexanol may not only be limited to changes in sensory neuron responses; it can also be a result of changes in response properties in downstream interneurons. Moreover, as mentioned in Chapter 1, *C. elegans* can use different navigational strategies towards to chemotax towards or away from odorant cues. It is currently unclear which interneurons are involved in driving plasticity of hexanol responses under different conditions and it also remains unclear if there are any underlying context-dependent differences in the navigation strategies.

Finally, it is important to speculate why the behavioral preference of hexanol changes so drastically in the presence of IAA. It is well known that bacteria emit an array of volatile compounds which accounts for their odors. Straight-chain alcohols and IAA have been previously shown to be produced by several bacterial isolates in the natural environment of *C*. *elegans* (Worthy, Haynes, et al., 2018; Worthy, Rojas, et al., 2018). Thus, they have the potential to serve as food signals for *C. elegans.* The chemical structure of hexanol is closely related to octanol, a longer-chain alcohol that has been reported to be produced by several bacterial strains, including pathogenic bacteria, and it has been shown trigger aversive responses in *C. elegans* (Baidya et al., 2014; Chao et al., 2004; Hamilton-Kemp et al., 2005; O'Donnell et al., 2020; Troemel et al., 1995). It is possible that hexanol is a potential toxin and that the olfactory circuit is employing a risk vs. reward paradigm, where in the absence of other volatile food signaling odorants, the risk of a potential toxin is not significant and therefore worms find it attractive. In the presence of the more potent, food-signaling odorant IAA, responses to hexanol may be inverted from attraction to avoidance as a way to avoid a potential toxin. To test this hypothesis, preliminary experiments were conducted that looked into responses to hexanol in the presence of different bacterial strains and upon starvation. However, the ethological relevance of hexanol induced avoidance in the presence of other attractive chemicals remains to be determined.

Findings shared in this dissertation further highlights the extraordinary computational ability of the nervous system. It is not only able to respond to sensory cues based on experience and context; it can also generate appropriate responses to novel stimuli. Many neurological diseases, such as schizophrenia and autism spectrum

disorders, stem from deficits in neuroplasticity mechanisms and sensory processing. This work and the study of chemosensory behaviors in *C. elegans* has important implications in understanding how animals respond precisely and robustly to environmental stimuli, and how misregulation of these mechanisms leads to neurophysiological and behavioral disorders. In conclusion, I hope the work of this thesis provides insight into context-dependent sensory processing mechanisms and how similar computations are executed in diverse nervous systems.

References

Akerboom, J., et al. (2012). Optimization of a GCaMP calcium indicator for neural activity imaging. *J Neurosci, 32*(40), 13819-13840. doi:10.1523/JNEUROSCI.2601-12.2012

Baidya, M., et al. (2014). Dopamine modulation of avoidance behavior in Caenorhabditis elegans requires the NMDA receptor NMR-1. *PLoS One, 9*(8), e102958. doi:10.1371/journal.pone.0102958

Bargmann, C. I., et al. (1993). Odorant-selective genes and neurons mediate olfaction in C. elegans. *Cell, 74*(3), 515-527. doi:10.1016/0092-8674(93)80053-h

Birnby, D. A., et al. (2000). A transmembrane guanylyl cyclase (DAF-11) and Hsp90 (DAF-21) regulate a common set of chemosensory behaviors in caenorhabditis elegans. *Genetics, 155*(1), 85-104. doi:10.1093/genetics/155.1.85

Buck, L., et al. (1991). A novel multigene family may encode odorant receptors: a molecular basis for odor recognition. *Cell, 65*(1), 175-187. doi:10.1016/0092-8674(91)90418-x

Cao, L. H., et al. (2017). Odor-evoked inhibition of olfactory sensory neurons drives olfactory perception in Drosophila. *Nat Commun, 8*(1), 1357. doi:10.1038/s41467-017-01185-0

Chalasani, S. H., et al. (2007). Dissecting a circuit for olfactory behaviour in Caenorhabditis elegans. *Nature, 450*(7166), 63-70. doi:10.1038/nature06292

Chao, M. Y., et al. (2004). Feeding status and serotonin rapidly and reversibly modulate a Caenorhabditis elegans chemosensory circuit. *Proc Natl Acad Sci U S A, 101*(43), 15512-15517. doi:10.1073/pnas.0403369101

Chen, N., et al. (2005). Identification of a nematode chemosensory gene family. *Proc Natl Acad Sci U S A, 102*(1), 146-151. doi:10.1073/pnas.0408307102

Coburn, C. M., et al. (1996). A putative cyclic nucleotide-gated channel is required for sensory development and function in C. elegans. *Neuron, 17*(4), 695-706. doi:10.1016/s0896-6273(00)80201-9

Colosimo, M. E., et al. (2004). Identification of thermosensory and olfactory neuron-specific genes via expression profiling of single neuron types. *Curr Biol, 14*(24), 2245-2251. doi:10.1016/j.cub.2004.12.030

Ferkey, D. M., et al. (2021). Chemosensory signal transduction in Caenorhabditis elegans. *Genetics, 217*(3). doi:10.1093/genetics/iyab004

Flytzanis, N. C., et al. (2014). Archaerhodopsin variants with enhanced voltage-sensitive fluorescence in mammalian and Caenorhabditis elegans neurons. *Nat Commun, 5*, 4894. doi:10.1038/ncomms5894

Gray, J. M., et al. (2005). A circuit for navigation in Caenorhabditis elegans. *Proc Natl Acad Sci U S A, 102*(9), 3184-3191. doi:10.1073/pnas.0409009101

Hallem, E. A., et al. (2006). Coding of odors by a receptor repertoire. *Cell, 125*(1), 143-160. doi:10.1016/j.cell.2006.01.050

Hallem, E. A., et al. (2004). The molecular basis of odor coding in the Drosophila antenna. *Cell, 117*(7), 965-979. doi:10.1016/j.cell.2004.05.012

Hamilton-Kemp, T., et al. (2005). Production of the long-chain alcohols octanol, decanol, and dodecanol by Escherichia coli. *Curr Microbiol, 51*(2), 82-86. doi:10.1007/s00284-005-4469-x

Hammarlund, M., et al. (2018). The CeNGEN Project: The Complete Gene Expression Map of an Entire Nervous System. *Neuron, 99*(3), 430-433. doi:10.1016/j.neuron.2018.07.042

Iino, Y., et al. (2009). Parallel use of two behavioral mechanisms for chemotaxis in Caenorhabditis elegans. *J Neurosci, 29*(17), 5370-5380. doi:10.1523/JNEUROSCI.3633-08.2009

L'Etoile, N. D., et al. (2000). Olfaction and odor discrimination are mediated by the C. elegans guanylyl cyclase ODR-1. *Neuron, 25*(3), 575-586. doi:10.1016/s0896-6273(00)81061-2

Lans, H., et al. (2004). A network of stimulatory and inhibitory Galpha-subunits regulates olfaction in Caenorhabditis elegans. *Genetics, 167*(4), 1677-1687. doi:10.1534/genetics.103.024786

Larsch, J., et al. (2015). A Circuit for Gradient Climbing in C. elegans Chemotaxis. *Cell Rep, 12*(11), 1748-1760. doi:10.1016/j.celrep.2015.08.032

Luo, L., et al. (2014). Dynamic encoding of perception, memory, and movement in a C. elegans chemotaxis circuit. *Neuron, 82*(5), 1115-1128. doi:10.1016/j.neuron.2014.05.010

McCarroll, S. A., et al. (2005). Identification of transcriptional regulatory elements in chemosensory receptor genes by probabilistic segmentation. *Curr Biol, 15*(4), 347-352. doi:10.1016/j.cub.2005.02.023

O'Donnell, M. P., et al. (2020). A neurotransmitter produced by gut bacteria modulates host sensory behaviour. *Nature, 583*(7816), 415-420. doi:10.1038/s41586-020-2395-5

Piggott, B. J., et al. (2011). The neural circuits and synaptic mechanisms underlying motor initiation in C. elegans. *Cell, 147*(4), 922-933. doi:10.1016/j.cell.2011.08.053

Roayaie, K., et al. (1998). The G alpha protein ODR-3 mediates olfactory and nociceptive function and controls cilium morphogenesis in C. elegans olfactory neurons. *Neuron, 20*(1), 55-67. doi:10.1016/s0896-6273(00)80434-1

Shidara, H., et al. (2017). Compartmentalized cGMP Responses of Olfactory Sensory Neurons in Caenorhabditis elegans. *J Neurosci, 37*(14), 3753-3763. doi:10.1523/JNEUROSCI.2628-16.2017

Solessio, E., et al. (1993). Antagonistic chromatic mechanisms in photoreceptors of the parietal eye of lizards. *Nature, 364*(6436), 442-445. doi:10.1038/364442a0

Su, C. Y., et al. (2006). Parietal-eye phototransduction components and their potential evolutionary implications. *Science, 311*(5767), 1617-1621. doi:10.1126/science.1123802

Tian, L., et al. (2009). Imaging neural activity in worms, flies and mice with improved GCaMP calcium indicators. *Nat Methods, 6*(12), 875-881. doi:10.1038/nmeth.1398

Troemel, E. R., et al. (1995). Divergent seven transmembrane receptors are candidate chemosensory receptors in C. elegans. *Cell, 83*(2), 207-218. doi:10.1016/0092-8674(95)90162-0

Tsalik, E. L., et al. (2003). Functional mapping of neurons that control locomotory behavior in Caenorhabditis elegans. *J Neurobiol, 56*(2), 178-197. doi:10.1002/neu.10245

Wei, Z., et al. (2020). A comparison of neuronal population dynamics measured with calcium imaging and electrophysiology. *PLoS Comput Biol, 16*(9), e1008198. doi:10.1371/journal.pcbi.1008198

White, J. G., et al. (1986). The structure of the nervous system of the nematode Caenorhabditis elegans. *Philos Trans R Soc Lond B Biol Sci, 314*(1165), 1-340. doi:10.1098/rstb.1986.0056

Worthy, S. E., et al. (2018). Identification of attractive odorants released by preferred bacterial food found in the natural habitats of C. elegans. *PLoS One, 13*(7), e0201158. doi:10.1371/journal.pone.0201158

Worthy, S. E., et al. (2018). Identification of Odor Blend Used by Caenorhabditis elegans for Pathogen Recognition. *Chem Senses, 43*(3), 169-180. doi:10.1093/chemse/bjy001